A Hermite Cubic Immersed Finite Element Space for Beam Design Problems

Tzin S. Wang

Thesis submitted to the Faculty of the
Virginia Polytechnic Institute and State University
in partial fulfillment of the requirements for the degree of

Master of Science
in
Mathematics

Tao Lin, Chair
David Russell
Shu-Ming Sun

April 28, 2005
Blacksburg, Virginia

Keywords: Euler-Bernoulli Beam, Finite Element, Immersed Finite Element,
Interface Problem, Discontinuous Coefficient, Inverse Problem

A Hermite Cubic Immersed Finite Element Space for Beam Designs

Tzin S. Wang

(ABSTRACT)

This thesis develops an immersed finite element (IFE) space for numerical simulations arising from beam design with multiple materials. This IFE space is based upon meshes that can be independent of interface of the materials used to form a beam. Both the forward and inverse problems associated with the beam equation are considered. The order of accuracy of this IFE space is numerically investigated from the point of view of both the interpolation and finite element solution of the interface boundary value problems. Both single and multiple interfaces are considered in our numerical simulation. The results demonstrate that this IFE space has the optimal order of approximation capability.

for mom

Acknowledgments

First I would like to thanks my parents for raising me and supporting me through my life.

I would also like to thank my high school math teacher, Linda Osborne, without whose encouragement and guidance I would not have reached this far on my study of mathematics.

I also want to thank all the professors who have taught me mathematics at Virginia Tech, I have learned very much form each of you all. Dr. Arnold, I want to thank you for listening to my stories and giving me wonderful advice.

Dr. Lin, you are more than just an excellent advisor to me. I cannot express how valuable your guidance has been. You have given me appreciation for mathematics and taught me many things that are needed in specialized mathematics. Also, you have been patient with me and given up much of your time to me; you always take your time to explain many of the mathematical ideas until I have understood them. I am very grateful to have you as my advisor; thank you for giving me this opportunity to learn from you. Dr. Lin, you are a wonderful mentor, I will always be indebted to you.

Valery, without you and the encouragement from your family, I probably would not have this success in my graduate studies. Also, thank you to all my friends, without you all, I would not be the person that I am today. Andrew Vance, Brian Skinner, and Daniel Sutton, I want to thank you all for always listening to the problems that I had in my life and giving me advice and help in solving them.

Contents

List of Figures

List of Tables

Chapter 1

Introduction

The purpose of this thesis is to develop a new finite element (FE) space as a tool for solving both forward and inverse interface problems involving the following ordinary differential equation (ODE):

$$(B(x)w''(x))'' = f(x) \tag{1.1}$$

together with a certain boundary condition, say:

$$w(0) = b_1, w'(0) = b_2, w(1) = b_3, w'(1) = b_4, \tag{1.2}$$

on a domain $x \in \Omega = (0, 1)$ that contains an interface α separating Ω into two sub-domains $\Omega_1 = (0, \alpha)$ and $\Omega_2 = (\alpha, 1)$ such that $\Omega = \Omega_1 \cup \{\alpha\} \cup \Omega_2$. The coefficient function B is piecewise defined by

$$B(x) = \begin{cases} B^- & \text{if } x < \alpha, \\ B^+ & \text{if } \alpha < x \end{cases} \tag{1.3}$$

with B^+ and B^- greater than 0. In addition, we impose the rigid connection condition at the interface α as follows:

$$\begin{aligned} w(\alpha-) &= w(\alpha+), && \text{continuity in the deflection,} \\ w'(\alpha-) &= w'(\alpha+), && \text{continuity in the bending angle,} \\ B(\alpha-)w''(\alpha-) &= B(\alpha+)w''(\alpha+), && \text{continuity of the bending moment,} \\ (B(\alpha-)w''(\alpha-))' &= (B(\alpha+)w''(\alpha+))', && \text{continuity of the shear.} \end{aligned} \tag{1.4}$$

Here the right-handed and left-handed limits of a given function g at the interface are defined as follows:

$$\begin{aligned} g(\alpha-) &\equiv \lim_{x \to \alpha-} g(x), \\ g(\alpha+) &\equiv \lim_{x \to \alpha+} g(x). \end{aligned}$$

The so called interface problem is to solve for $w(x)$ from (1.1), (1.2) and (1.4), which arises from a well known application: namely, the Euler-Bernoulli beam. We will give a derivation of the differential equation for Euler-Bernoulli beam with its physical meaning in the Chapter 2.

A typical forward problem associated with (1.1) is:

Problem(**F**): Given the coefficient B and the forcing function f, together with the boundary conditions (1.2) and the interface condition (1.4), determine w.

On the other hand, the inverse problem associated with (1.1) considered in this thesis is:

Problem(**I**): Determine the interface location α based upon some expectation about the solution w to the forward problem. Specifically, we will consider the problem of determining α assuming that $B(1)w''(1) = \gamma$ is given.

The purpose of this thesis, in particular, is to develop an immersed finite element (IFE) space that can be used together with a mesh independent of the interface to efficiently solve the inverse interface problems associated with (1.1). However, before we go on to develop this IFE space, we first look at an application involving interface.

Suppose we want to construct a composite beam formed by two shorter beams, each of which is made from a different material. For simplicity, let us assume that the length of the shorter beams are over the domain Ω_1 and Ω_2, and the joint point is α, so that the length of the composite beam is over the domain $\Omega = \Omega_1 \cup \{\alpha\} \cup \Omega_2 = (0, 1)$. In addition, we assume that the Young's Modulus, E, and the moment of inertia, I, in each shorter beam is given such that $B_1 = E_1 I_1$ and $B_2 = E_2 I_2$ corresponding to each of the shorter beam remains as a constant. Moreover, the bending moment at right end of the composite beam is required to be equal to or as close to a given amount, say γ (foot·lbs or Newton·meters), as possible. In addition, the two shorter beams are to be connected at the interface α with the rigid connection conditions defined in (1.4). With these criteria enforced, the remaining variable that would give a variation to the bending moment at the right end of the beam is the joining position α.

Here, we let $w(\eta, \alpha)$ be the deformation of the beam at the location η, and the parameter α is the position of the interface. Then the bending moment of the beam is given by $B(\eta)w''(\eta, \alpha)$. Let $g(\alpha) = B(1)w''(1, \alpha)$. Then, we can see that different α values will result in different bending moment responses at $\eta = 1$.

Since the position of the joint is the only variable remaining that would give a variation of the bending moment at the right end, the above beam design problem leads to the following inverse problem of the beam equation:

Inverse Problem: find all $\alpha^* \in \Omega$ such that

$$g(\alpha^*) = \gamma, \tag{1.5}$$

for a prescribed bending moment requirement γ, if possible; otherwise, find α^* such that

$$|g(\alpha^*) - \gamma|^2 \leq |g(\alpha) - \gamma|^2, \qquad \forall \alpha \in \Omega. \tag{1.6}$$

Now, we discuss in general how to solve this inverse problem. First, let us assume that the condition (1.5) holds. We note that the curve of $g(\alpha)$ for $\alpha \in \Omega$ may meet the line $y = \gamma$ at multiple points, and each of these points is a solution to the inverse problem. Hence, we need to develop a procedure that can determine these locations. Since the condition (1.5) holds, we know that

$$\gamma \in [\min_{\alpha \in \Omega} g(\alpha), \max_{\alpha \in \Omega} g(\alpha)]. \tag{1.7}$$

Without lost of generality, let us assume that $g(\kappa_1)$ gives the $\max(g(\alpha))$ and $g(\kappa_2)$ gives the $\min(g(\alpha))$ where $\kappa_1 \leq \kappa_2$ and $\kappa_1, \kappa_2 \in \Omega$. To find a solution of the inverse problem, let us first define a function J such that $J : \overline{\Omega} \to \mathbf{R}$ as follows:

$$J(x) = g(x) - \gamma.$$

Thus, from the assumption that g is a continuous function, we have J being a continuous function. Then by the intermediate value theorem, we know that J has at least one root in the interval $[\kappa_1, \kappa_2]$; moreover, roots of J are solutions to (1.5). To find a root of J, we can apply an iterative method such as the bisection method on J with the initial interval of $[\kappa_1, \kappa_2]$. Note: a root of J is guaranteed to be found when using the bisection method with the starting interval $[\kappa_1, \kappa_2]$. Thus, a solution to (1.5) can be obtained.

However, if we want to find all of the solutions to (1.5), besides using the assumption in (1.7), we will make an additional assumption: g has a finite number of local extremes. So let us suppose that these two assumptions hold; we now want to determine all the solutions to the inverse problem.

Since g maps from $\overline{\Omega}$ to $\mathbf{R}$, from calculus, we know that the function g changes from increasing to decreasing or went from decreasing to increasing at local extremes. So we will first sample g at a partition $p = \{0, h, 2h, \ldots, nh = 1\}$, where h is the step size. Now, let us define a function H as follows:

$$H(i) = (g(i * h) - g((i-1)h))\,(g((i+1)h) - g(i * h)) \text{ for } i = 1, 2, \ldots, n-1.$$

Then if $H(i) \leq 0$, we know that there exists a local extremum in the interval $[(i+1)h, (i-1)h]$. However, depending on the partition p, the condition $H(i) > 0$ does not guarantee that there

are no local extrema in the interval $[(i+1)h, (i-1)h]$.

After we obtain the intervals that contain the local extremes of $g(\alpha)$, we can take these intervals and apply the golden section (golden ratio) search algorithm [15, 19] to locate the positions of local maxima or local minima of $g(\alpha)$ in these intervals. In general, the golden search algorithm find the positions such that the absolute minimum occurs in the giving interval; however, the algorithm can be easily modified to find the local maximum or local minimum upon the user input. With the assumption that we have found all the positions in Ω that give local extremes of g, we then add the boundary of Ω to have a complete list of local extreme locations.

Now suppose E is an ordered set that contains all the local extremes of $g(\alpha)$ as follows:

$$E = \{0 = x_1, x_2, x_3, \ldots, x_m = 1\}.$$

First, we calculate $g(x_i)$ for $x = 1, 2, 3 \ldots, m$. If $g(x_i) = \gamma$, then x_i is a solution to our inverse problem. Then we check whether $g(x_i) < \gamma < g(x_{i+1})$ for $i = 1$ to $m - 1$. If $g(x_i) < \gamma < g(x_{i+1})$ for some i, we can look for the zero ξ of $J(x)$ in the interval (x_i, x_{i+1}), and this ξ is a solution to the inverse problem. There are many ways to find the zero of J over an interval; however, we will only discuss the uses of the bisection method and the secant method and compare the differences between these two methods because they do not require a complicated differentiation procedure on $g(\alpha)$.

Now let us suppose that there is no α^* such that α^* satisfies the equation (1.5). We then have to find α^* such that α^* satisfies the condition in (1.6). Thus our problem is now to minimize the difference between $g(x)$ and γ. To solve this problem, we simply find the absolute maximum or absolute minimum of g and compare it to γ. If γ is greater than absolute maximum of g, we will let α^* be the position such that $g(\alpha^*)$ gives the absolute maximum of g; otherwise we will let α^* be the position such that $g(\alpha^*)$ gives the absolute minimum of g. Thus α^* solves the inverse problem.

Therefore, our inverse problem can be solved when the function g is continuous and g contains finitely many local extremes.

We notice that the above procedure to solve the inverse problem requires to solve the forward problem for each evaluation of g. In addition, we know that in order to use the standard Galerkin finite element method to solve boundary value problems with discontinuities efficiently, it is necessary to make the partition of Ω be such that the point of discontinuity is one of the nodes in this partition [13]. Therefore, each evaluation of g requires a different partition, and this takes time to generate the partition, and as the dimension of Ω increases, the time needed to generate the partition is then increased dramatically.

The recently developed immersed finite element (IFE) methods can solve boundary value

problems with a partition independent of the discontinuity of the coefficients in the differential equations [3, 4, 13]. The two fundamental ideas of an IFE method are:

- The partition used can be independent of the discontinuity. If necessary, a uniform partition can be used.
- The basis functions of the IFE method are formed according to interface jump conditions.

Thus, the immersed finite element idea is desirable for solving the inverse problem for identifying the interfaces. The objective of this thesis is to develop an immersed finite element space for solving the forward problem and inverse problem in multiple material beam design.

The remainder of this thesis is divided into five chapters. Chapter 2 gives a derivation of the Euler-Bernoulli beam equation and the weak form for the differential equation (1.1) with boundary conditions (1.2). In Chapter 3, we review a well known finite element space: namely, Hermite cubic FE space. In Chapter 4, we will construct an IFE space which we call immersed Hermite cubic IFE space and discuss some of its properties. Furthermore, we will investigate its accuracy and approximation capabilities on forward interface problems. Chapter 5 gives an example of solving an inverse interface problem with the immersed Hermite cubic IFE space developed in Chapter 4. Finally, in Chapter 6 we will look at a class of time-dependent beam problems and solve it with immersed Hermite cubic IFE space. In addition, we will discuss the approximation capabilities of the immersed Hermite cubic IFE space on this time-dependent beam problem.

Chapter 2

The Euler-Bernoulli Beam Equation

In this section we will briefly discuss the models of the Euler-Bernoulli beam in both its static state and time-dependent state. For the static state we have

$$\frac{d^2}{dx^2}\left[EI\frac{d^2w(x)}{dx^2}\right] = p(x), \tag{2.1}$$

and for time-dependent state we have

$$\frac{d^2}{dx^2}\left[EI\frac{d^2w(x,t)}{dx^2}\right] + \rho(x)\frac{d^2w(x,t)}{dt^2} = p(x,t). \tag{2.2}$$

We will explain the meaning of these beam equations and show how the static Euler-Bernoulli beam equation can be derived from the theories of kinematics, constitutive, force resultant, and equilibrium. Then we will show how can we derive the time-dependent Euler-Bernoulli beam equation from a variational point of view.

2.1 The static Euler-Bernoulli beam equation and its weak form

In this section we will derive the static Euler-Bernoulli beam equation:

$$\frac{d^2}{dx^2}\left[EI\frac{d^2w(x)}{dx^2}\right] = p(x),$$

from the theories of kinematics, constitutive, force resultant, and equilibrium. Further, we will give a derivation of the weak form for this beam equation.

2.1.1 Theory of kinematics

Kinematics describes the way in which a beam deflects. First, let us consider a beam on the standard $x - y - z$ coordinate system, where the length is along the x direction, the height of the beam is along the y direction, and the width of the beam is along the z direction. For convenience, let us set the neutral plane of the beam on the plane $y = 0$. We define the neutral plane to be the plane such that the center of deflection of the beam lies on it when the beam is not deflected. (Note: the neutral plane changes as beam is deflected, and it is perpendicular to the cross section of the beam.) Now, we will consider the Kirchhoff Assumptions, [7], on the Euler-Bernoulli beam equation:

1. Normals remains straight (they do not bend).
2. Normals remain unstretched (they keep the same length).
3. Normals remain normal (they always make a right angle to the neutral plane).

The normals are defined to be lines along the cross section of the beam in the $y - z$ plane when the beam is in its neutral position, i.e, the beam is in the straight position with no deflection. Let us consider θ to be the angle formed from the beam's neutral position with the $x - z$ plane, with $\theta < 0$ if the neutral plane lies below the $x - z$ plane in the positive x direction. The beam is then deformed, and according to Kirchhoff's Assumptions, we know that the degree banked on the cross section is the same as θ. Let us define the function $w(x, y)$ to be the displacement in the x-direction such that the line alone $w(x, y)$ is perpendicular to the banked cross section of the beam; in addition, $w(x, y)$ is defined to be the displacement between the banked cross section of the beam and the neutral cross section of the beam. Let us consider y to be the displacement from the neutral plane to any point in the beam along the y direction. Since the normals remain straight and unstretched, we can assume that there is negligible strain in the cross section of the beam. Here, both the deformed state and the undeformed state of the beam are shown in Figure 2.1. Now we can write $w(x, y)$ as follows:

$$w(x, y) = \chi(x) \cdot y$$

where

$$\chi(x) = \sin(-\theta), \text{ where } \theta \text{ varies with } x.$$

The strain, ε, describes the resulting deformation, so we can write

$$\varepsilon = \frac{dw}{dx}.$$

Then it follows that

$$\varepsilon(x, y) = \frac{d\chi}{dx} \cdot y.$$

Finally, with normals always normal, we can tie the cross section rotation χ to the neutral plane rotation θ, and eventually to the beam's displacement w [18],

$$\chi = -\theta = -\frac{dw}{dx}. \tag{2.3}$$

Thus, we have

$$\frac{d\chi}{dx} = -\frac{d^2w}{dx^2}. \tag{2.4}$$

2.1.2 Theory of constitutive

The theory of constitutive describes how the direct stress, σ, relates to the direct strain, ε. Here, we use Hooke's law [10] to describe this relationship, i.e.,

$$\frac{\text{Stress}}{\text{Strain}} = \text{Elastic modulus.}$$

So in beam theory, it becomes:

$$\frac{\sigma(x,y)}{\varepsilon(x,y)} = E, \text{ or } \sigma(x,y) = E \cdot \varepsilon(x,y),$$

with E being Young's Modulus.

2.1.3 Theory of resultants

In this subsection, we will talk about how the stresses in a beam are being tracked.

Let us consider the cross section of a beam. There exists a distribution of direct stresses, $\sigma(y)$, and shear stresses, $\sigma_{xy}(y)$ at this cross section. Now we will show how force resultants are generated by these stresses.

Each differential portion of direct stress acting on the cross section creates a corresponding moment about the neutral plane; and the sum of these individual moments over the area of the cross-section can be written as

$$\int\int y \cdot \sigma(x,y)\ dydz.$$

But this is just the definition of the moment resultants [7], M. Thus, we have

$$M(x) = \int\int y \cdot \sigma(x,y) dydz$$

Similarly, the sum of the shear stresses on the cross-section can be written as

$$\int\int \sigma_{xy}(x,y)\cdot dydz$$

But this is just the definition of the shear resultants, V. Thus we have

$$V(x) = \int\int \sigma_{xy}(x,y)dydz.$$

Finally, the force resultant is the integral of direct stresses over the cross-sectional area. This resultant, N, is then given by

$$N(x) = \int\int \sigma(x,y)dydz.$$

So, $N(x)$ is the total direct force within the beam at some point x. However, $N(x)$ does not play a role in the derivation of the Euler-Bernoulli beam equation since it does not cause displacement in w.

2.1.4 Theory of equilibrium

Finally, we will discuss the theory of equilibrium. Suppose we cut out a small section of the beam, i.e, a small variation, dx, in length; then we can find the shear resultant, V, acting in the $-y$ direction on the left side of the beam. Similarly, we can find $V + \frac{dV}{dx}dx$ shear resultants on the right side of the beam. Also, we have the loading force, pdx, acting in the $+y$ direction. Now, in order to achieve a static state in the beam, the sum of these forces must be zero [11]. Thus, we have

$$-V + (V + \frac{dV}{dx}dx) + pdx = 0,$$

or

$$\frac{dV}{dx} = -p.$$

The other requirement for the beam to be in a static state is that the moments must be balanced. Let us consider the moment equilibrium about a point on the right side of the beam. Then then we have moments M on the left side of the beam with counter-clockwise direction, and $(M + \frac{dM}{dx}dx)$ on the right side of the beam with clockwise direction. Also, we have $V\frac{dx}{2}$ on the left side of the beam with counter-clockwise direction and $(V + \frac{dV}{dx}dx)\frac{dx}{2}$ on the right side of the beam with clockwise direction. Then with the sum of the moments equal to zero, we get

$$M - (M + \frac{dM}{dx}dx) + V\frac{dx}{2} + (V + \frac{dV}{dx}dx)\frac{dx}{2} = 0.$$

then by neglecting differential quantities of second order, we can simplify the equation above as follows:

$$\frac{dM}{dx} = V.$$

Thus, from the theory of equilibrium, we have derived the relation between load, shear, and bending moment as $\frac{dV}{dx} = -p$ and $\frac{dM}{dx} = V$ [16].

2.1.5 The Euler-Bernoulli beam equation in the static state

Now we are ready to construct the Euler-Bernoulli beam equation [7, 8, 11, 17, 18], i.e.,

$$\frac{d^2}{dx^2}\left[EI\frac{d^2w}{dx^2}\right] = p,$$

where p is the is the distributed loading force acting on the $+y$ direction, E is the Young's Modulus, I is the moment of inertia, and w is the deformation of the beam.

From the theory of equilibrium, we have

$$\frac{dM}{dx} = V, \text{ and } \frac{dV}{dx} = -p.$$

Then by taking derivatives on $\frac{dM}{dx} = V$, we have

$$\frac{d^2M}{dx^2} = -p.$$

Next, by replacing the moment resultant, M, with its definition in terms of direct stress, σ, we get

$$\frac{d^2}{dx^2}\left(\int\int y \cdot \sigma \cdot dy \cdot dz\right) = -p.$$

And from theory of constitutive, we know $\sigma(x, y) = E\varepsilon(x, y)$. Then by replacing $\sigma(x, y)$ with $E\varepsilon(x, y)$, we get

$$\frac{d^2}{dx^2}E\left(\int\int y \cdot \varepsilon(x, y) \cdot dy \cdot dz\right) = -p.$$

But from the theory of kinematics, we know $\varepsilon(x, y) = \frac{d\chi}{dx} \cdot y$ and $\frac{d\chi}{dx} = \frac{-d^2w}{dx^2}$. So we can replace ε with $\frac{d\chi}{dx} \cdot y$ and get

$$\frac{d^2}{dx^2}E\frac{d\chi}{dx}\left(\int\int y^2 \cdot dy \cdot dz\right) = -p.$$

Now by replacing $\frac{d\chi}{dx}$ with $\frac{-d^2w}{dx^2}$, we get

$$\frac{d^2}{dx^2}E\frac{-d^2w}{dx^2}\left(\int\int y^2 \cdot dy \cdot dz\right) = -p.$$

But

$$I = \int\int y^2 \cdot dy \cdot dz,$$

is defined as the moment of inertia, [18]. Therefore, we can finally arrive at the Euler-Bernoulli beam equation,

$$\frac{d^2}{dx^2}\left[EI(x)\frac{d^2w(x)}{dx^2}\right] = p(x), \tag{2.5}$$

or

$$(B(x)u''(x))'' = f(x)$$

where $B(x) = EI(x)$ and $f(x) = p(x)$ at cross section x.

Note here, possible boundary conditions for solving Euler-Bernoulli beam equation can be found in [8] as in two sets of possibility as follows:

Boundary Conditions

$$\begin{aligned} w'''(0) = 0 \quad &\text{or} \quad w(0) = 0, \\ w''(0) = 0 \quad &\text{or} \quad w'(0) = 0, \end{aligned}$$

and

$$\begin{aligned} w'''(L) = 0 \quad &\text{or} \quad w(L) = 0, \\ w''(L) = 0 \quad &\text{or} \quad w'(L) = 0. \end{aligned}$$

The physical description of these boundary conditions are shown in the Figure 2.2.

2.1.6 Weak form of the static Euler-Bernoulli beam equation

By combining the static Euler-Bernoulli equation or (1.1), and the boundary conditions (1.2), we get a boundary value problem as follows:

$$(B(x)w''(x))'' = f(x), x \in \Omega = (0,1), \tag{2.6}$$

$$w(0) = b_1, w'(0) = b_2, w(1) = b_3, w'(1) = b_4. \tag{2.7}$$

Now we will derive the weak form for this boundary value problem.

First, by formally multiplying the test function $v(x)$ on (2.6) and integrating from 0 to 1, we obtain the following equation:

$$\int_0^1 v(x)(B(x)w''(x))''dx = \int_0^1 v(x)f(x)dx. \tag{2.8}$$

Since $B(x)$ is discontinuous at the interface α, we will write (2.8) as follows:

$$\int_0^\alpha v(x)(B(x)w''(x))''dx + \int_\alpha^1 v(x)(B(x)w''(x))''dx = \int_0^1 v(x)f(x)dx. \tag{2.9}$$

Then using integration by parts on $\int_0^\alpha v(x)(B(x)w''(x))''dx$ and $\int_0^\alpha v(x)(B(x)w''(x))''dx$, equation (2.9) becomes

$$\begin{aligned} v(x)(B(x)w''(x))'|_0^\alpha &- \int_0^\alpha v'(x)(B(x)w''(x))'dx \\ +v(x)(B(x)w''(x))'|_\alpha^1 &- \int_\alpha^1 v'(x)(B(x)w''(x))'dx \\ &= \int_0^1 v(x)f(x)dx, \end{aligned}$$

or

$$\begin{aligned} v(\alpha-)(B(\alpha-)w''(\alpha-))' - v(0)(B(0)w''(0))' &- \int_0^\alpha v'(x)(B(x)w''(x))'dx \\ +v(1)(B(1)w''(1))' - v(\alpha+)(B(\alpha+)w''(\alpha+))' &- \int_\alpha^1 v'(x)(B(x)w''(x))'dx \\ &= \int_0^1 v(x)f(x)dx. \end{aligned} \tag{2.10}$$

By choosing a function v such that $v(0) = v(1) = 0$ and $v(\alpha-) = v(\alpha+)$, the equation (2.10) becomes

$$-\int_0^\alpha v'(x)(B(x)w''(x))'dx - \int_\alpha^1 v'(x)(B(x)w''(x))'dx = \int_0^1 v(x)f(x)dx,$$

Now using integration by parts again on $-\int_0^\alpha v'(x)(B(x)w''(x))'dx$ and $-\int_\alpha^1 v'(x)(B(x)w''(x))'dx$ results in:

$$\begin{aligned} -v'(x)B(x)w''(x)|_0^\alpha &+ \int_0^\alpha v''(x)(B(x)w''(x))dx \\ -v'(x)B(x)w''(x)|_\alpha^1 &+ \int_\alpha^1 v''(x)(B(x)w''(x))dx \\ &= \int_0^1 v(x)f(x)dx. \end{aligned} \tag{2.11}$$

Choosing $v'(0) = v'(1) = 0$ and $v'(\alpha-) = v'(\alpha+)$, the equation (2.11) becomes

$$\int_0^\alpha v''(x)B(x)w''(x)dx + \int_\alpha^1 v''(x)B(x)w''(x)dx = \int_0^1 v(x)f(x)dx.$$

Thus the weak form for this boundary value problem is:

Find

$$w \in S = \{w | w \in H^2(\Omega), w(0) = b_1, w'(0) = b_2, w(1) = b_3, w'(1) = b_4\}$$

such that

$$\int_0^1 v''(x)B(x)w''(x)dx = \int_0^1 v(x)f(x)dx, \tag{2.12}$$

for any

$$v \in T = H_0^2(\Omega).$$

Here, we call S the solution set for the weak form, and T the test function space. Also, $H^n(\Omega)$ is defined as [13]:

$$H^n(\Omega) = \left\{ g | \int_\Omega \left(g^{(k)}(x) \right)^2 dx < \infty, k = 0, 1, \cdots, n \right\},$$

and H_0^n is a subspace of H^n whose elements have 0 derivatives at boundary up $(n-1)$-th order.

2.2 The time-dependent Euler-Bernoulli beam equation and its weak form

In this section we will give a derivation of the Timoshenko beam and show how the time-dependent Euler-Bernoulli beam can be derive from the Timoshenko beam. However, before we proceed to the derivation, we will first examine *D'Alembert's principle*, then we will use D'Alembert's principle in the derivation of *Hamilton's principle*. Finally, we will use Hamilton's principle in the derivation of the Euler-Bernoulli beam equation. After we have derived these beam equations, we will then give a derivation of the weak form for the Euler-Bernoulli beam in the time-dependent state. This weak form will later be used in this thesis to assemble the finite element solution to the initial-boundary value problem which is created in later chapters for the investigation of the order of accuracy of the developed IFE space.

2.2.1 D'Alembert's principle

D'Alembert extended the applicability of the principle of virtual work to dynamic problems. Let us first recall Newton's law of motion [10]:

$$\mathbf{F} = m\mathbf{a}$$

where $\mathbf{F}$ is the force applied on a particle with mass m and $\mathbf{a}$ is the acceleration of the particle due to the force $\mathbf{F}$. Newton's law can be rewritten as d'Alembert's principle in the following form for N particles [2],

$$\mathbf{F}_i + \mathbf{f}_i - m_i\ddot{\mathbf{r}}_i = 0, \qquad i = 1, 2, \ldots, N, \tag{2.13}$$

where $\mathbf{F}_i$ represents the external forces on the system, $\mathbf{f}_i$ represents the constraint forces on the system, and the term $-m_i\ddot{\mathbf{r}}_i$ may be considered to be an *inertia force*. Note that each of the forces in the equation (2.13) may be a constant or a function of time; also $\dot{\mathbf{r}}$ denotes $\frac{d\mathbf{r}}{dt}$ and $\ddot{\mathbf{r}}$ denotes $\frac{d^2\mathbf{r}}{dt^2}$. The virtual work for the ith particle is

$$(\mathbf{F}_i + \mathbf{f}_i - m_i\ddot{\mathbf{r}}_i) \cdot \delta\mathbf{r}_i = 0,$$

where the virtual displacements $\delta\mathbf{r}_i$ are compatible with the constraints. If we assume that virtual work due to constraint forces is zero, then the virtual work for the system becomes

$$\sum_{i=1}^{N} (\mathbf{F}_i - m_i\ddot{\mathbf{r}}_i) \cdot \delta\mathbf{r}_i = 0. \tag{2.14}$$

The equation (2.14) above is called the *generalized principle of d'Alembert* [2].

2.2.2 Hamilton's principle

In this subsection, we will give a derivation of Hamilton's principle [2]. First, let us consider the following relation:

$$\frac{d}{dt}(\dot{\mathbf{r}}_i \cdot \delta\mathbf{r}_i) = \ddot{\mathbf{r}}_i \cdot \delta\mathbf{r}_i + \dot{\mathbf{r}}_i \cdot \delta\dot{\mathbf{r}}_i = \ddot{\mathbf{r}}_j \cdot \delta\mathbf{r}_i + \delta(\frac{1}{2}\dot{\mathbf{r}}_i \cdot \dot{\mathbf{r}}_i).$$

We can rewrite $\sum_{i=1}^{N} m_i\ddot{\mathbf{r}}_i \cdot \delta\mathbf{r_i}$ as

$$\begin{aligned} \sum_{i=1}^{N} m_i\ddot{\mathbf{r}}_i \cdot \delta\mathbf{r}_i &= \sum_{i=1}^{N} m_i\frac{d}{dt}(\dot{\mathbf{r}}_i \cdot \delta r_i) - \delta\sum_{i=1}^{N} m_i(\dot{\mathbf{r}}_i \cdot \dot{r}_i) \\ &= \sum_{i=1}^{N} m_i\frac{d}{dt}(\dot{\mathbf{r}}_i \cdot \delta\mathbf{r}_i) - \delta T, \end{aligned} \tag{2.15}$$

where T is the kinetic energy defined as follows:

$$T = \frac{1}{2}\sum_{i=1}^{N} m_i\dot{\mathbf{r}}_i \cdot \dot{\mathbf{r}}_i.$$

Also, we know the work W is defined as

$$W = \mathbf{F} \cdot \mathbf{r},$$

[10], so it follows that

$$\delta W = \sum_{i=1}^{N} \mathbf{F}_i \cdot \delta \mathbf{r}_j,$$

[2]. Now, using d'Alembert's principle from the equation (2.14):

$$\sum_{i=1}^{N} (\mathbf{F}_i - m_i \ddot{\mathbf{r}}_i) \cdot \delta \mathbf{r}_i = 0,$$

we can substitute the equation (2.15) and $\delta W = \sum_{i=1}^{N} F_i \cdot \delta \mathbf{r}_j$ into d'Alembert's principle, giving

$$\delta T + \delta W = \sum_{i=1}^{N} m_i \frac{d}{dt}(\dot{\mathbf{r}}_i \cdot \delta \mathbf{r}_i).$$

Now let us consider a varied path, as shown in Figure 2.3, where the paths coincide at the initial and final times (t_1 and t_2), and let us integrate from t_1 to t_2 to get

$$\begin{aligned}
\int_{t_1}^{t_2} (\delta T + \delta W)\, dt &= \int_{t_1}^{t_2} \sum_{i=1}^{N} m_i \frac{d}{dt}(\dot{\mathbf{r}}_i \cdot \delta \mathbf{r}_i) dt \\
&= \sum_{i=1}^{N} \int_{t_1}^{t_2} m_i \frac{d}{dt}(\dot{\mathbf{r}}_i \cdot \delta \mathbf{r}_i) dt \\
&= \sum_{i=1}^{N} m_i \dot{\mathbf{r}}_i \cdot \delta \mathbf{r}_i |_{t_1}^{t_2} \\
&= 0.
\end{aligned}$$

Note: $\delta \mathbf{r}_i = 0$ at t_1 and t_2. Therefore,

$$\int_{t_1}^{t_2} (\delta T + \delta W)\, dt = 0.$$

The equation above is called *the extended Hamilton's principle* [2]. Here, δW includes both conservative and non-conservative work.

2.2.3 The Timoshenko beam and the time-dependent Euler-Bernoulli beam

In this section we will give a derivation of the equation governing the transverse vibration of a beam of length L, with the following properties at section x: $m(x)$ is the mass per unit length, $A(x)$ is the cross-section area of the beam, E is the Young's Modulus, and $I(x)$ is the moment of inertia. We assume small deflections $y(x,t)$ and rotations $\partial y/\partial x$, and include

the bending $M(x,t)$ and shear $Q(x,t)$ effects.

Now let us consider a free body of a section of length dx as shown in Figure 2.4. Its slope due to a bending component ψ, and a shear distortion component α is as follows:

$$\frac{\partial y}{\partial x} = \psi(x,t) + \alpha(x,t). \tag{2.16}$$

The bending moment is defined as [2]:

$$\frac{M}{EI} = \frac{y''}{[1+(y')^2]^{3/2}}.$$

However, for small displacements and slopes, y' is very small compared to 1 and can be ignored. Now we consider the bending moment as:

$$\frac{M}{EI} = y'',$$

and the bending moment can be related to the slope by

$$M = EI\frac{\partial \psi}{\partial x}.$$

The shear is related to the slope by

$$Q = s\alpha A(x)G,$$

from elementary beam theory, where s is a number that depends on the shape of the cross-section, and G is the constant shear modulus of the material [2]. From equation (2.16), we can rewrite Q as

$$Q = s\left(\frac{\partial y}{\partial x} - \psi\right)A(x)G.$$

Now, we will use Hamilton's principle, $\int_{t_1}^{t_2}(\delta T + \delta W)dt = 0$, to derive the boundary value problem and proceed to derive the kinetic and potential energies, and their variations. The kinetic energy due to translation and rotation for the whole beam is given by [2]

$$T(t) = \frac{1}{2}\int_0^L m(x)\left[\frac{\partial y}{\partial t}\right]^2 dx + \frac{1}{2}\int_0^L J(x)\left[\frac{\partial \psi}{\partial t}\right]^2 dx, \tag{2.17}$$

where

$$J(x) = \rho(x)I(x) = \frac{m(x)}{A(x)}I(x) = k(x)^2 m(x).$$

$J(x)$ is the mass moment of inertia per unit length, $\rho(x)$ is the density of the material at the cross section, and $k(x)$ is the radius of gyration; here $J(x)$ and $k(x)$ are about the neutral bending axis. Now let us define

$$F_T(\lambda) = \frac{1}{2}\int_0^L m(x)\left[\frac{\partial\left(y+\lambda\delta_y\right)}{\partial t}\right]^2 dx + \frac{1}{2}\int_0^L J(x)\left[\frac{\partial\left(\psi+\lambda\delta_\psi\right)}{\partial t}\right]^2 dx.$$

Then we have

$$\begin{aligned} F_T'(\lambda)|_{\lambda=0} &= \left(\int_0^L m(x)\left[\frac{\partial\left(y+\lambda\delta_y\right)}{\partial t}\right]\frac{\partial\delta_y}{\partial t}dx + \int_0^L J(x)\left[\frac{\partial\left(\psi+\lambda\delta_\psi\right)}{\partial t}\right]\frac{\partial\delta_\psi}{\partial t}dx\right)\Bigg|_{\lambda=0} \\ &= \int_0^L m(x)\frac{\partial y}{\partial t}\frac{\partial\delta_y}{\partial t}dx + \int_0^L J(x)\frac{\partial\psi}{\partial t}\frac{\partial\delta_\psi}{\partial t}dx \\ &= \delta T(t). \end{aligned}$$

Thus, we have the variation in kinetic energy δT as follows:

$$\delta T(t) = \int_0^L m(x)\frac{\partial y}{\partial t}\frac{\partial\delta_y}{\partial t}dx + \int_0^L J(x)\frac{\partial\psi}{\partial t}\frac{\partial\delta_\psi}{\partial t}dx. \tag{2.18}$$

Before proceeding with the variation of the work done on the structure, δW, we partition the work into a *conservative* (δW_c) part that is equal to the change in potential and strain energy, and a *non-conservative* (δW_{nc}) part that includes the work done by external forces $p(x,t)$,

$$\begin{aligned} \delta W(t) &= \delta W_c(t) + \delta W_{nc}(t) \\ &= -\delta V(t) + \int_0^L p(x,t)\delta_y(x,t)dx. \end{aligned} \tag{2.19}$$

The change in potential energy equals the work done by the conservative actions due to the moment and the shear force [2],

$$\begin{aligned} V(t) &= \frac{1}{2}\int_0^L M(x,t)\frac{\partial\psi}{\partial x}dx + \frac{1}{2}\int_0^L Q(x,t)\alpha dx \\ &= \frac{1}{2}\int_0^L EI(x)\left(\frac{\partial\psi}{\partial x}\right)^2 dx + \frac{1}{2}\int_0^L s\alpha^2 A(x)Gdx. \end{aligned}$$

By letting

$$F_V(\lambda) = \frac{1}{2}\int_0^L EI(x)\left(\frac{\partial\left(\psi+\lambda\delta_\psi\right)}{\partial x}\right)^2 dx + \frac{1}{2}\int_0^L sA(x)G\left(\alpha+\lambda\delta_\alpha\right)^2 dx,$$

we have

$$\begin{aligned} F_V'(\lambda)|_{\lambda=0} &= \left(\int_0^L EI(x)\left(\frac{\partial\left(\psi+\lambda\delta_\psi\right)}{\partial x}\right)\frac{\partial\delta_\psi}{\partial x}dx + \int_0^L sA(x)G\left(\alpha+\lambda\delta_\alpha\right)\delta_\alpha dx\right)\Bigg|_{\lambda=0} \\ &= \int_0^L EI(x)\left(\frac{\partial\psi}{\partial x}\right)\frac{\partial\delta_\psi}{\partial x}dx + \int_0^L sA(x)G\alpha\delta_\alpha dx \\ &= \delta V(t). \end{aligned}$$

Therefore, we have the variation $\delta V(t)$ as follows:

$$\delta V(t) = \int_0^L EI(x)\left(\frac{\partial \psi}{\partial x}\right)\frac{\partial \delta_\psi}{\partial x}dx + \int_0^L sA(x)G\alpha\delta_\alpha dx.$$

Now by applying Hamilton's variational principle on equations (2.18) and (2.19), we get

$$\begin{aligned}\int_{t_1}^{t_2}\Bigg\{&\left[\int_0^L m(x)\frac{\partial y}{\partial t}\left(\frac{\partial \delta_y}{\partial t}\right)dx + \int_0^L k(x)^2 m(x)\frac{\partial \psi}{\partial t}\left(\frac{\partial \delta_\psi}{\partial t}\right)dx\right] \\ &-\left[\int_0^L EI(x)\frac{\partial \psi}{\partial x}\left(\frac{\partial \delta_\psi}{\partial x}\right)dx + \int_0^L sA(x)G\alpha\delta_\alpha dx\right] + \int_0^L p(x,t)\delta_y(x,t)dx\Bigg\}dt = 0.\end{aligned} \tag{2.20}$$

However, recalling the equation (2.16), we have $\alpha = \frac{\partial y}{\partial x} - \psi(x,t)$. Thus, we can rewrite equation (2.20) as follows:

$$\begin{aligned}\int_{t_1}^{t_2}\Bigg\{&\left[\int_0^L m(x)\frac{\partial y}{\partial t}\left(\frac{\partial \delta_y}{\partial t}\right)dx + \int_0^L k(x)^2 m(x)\frac{\partial \psi}{\partial t}\left(\frac{\partial \delta_\psi}{\partial t}\right)dx\right] \\ &-\left[\int_0^L EI(x)\frac{\partial \psi}{\partial x}\left(\frac{\partial \delta_\psi}{\partial x}\right)dx + \int_0^L sA(x)G\left(\frac{\partial y}{\partial x} - \psi(x,t)\right)\left(\frac{\partial \delta_y}{\partial x} - \delta_\psi(x,t)\right)dx\right] \\ &+\int_0^L p(x,t)\delta_y(x,t)dx\Bigg\}dt = 0.\end{aligned} \tag{2.21}$$

Now we apply integration by parts on

$$\int_{t_1}^{t_2}\int_0^L m(x)\frac{\partial y}{\partial t}\left(\frac{\partial \delta_y}{\partial t}\right)dxdt$$

to get

$$\int_{t_1}^{t_2}\int_0^L m(x)\frac{\partial y}{\partial t}\left(\frac{\partial \delta_y}{\partial t}\right)dx = \int_0^L m(x)\frac{\partial y}{\partial t}\delta_y\Big|_{t_1}^{t_2}dx - \int_{t_1}^{t_2}\int_0^L m(x)\frac{\partial^2 y}{\partial t^2}\delta_y dxdt.$$

Similarly, integration by parts on

$$\int_{t_1}^{t_2}\int_0^L k(x)^2 m(x)\frac{\partial \psi}{\partial t}\left(\frac{\partial \delta_\psi}{\partial t}\right)dxdt$$

give us

$$\int_{t_1}^{t_2}\int_0^L k(x)^2 m(x)\frac{\partial \psi}{\partial t}\left(\frac{\partial \delta_\psi}{\partial t}\right)dx = \int_0^L k(x)^2 m(x)\left(\frac{\partial \psi}{\partial t}\right)\delta_\psi\Big|_{t_1}^{t_2}dx - \int_{t_1}^{t_2} k(x)^2 m(x)\left(\frac{\partial \psi}{\partial t}\right)^2\delta_\psi dxdt.$$

Also, by applying integration by parts on

$$\int_0^L EI(x)\frac{\partial \psi}{\partial x}\left(\frac{\partial \delta_\psi}{\partial x}\right)dx,$$

we get

$$\int_0^L EI(x)\frac{\partial\psi}{\partial x}\delta\left(\frac{\partial\psi}{\partial x}\right)dx \;=\; EI(x)\frac{\partial\psi}{\partial x}\delta_\psi\Big|_0^L - \int_0^L \frac{\partial}{\partial x}\left(EI(x)\frac{\partial\psi}{\partial x}\right)\delta_\psi dx.$$

Finally, we will simply the following:

$$\begin{aligned}
&\int_0^L sA(x)G\left(\frac{\partial y}{\partial x}-\psi\right)\left(\frac{\partial\delta_y}{\partial x}-\delta_\psi\right)dx\\
&\quad=\int_0^L sA(x)G\left(\frac{\partial y}{\partial x}-\psi\right)\frac{\partial\delta_y}{\partial x} - sA(x)G\left(\frac{\partial y}{\partial x}-\psi\right)\delta_\psi dx\\
&\quad=\int_0^L sA(x)G\left(\frac{\partial y}{\partial x}-\psi\right)\frac{\partial\delta_y}{\partial x}dx - \int_0^L sA(x)G\left(\frac{\partial y}{\partial x}-\psi\right)\delta_\psi dx\\
&\quad= sA(x)G\left(\frac{\partial y}{\partial x}-\psi\right)\delta_y\Big|_0^L - \int_0^L \frac{\partial\left(sA(x)G\left(\frac{\partial y}{\partial x}-\psi\right)\right)}{\partial x}\delta_y dx\\
&\qquad-\int_0^L sA(x)G\left(\frac{\partial y}{\partial x}-\psi\right)\delta_\psi dx.
\end{aligned}$$

Therefore, we can rewrite equation (2.21) as follows:

$$\begin{aligned}
\int_{t_1}^{t_2}\Bigg[\int_0^L &\left\{\frac{\partial}{\partial x}\left[sGA(x)\left(\frac{\partial y}{\partial x}-\psi\right)\right]-m(x)\frac{\partial^2 y}{\partial t^2}+p(x,t)\right\}\delta_y dx\\
&+\int_0^L\left\{\frac{\partial}{\partial x}\left(EI(x)\frac{\partial\psi}{\partial x}\right)+sGA(x)\left(\frac{\partial y}{\partial x}-\psi\right)-k(x)^2m(x)\frac{\partial^2\psi}{\partial t^2}\right\}\delta_\psi dx\\
&-\left(EI(x)\frac{\partial\psi}{\partial x}\right)\delta_\psi\Big|_0^L-\left[sGA(x)\left(\frac{\partial y}{\partial x}-\psi\right)\right]\delta_y\Big|_0^L\Bigg]dt=0. \qquad (2.22)
\end{aligned}$$

To proceed, we note that δ_ψ and δ_y are arbitrary and independent. We can let

$$\begin{aligned}
&\delta_\psi = 0 \text{ at } x=0, x=L\\
&\delta_y = 0 \text{ at } x=0, x=L.
\end{aligned}$$

Therefore, we can rewrite (2.22) as follows:

$$\begin{aligned}
\int_{t_1}^{t_2}\Bigg[\int_0^L &\left\{\frac{\partial}{\partial x}\left[sGA(x)\left(\frac{\partial y}{\partial x}-\psi\right)\right]-m(x)\frac{\partial^2 y}{\partial t^2}+p(x,t)\right\}\delta_y dx\\
&+\int_0^L\left\{\frac{\partial}{\partial x}\left(EI(x)\frac{\partial\psi}{\partial x}\right)+sGA(x)\left(\frac{\partial y}{\partial x}-\psi\right)-k(x)^2m(x)\frac{\partial^2\psi}{\partial t^2}\right\}\delta_\psi dx\Bigg]dt=0.
\end{aligned}$$

δ_ψ and δ_y are arbitrary for $0<x<L$. Thus we have the governing equations as follows:

$$\frac{\partial}{\partial x}\left[sGA(x)\left(\frac{\partial y}{\partial x}-\psi\right)\right]-m(x)\frac{\partial^2 y}{\partial t^2}+p(x,t)=0, \qquad (2.23)$$

and

$$\frac{\partial}{\partial x}\left(EI(x)\frac{\partial \psi}{\partial x}\right) + sGA(x)\left(\frac{\partial y}{\partial x} - \psi\right) - k(x)^2 m(x)\frac{\partial^2 \psi}{\partial t^2} = 0, \tag{2.24}$$

and the possible boundary conditions are given by

$$\left[EI(x)\frac{\partial \psi}{\partial x}\right]\delta_\psi\Big|_0^L = 0,$$

and

$$\left[sGA(x)\left(\frac{\partial y}{\partial x} - \psi\right)\right]\delta_y\Big|_0^L = 0.$$

The equations (2.23) and (2.24) are the governing equations of motion for the transverse vibration of a Timoshenko beam. By assuming a uniform beam, where $A(x) = A$, $m(x) = m$, $k(x) = k$, and $I(x) = I$, the governing equations are now reduced to

$$sGA\left(\frac{\partial^2 y}{\partial x^2} - \frac{\partial \psi}{\partial x}\right) - m\frac{\partial y^2}{\partial t^2} + p(x,t) = 0 \tag{2.25}$$

and

$$EI\frac{\partial^2 \psi}{\partial x^2} + sGA\left(\frac{\partial y}{\partial x} - \psi\right) - k^2 m\frac{\partial^2 \psi}{\partial t^2} = 0. \tag{2.26}$$

Now we will combine these two governing equations to eliminate ψ. First, by differentiating equation (2.26) with respect to x, we get

$$EI\frac{\partial^3 \psi}{\partial x^3} + sGA\left(\frac{\partial^2 y}{\partial x^2} - \frac{\partial \psi}{\partial x}\right) - k^2 m\frac{\partial^3 \psi}{\partial x \partial t^2} = 0. \tag{2.27}$$

We then solve for $\frac{\partial \psi}{\partial x}$ in equation (2.25) and obtain other derivatives that appear in equation (2.26) such as $\frac{\partial^3 \psi}{\partial x^3}$ and $\frac{\partial^2 \psi}{\partial x \partial t^2}$. Therefore, we get

$$\begin{aligned}
\frac{\partial \psi}{\partial x} &= \frac{\partial^2 y}{\partial x^2} - \frac{m}{sGA}\frac{\partial y^2}{\partial t^2} + \frac{p(x,t)}{sGA}, \\
\frac{\partial^3 \psi}{\partial x^3} &= \frac{\partial^4 y}{\partial x^4} - \frac{m}{sGA}\frac{\partial y^4}{\partial x^2 \partial t^2} + \frac{1}{sGA}\frac{\partial p^2}{\partial x^2}, \\
\frac{\partial^3 \psi}{\partial x \partial t^2} &= \frac{\partial^4 y}{\partial x^2 \partial t^2} - \frac{m}{sGA}\frac{\partial y^4}{\partial t^4} + \frac{1}{sGA}\frac{\partial p^2}{\partial t^2}.
\end{aligned}$$

By substituting these derivatives into equation (2.27), we get

$$\begin{aligned}
EI\left(\frac{\partial^4 y}{\partial x^4} - \frac{m}{sGA}\frac{\partial y^4}{\partial x^2 \partial t^2} + \frac{1}{sGA}\frac{\partial p^2}{\partial x^2}\right) \\
+ sGA\left(\frac{\partial^2 y}{\partial x^2} - \left(\frac{\partial^2 y}{\partial x^2} - \frac{m}{sGA}\frac{\partial y^2}{\partial t^2} + \frac{p(x,t)}{sGA}\right)\right) \\
- k^2 m\left(\frac{\partial^4 y}{\partial x^2 \partial t^2} - \frac{m}{sGA}\frac{\partial y^4}{\partial t^4} + \frac{1}{sGA}\frac{\partial p^2}{\partial t^2}.\right) = 0,
\end{aligned}$$

or

$$EI\frac{\partial y^4}{\partial x^4} + m\frac{\partial^2 y}{\partial t^2} - \left(k^2 m + \frac{EIm}{sGA}\right)\frac{\partial^4 y}{\partial x^2 \partial t^2} + \frac{(km)^2}{sGA}\frac{\partial^4 y}{\partial t^4} = p(x,t) + \frac{k^2 m}{sGA}\frac{\partial^2 p}{\partial t^2} - \frac{EI}{sGA}\frac{\partial p^2}{\partial x^2}. \tag{2.28}$$

The equation above is the governing equation for Timoshenko beam [2]. Now, if the rotary effects can be neglected, we set $k = 0$ in equation (2.28), and if the shear effect can be neglected, we set $s = 0$ in equations (2.25) and (2.26), which results in $Q = 0$. This then leads to the well known Euler-Bernoulli beam equation [2]:

$$EI\frac{\partial y^4}{\partial x^4} + m\frac{\partial y^2}{\partial t^2} = p(x,t).$$

2.2.4 Weak form for the time-dependent beam problem

Consider the following initial-boundary value problem (IBVP):

$$\begin{aligned}
&\rho(x)w_{tt}(x,t) + (B(x)w_{xx}(x,t))_{xx} = f(x,t), \qquad x \in (0,1), t \in (0,T_{end}),\\
&w(0,t) = b_1(t), w_x(0,t) = b_2(t), w(1,t) = b_3(t), w_x(1,t) = b_4(t),\\
&B(x)w(x,0) = g_1(x), B(x)w_t(x,0) = g_2(x)
\end{aligned}$$

and the rigid connection condition for time-dependent beam is defined as follows:

$$\begin{aligned}
w(\alpha-,t) &= w(\alpha+,t), && \text{continuity in the deflection,}\\
w'(\alpha-,t) &= w'(\alpha+,t), && \text{continuity in the bending angle,}\\
B(\alpha-)w''(\alpha-,t) &= B(\alpha+)w''(\alpha+,t), && \text{continuity of the bending moment,}\\
(B(\alpha-)w''(\alpha-,t))' &= (B(\alpha+)w''(\alpha+,t))', && \text{continuity of the shear.}
\end{aligned}$$

Let us multiply a test function $v(x)$ on both sides of the differential equation $\rho(x)w_{tt}(x,t) + (B(x)w_{xx}(x,t))_{xx} = f(x,t)$ and integrate it from 0 to 1 with respect to x:

$$\int_0^1 v(x)\rho(x)w_{tt}(x,t)dx + \int_0^1 v(x)(B(x)w_{xx}(x,t))_{xx}dx = \int_0^1 v(x)f(x,t)dx, \qquad t \in (0,T_{end}).$$

Then use integration by parts on $\int_0^1 v(x)(B(x,t)w_{xx}(x,t))_{xx}dx$ with respect to x, to get

$$\begin{aligned}
&\int_0^1 v(x)\rho(x)w_{tt}(x,t)dx + v(x)(B(x)w_{xx}(x))_x|_0^1 - \int_0^1 v'(x)(B(x)w_{xx}(x,t))_x dx\\
=\ &\int_0^1 v(x)f(x,t)dx.
\end{aligned}$$

By choosing $v(0) = v(1) = 0$, we get

$$\int_0^1 v(x)\rho(x,t)w_{tt}(x,t)dx - \int_0^1 v'(x)(B(x)w_{xx}(x,t))_x dx = \int_0^1 v(x)f(x,t)dx.$$

Using integration by parts again on $\int_0^1 v'(x)(B(x,t)w_{xx}(x,t))_x dx$ with respect to x, we have

$$\int_0^1 v(x)\rho(x)w_{tt}(x,t)dx - v'(x)B(x)u_{xx}(x,t)|_0^1 + \int_0^1 v''(x)B(x)w_{xx}(x,t)dx = \int_0^1 v(x)f(x,t)dx.$$

By choosing $v'(0) = v'(1) = 0$, we get

$$\int_0^1 v(x)\rho(x)w_{tt}(x,t)dx + \int_0^1 v''(x)B(x)w_{xx}(x,t)dx = \int_0^1 v(x)f(x,t)dx.$$

Thus the weak form for this IBVP is:

Find $w \in S$ such that

$$\int_0^1 v(x)\rho(x)w_{tt}(x,t)dx + \int_0^1 v''(x)B(x)w_{xx}(x,t)dx = \int_0^1 v(x)f(x,t)dx, \forall v \in T,$$

where

$$S = \{w \in C^2((0,T_{end}), L^2(0,1)) \cap C((0,T_{end}), H^2(0,1))| \\ w(0,t) = b_1(t), w'(0,t) = b_2(t), w(1,t) = b_3(t), w'(1,t) = b_4(t)\},$$
$$T = \{v \in H^2(0,1) | v(0) = v'(0) = v(1) = v'(1) = 0\}.$$

Note that S is the solution set for the weak form and T is the test function space. Here $C^n((0,T_{end}), H^k(\Omega))$ is a space whose elements are functions mapping $(0,T_{end})$ to $H^k(\Omega)$ with continuous derivatives up to n-th order. Also,

$$L^p(\Omega) = \left\{u | \int_\Omega |u|^p (x)dx < \infty\right\},$$

for $p \geq 1$ [13].

2.3 A finite element method for the beam equation

In this section we will discuss how to solve the BVP of the beam equation, formed by (1.1) and (1.2), by the standard Hermite finite element method. The framework for this method will be extended later to the immersed finite element method.

2.3.1 A Hermite cubic finite element space

From the weak form for the beam equation, we see that the test and trial functions must be in H^2. If we choose the test and trial functions from a finite dimensional space, a finite

element space for example, then the basis functions of this finite dimensional space must also be in H^2.

However, there are many finite element developed that are in H^2, perhaps the most popular one is the Hermite cubic finite element functions [1, 6, 12, 13, 18]. Here, we will show how the Hermite cubic finite element functions can be constructed.

For simplicity in constructing the Hermite cubic local basis functions, let us start with the reference domain $\overline{\Omega} = [0, 1]$ where $\Omega = (0, 1)$. We first introduce the local nodal basis functions on the reference domain. We then use them to define the local nodal basis functions in an arbitrary element $[x_l, x_r]$. Furthermore, the local nodal basis functions in elements are used to define the global Hermite cubic basis functions.

Let $N_1(\xi)$ be a cubic polynomial with $\xi \in \overline{\Omega}$:

$$N_1(\xi) = a\xi^3 + b\xi^2 + c\xi + d$$

such that the following nodal value specifications are satisfied:

$$N_1(0) = 1, N_1'(0) = 0, N_1(1) = 0, N_1'(1) = 0.$$

Then the coefficients of $N_1(\xi)$ can be determined by solving the following linear system:

$$\begin{pmatrix} 0 & 0 & 0 & 1 \\ 0 & 0 & 1 & 0 \\ 1 & 1 & 1 & 1 \\ 3 & 2 & 1 & 0 \end{pmatrix} \begin{pmatrix} a \\ b \\ c \\ d \end{pmatrix} = \begin{pmatrix} 1 \\ 0 \\ 0 \\ 0 \end{pmatrix},$$

from which we have $a = 2$, $b = -3$, $c = 0$, and $d = 1$. Thus,

$$N_1(\xi) \;=\; 2\xi^3 - 3\xi^2 + 1 \tag{2.29}$$

Similarly, $N_2(\xi), N_3(\xi)$, and $N_4(\xi)$ can be found to have the following formulas:

$$\begin{aligned} N_2(\xi) &= \xi^3 - 2\xi^2 + \xi \\ N_3(\xi) &= -2\xi^3 + 3\xi^2 \\ N_4(\xi) &= \xi^3 - \xi^2 \end{aligned} \tag{2.30}$$

where the Hermite nodal value specifications for $N_2(\xi), N_3(\xi)$, and $N_4(\xi)$ are as follows:

$$\begin{aligned} &N_2(0) = 0, N_2'(0) = 1, N_2(1) = 0, N_2'(1) = 0 \\ &N_3(0) = 0, N_3'(0) = 0, N_3(1) = 1, N_3'(1) = 0 \\ &N_4(0) = 0, N_4'(0) = 0, N_4(1) = 0, N_4'(1) = 1 \end{aligned}$$

The plots of $N_i(\xi)$ for $i = 1, 2, 3, 4$ are shown in Figure 2.5.

In general, we need to use the Hermite cubic nodal basis functions in an arbitrary interval rather than the reference interval $[0, 1]$. This can be done by transforming our formulas in (2.29) and (2.30) to an arbitrary interval, for example $[x_l, x_r]$ with the function $\zeta : [x_l, x_r] \to [0, 1]$ as

$$\zeta(x) = \frac{x - x_l}{x_r - x_l}.$$

This leads to functions $\psi_i : [x_l, x_r] \to \mathbf{R}$, $i = 1, 2, 3, 4$ defined as

$$\begin{array}{ll} \psi_1(x) = N_1(\zeta(x)), & \psi_2(x) = (x_r - x_l)(N_2(\zeta(x))), \\ \psi_3(x) = N_3(\zeta(x)), & \psi_4(x) = (x_r - x_l)(N_4(\zeta(x))). \end{array} \tag{2.31}$$

Then ψ_1, ψ_2, ψ_3, and ψ_4 are now the Hermite cubic nodal basis function defined over an arbitrary interval $[x_l, x_r]$. Notice that the nodal value of $\psi_i(x)$ is equal the nodal value of $N_i(x)$ for $i = 1, 2, 3, 4$, and $\psi_i(x)$ preserves the properties of the Hermite cubic nodal basis functions.

We then use the local nodal basis functions to form the global nodal basis functions which can be used to form the Hermite cubic space for our BVP.

First, let us introduce a partition of $\overline{\Omega} = [0, 1]$ defined by

$$\mathcal{T}_h = \bigcup_{k=1}^{n-1} e_k, \tag{2.32}$$

where $e_k = [x_k, x_{k+1}]$ for $k = 1, 2, \ldots, n-1$ is called an element of this partition, and we assume that these elements are formed by node points:

$$0 = x_1 < x_2 < \cdots < x_{n-1} < x_n = 1,$$

with $n - 1$ being the number of elements. For each element $e_k = [x_k, x_{k+1}]$, we will use the notation $\psi_{k,i} : [x_k, x_{k+1}] \to \mathbf{R}$, $i = 1, 2, 3, 4$ to denote the Hermite cubic local nodal basis functions defined over this element.

At each node $x_i, i = 1, 2, \cdots, n$, we define two global nodal basis functions as follows.

At x_1, we define

$$\phi_1(x) = \begin{cases} 0, & \text{if } x \notin [x_1, x_2] \\ \psi_{1,1}(x) & \text{if } x \in [x_1, x_2], \end{cases}$$

$$\phi_2(x) = \begin{cases} 0, & \text{if } x \notin [x_1, x_2] \\ \psi_{1,2}(x) & \text{if } x \in [x_1, x_2], \end{cases}$$

at $x_k, k = 2, 3, \cdots, n-1$, we define

$$\phi_{2k-1}(x) = \begin{cases} 0, & \text{if } x \notin [x_{k-1}, x_{k+1}] \\ \psi_{k-1,3}(x) & \text{if } x \in [x_{k-1}, x_k] \\ \psi_{k,1}(x) & \text{if } x \in [x_k, x_{k+1}], \end{cases}$$

$$\phi_{2k}(x) = \begin{cases} 0, & \text{if } x \notin [x_{k-1}, x_{k+1}] \\ \psi_{k-1,4}(x) & \text{if } x \in [x_{k-1}, x_k] \\ \psi_{k,2}(x) & \text{if } x \in [x_k, x_{k+1}], \end{cases}$$

and at x_n we define

$$\phi_{2n-1}(x) = \begin{cases} 0, & \text{if } x \notin [x_{n-1}, x_n] \\ \psi_{n-1,3}(x) & \text{if } x \in [x_{n-1}, x_n], \end{cases}$$

$$\phi_{2n}(x) = \begin{cases} 0, & \text{if } x \notin [x_{n-1}, x_n] \\ \psi_{n-1,4}(x) & \text{if } x \in [x_{n-1}, x_n]. \end{cases}$$

Thus, the nodal value for $\phi_k(x_j)$ for $k = 1, 2, \ldots, 2n$ and $j = 1, 2, \ldots, n$ is given as follows:

$$\phi_{2i-1}(x_j) = \begin{cases} 0, & \text{if } x_j \neq x_i \\ 1. & \text{if } x_j = x_i, \end{cases}$$

for $i = 1, 2, \ldots, n$, and

$$\phi'_{2i}(x_j) = \begin{cases} 0, & \text{if } x_j \neq x_i \\ 1. & \text{if } x_j = x_i, \end{cases}$$

for $i = 1, 2, \ldots, n$.

Notice that the nodal values for ϕ_k, $k = 1, 2, \ldots, 2n-1, 2n$, are carried from the properties of the Hermite cubic local nodal basis functions $\psi_{k,i}(x), i = 1, 2, 3, 4$. Here, we plot the standard Hermite cubic global basis functions with nodes $x_1 = 0$, $x_2 = 0.2$, and $x_3 = 0.4$ on the domain [0, 1] to give a visualization of these global basis functions. This plot is shown in Figure 2.6.

Finally, our Hermite cubic finite element space is defined as:

$$S_h(\overline{\Omega}) = span\{\phi_1, \phi_2, \cdots, \phi_{2n-1}, \phi_{2n}\}.$$

Moreover, according to [13], if we use the Hermite cubic finite element space to do the interpolations, we can expect the order of convergence as follows:

$$||u - I_h u||_0 + h||u - I_h u||_1 + h^2||u - I_h u||_2 + h^3||u - I_h u||_3 \leq C(|u|_4)h^4,$$

where u is a function in $H^4(\Omega)$ and $I_h u$ is its interpolation solution with the Hermite cubic finite element space. Here, the norms $||f||_0$, $||f||_1$, $||f||_2$, and $||f||_3$ of a function f are defined as

$$\begin{aligned} ||f||_0 &= \sqrt{\int_\Omega f^2(x)dx}, \\ ||f||_1 &= \sqrt{\int_\Omega (f^2(x) + (f'(x))^2)dx}, \\ ||f||_2 &= \sqrt{\int_\Omega (f^2(x) + (f'(x))^2 + (f''(x))^2)dx}, \\ ||f||_3 &= \sqrt{\int_\Omega (f^2(x) + (f'(x))^2 + (f''(x)^2) + (f'''(x))^2)dx}, \end{aligned} \tag{2.33}$$

and the semi-norm $|f|_i, i = 1, 2, 3, 4$ is defined as

$$|f|_i = \sqrt{\int_\Omega (f^{(i)}(x))^2 dx}.$$

2.3.2 The Hermite finite element solution

In this subsection, we will discuss the Hermite finite element solution to our BVP (1.1) and (1.2). Recall that the weak form of this boundary value problem is listed in (2.12) as:

Find $w \in S = \{w | w \in H^2, w(0) = b_1, w'(0) = b_2, w(1) = b_3, w'(1) = b_4\}$ such that
$\int_0^1 v''(x)B(x)w''(x)dx = \int_0^1 v(x)f(x)dx,$
for any $v \in T = \{w | w \in H^2, w(0) = w(1) = w'(0) = w'(1) = 0\}$.

Since the Hermite cubic finite element space defined in the previous section is a subspace of H^2, we will use its basis functions to form the Hermite cubic finite element spaces for both of our test function space and trial function set. Thus we let

$$\begin{aligned} S_h(\overline{\Omega}) &= span\{\phi_1, \phi_2, \cdots, \phi_{2n-1}, \phi_{2n}\} \cap S, \\ T_h(\overline{\Omega}) &= span\{\phi_3, \phi_4, \cdots, \phi_{2n-3}, \phi_{2n-2}\} \subset T. \end{aligned}$$

However, recall that $B(x)$ is piecewise constant function and it is discontinuous at the interface α. In order to use the weak form in (2.12) to obtain the finite element equation, we need to place a node at the interface α. Hence we need to use a partition of $\overline{\Omega}$ by

$$\mathcal{T}_h = \bigcup_{k=1}^{n-1} e_k,$$

where $e_k = [x_k, x_{k+1}]$ for $k = 1, 2, \ldots, n-1$ is formed by the node points

$$0 = x_1 < x_2 < \cdots < x_i = \alpha < \cdots < x_n = 1.$$

Then we define the Hermite cubic finite element solution as the function $u_h = \sum_{j=1}^{2n} u_j \phi_j(x) \in S_h$ determined by the finite element equations as follows:

$$\int_0^1 \phi_i''(x) B(x) u_h''(x) dx = \int_0^1 \phi_i(x) f(x) dx, \qquad i = 3, 4, \ldots, 2n-2. \tag{2.34}$$

We can rewrite (2.34) as

$$\int_0^1 \phi_i''(x) B(x) \sum_{j=1}^{2n} u_j \phi_j''(x) dx = \int_0^1 \phi_i(x) f(x) dx,$$

or

$$\sum_{j=1}^{2n} u_j \int_0^1 \phi_i''(x) B(x) \phi_j''(x) dx = \int_0^1 \phi_i(x) f(x) dx, \tag{2.35}$$

with $i = 3, 4, \ldots, 2n-2$. However, from the definition of the finite element solution set S_h, we must have $u_h(0) = b_1$, $u_h'(0) = b_2$, $u_h(1) = b_3$, and $u_h'(1) = b_4$. Because of the nodal value properties of $\phi_1, \phi_2, \phi_{2n-1}$, and ϕ_{2n}, we have $u_1 = b_1, u_2 = b_2, u_{2n-1} = b_3$, and $u_{2n} = b_4$. This implies that only coefficients $u_3, u_4, \cdots, u_{2n-3}$ and u_{2n-2} are to be computed. Therefore (2.35) becomes:

$$\begin{aligned} \sum_{j=3}^{2n-2} u_j \int_0^1 \phi_i''(x) B(x) \phi_j''(x) dx &= \int_0^1 \phi_i(x) f(x) dx - b_1 K_{i,1} - b_2 K_{i,2} \\ &\quad - b_3 K_{i,2n-1} - b_4 K_{i,2n}, \end{aligned} \tag{2.36}$$

for $i = 3, 4, \ldots, 2n-3, 2n-2$, where

$$K_{i,j} = \int_0^1 \phi_i''(x) B(x) \phi_j''(x) dx.$$

We can write the finite element equations above in matrix form as follows:

$$K\vec{u} = \vec{f} + \vec{B}_e, \tag{2.37}$$

where

$$\begin{aligned} \vec{u} &= (u_i)_{i=3}^{2n-2}, \\ K &= (K_{i,j})_{i=3,j=3}^{2n-2}, \\ \vec{f} &= \left(\int_0^1 \phi_i(x) f(x) dx \right)_{i=3}^{2n-2}, \\ \vec{B}_e &= (B_{e,i})_{i=3}^{2n-2}, \text{ where } B_{e,i} = -b_1 K_{i,1} - b_2 K_{i,2} - b_3 K_{i,2n-1} - b_4 K_{i,2n}. \end{aligned}$$

We should note that when h is small, K is a banded matrix, and most of the entries of B_e are zero. In addition, the matrix K can be assembled element by element through the local matrix K_{e_k} with the standard procedure, where

$$\begin{aligned} K_{e_k} &= (K_{e_k,i,j})_{i,j=1}^{4}, \\ K_{e_k,i,j} &= \int_{e_k} \phi_{k,i}''(x) B(x) \phi_{k,j}''(x) dx, \qquad i, j = 1, 2, 3, 4. \end{aligned}$$

By solving the linear system in (2.37), we will obtain the vector $\vec{u}$ which can be used to form the finite element solution:

$$u_h(x) = u_1\phi_1(x) + u_2\phi_2(x) + \cdots + u_{2n-1}\phi_{2n-1}(x) + u_{2n}\phi_{2n}(x).$$

Since u_h is an approximation of w, we should notice its accuracy described as follows [13]:

$$||w - u_h||_0 \leq Ch^4,$$
$$|w - u_h|_2 \leq Ch^2,$$

where h is the partition size used in our finite element spaces, and C is a generic constant independent of h.

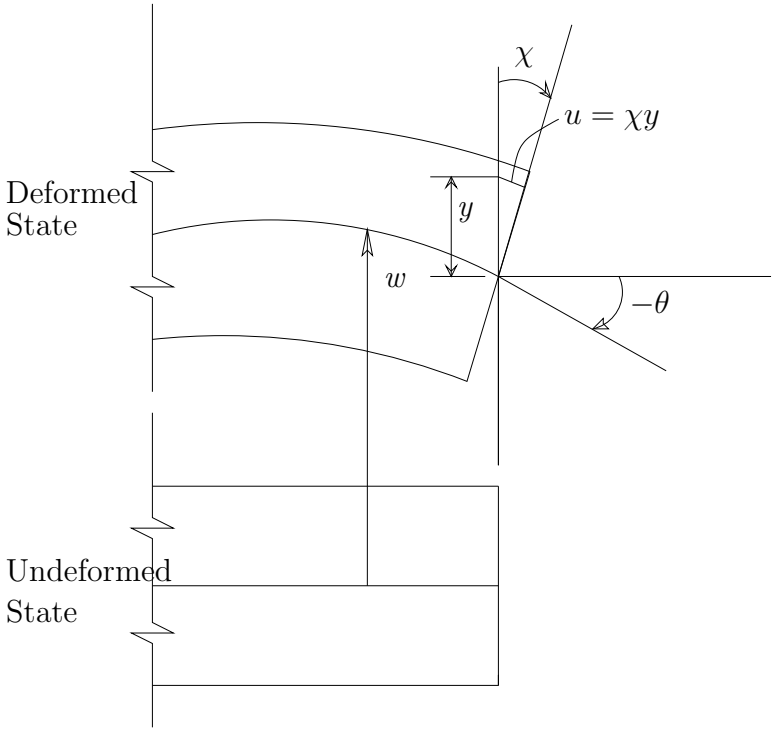

Figure 2.1: Deformed and undeformed state of a beam.

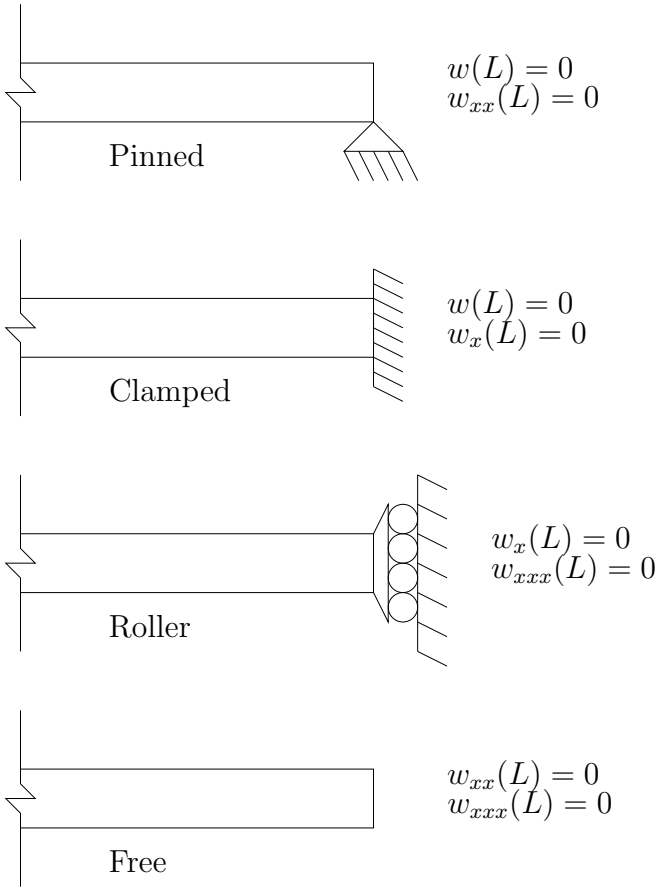

Figure 2.2: Possible boundary conditions for beam boundary value problem.

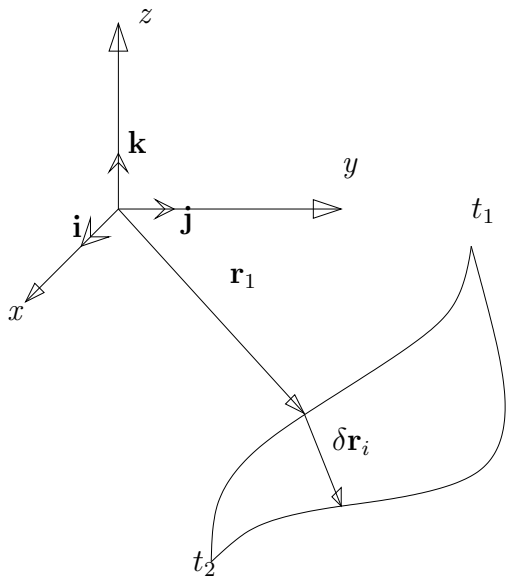

Figure 2.3: Path and varied path for Hamilton's principle.

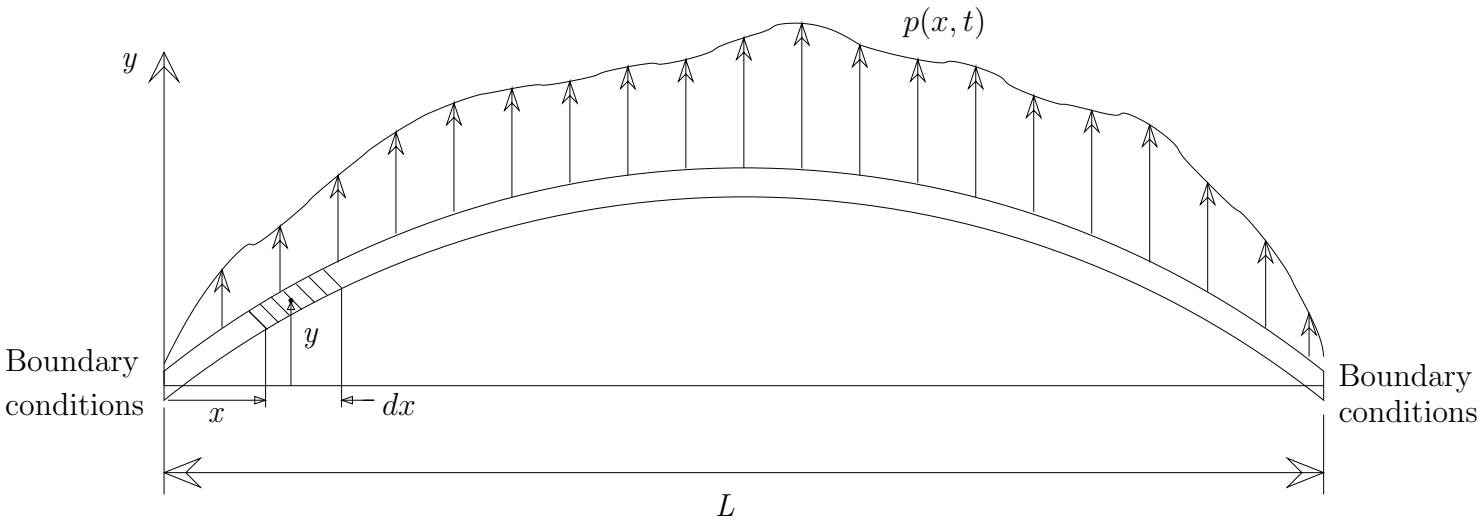

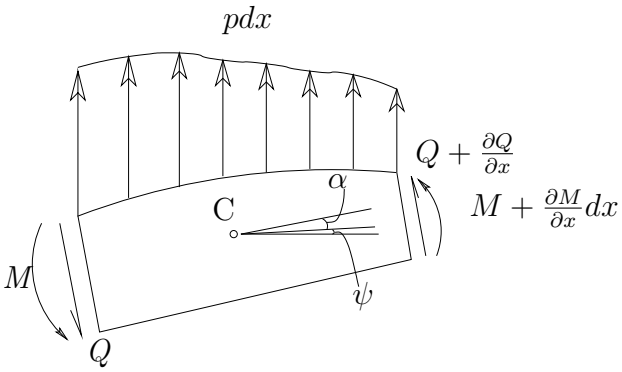

Figure 2.4: The transverse motion of a beam.

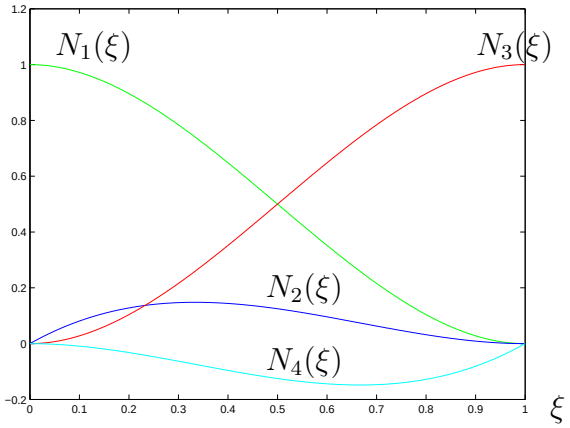

Figure 2.5: The standard Hermite cubic local basis functions $N_i(\xi)$, $i = 1, 2, 3, 4$.

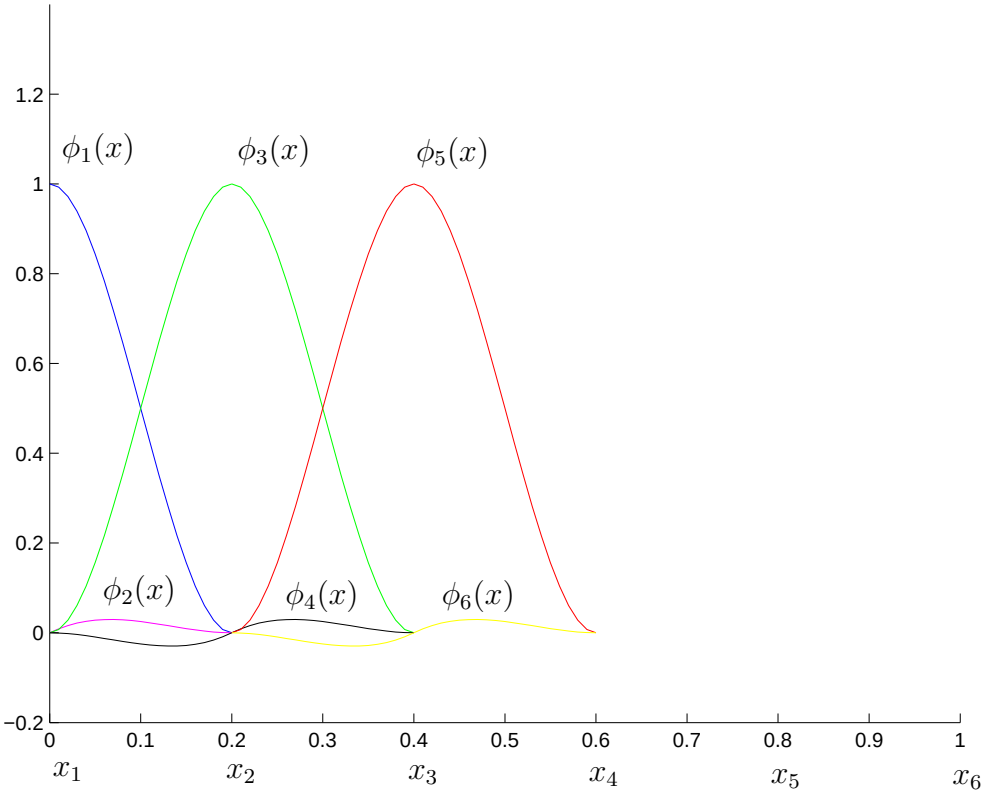

Figure 2.6: First six of the Hermite cubic global basis functions with 6 nodes partition on the domain [0, 1].

Chapter 3

An Immersed Finite Element Method for the Beam Equation

From previous sections, we see that in order for the standard Hermite cubic finite element space to solve our boundary value problem formed by (1.1) and (1.2), we need to have the interface α as one of the nodal points in the partition $\mathcal{T}_h$ of $\overline{\Omega}$. However, to solve the inverse interface problem, we need to solve our boundary value problem repeatedly, e.g., in the evaluation of $g(\alpha)$. Thus, a new partition $\mathcal{T}_h$ is needed for each evaluation of g. Our main purpose is to develop a Hermite cubic immersed finite element (IFE) space for solving interface beam problems, especially for solving the inverse beam problem efficiently.

Recall that the immersed finite element space is introduced to solve the interface problems without a repartition of $\overline{\Omega}$ [3, 4, 9]. However, the local nodal basis functions of an IFE space have to be formed according to the interface problem. Therefore, the central part of this thesis it to develop IFE basis functions suitable for solving the interface beam problem.

Let us consider a beam of length Ω that is formed by two smaller beams whose domain is Ω_1 and Ω_2 that join together at an interface α with rigid connection conditions as defined in (1.4); thus we have $\Omega = \Omega_1 \cup \{\alpha\} \cup \Omega_2$. In addition, let the Young's modulus and the moment of inertia for each beam be $E_1(x_1)$, $E_2(x_2)$, $I_1(x_1)$, and $I_2(x_2)$, respectively, for which

$$\begin{aligned} E_1(x_1)I_1(x_1) &= B^-, \forall x_1 \in \Omega_1, \\ E_2(x_2)I_2(x_2) &= B^+, \forall x_2 \in \Omega_2, \end{aligned}$$

such that B^- and B^+ are constants. Moreover, let us consider a loading force $f(x)$ over Ω, and for simplicity, we assume $\Omega = (0, 1)$. Now suppose $w(x)$ is the deflection of the beam and $w(0) = b_1$, $w'(0) = b_2$, $w(1) = b_3$, and $w'(1) = b_4$, where b_1, b_2, b_3, and b_4 in $\mathbf{R}$ are known, then by the Euler-Bernoulli Beam equation, $w(x)$ can be found by solving the

following boundary value problem:

$$(B(x)w(x)'')'' = f(x), x \in \Omega, \tag{3.1}$$

$$w(0) = b_1, w'(0) = b_2, w(1) = b_3, w'(1) = b_4, \tag{3.2}$$

where

$$B(x) = \begin{cases} B^- & \text{if } x < \alpha, \\ B^+ & \text{if } \alpha < x, \end{cases} \tag{3.3}$$

for which

$$\begin{aligned} w(\alpha-) &= w(\alpha+), && \text{(continuity in the deflection)}, \\ w'(\alpha-) &= w'(\alpha+), && \text{(continuity in the bending angle)}, \\ B(\alpha-)w''(\alpha-) &= B(\alpha+)w''(\alpha+), && \text{(continuity of the bending moment)}, \\ (B(\alpha-)w''(\alpha-))' &= (B(\alpha+)w''(\alpha+))', && \text{(continuity of the shear)}. \end{aligned} \tag{3.4}$$

3.1 Hermite cubic IFE local nodal basis functions with rigid connection

In this subsection, we construct the local nodal basis function for the Hermite cubic immersed finite element space.

As in the construction of the Hermite cubic local nodal basis functions from the weak form derivation, we must have the test and trial functions in H^2. Since the regular Hermite cubic nodal basis functions are in H^2 and are generally used to solve the beam problems, we will construct the immersed Hermite cubic local nodal basis functions based on the properties of regular Hermite cubic local nodal basis functions plus the interface conditions specified by (1.4).

Similar to the construction of the regular Hermite cubic local nodal basis functions, we first define our immersed Hermite cubic local nodal basis functions $\widetilde{N}_i(\xi)$ in the reference element $[0, 1]$, and an interface α such that $\alpha \in [0, 1]$. We let

$$\widetilde{N}_i(\xi) = \begin{cases} a_i + b_i\xi + \xi^2(c_i + d_i(\xi - \alpha)) & \text{if } 0 \le \xi \le \alpha, \\ e_i + f_i(\xi - 1) + (\xi - 1)^2(g_i + h_i(\xi - \alpha)) & \text{if } \alpha \le \xi \le 1, \end{cases}$$

where $\xi \in [0, 1]$. Note that if d_i and h_i are not zero, then $N_i(\xi)$ is a piecewise cubic polynomial.

Now suppose that $\widetilde{N}_i(\xi)$ satisfies the Hermite cubic local nodal conditions:

$$\begin{aligned} \widetilde{N}_i(0) &= \begin{cases} 1, & \text{if } i = 1, \\ 0, & \text{if } i \neq 1, \end{cases} & \widetilde{N}_i'(0) &= \begin{cases} 1, & \text{if } i = 2, \\ 0, & \text{if } i \neq 2, \end{cases} \\ \widetilde{N}_i(1) &= \begin{cases} 1, & \text{if } i = 3, \\ 0, & \text{if } i \neq 3, \end{cases} & \widetilde{N}_i'(1) &= \begin{cases} 1, & \text{if } i = 4, \\ 0, & \text{if } i \neq 4, \end{cases} \end{aligned} \tag{3.5}$$

and in addition, each of $\widetilde{N}_i$ satisfies rigid connection conditions at the interface α:

$$\begin{aligned}
\widetilde{N}_i(\alpha-) &= \widetilde{N}_i(\alpha+),\\
\widetilde{N}_i'(\alpha-) &= \widetilde{N}_i'(\alpha+),\\
B(\alpha-)\widetilde{N}_i''(\alpha-) &= B(\alpha+)\widetilde{N}_i''(\alpha+),\\
(B(\alpha-)\widetilde{N}_i''(\alpha-))' &= (B(\alpha+)\widetilde{N}_i''(\alpha+))'.
\end{aligned}$$

The nodal value conditions lead to

$$\begin{array}{llll}
a_1 = 1, & a_2 = 0, & a_3 = 0, & a_4 = 0,\\
b_1 = 0, & b_2 = 1, & b_3 = 0, & b_4 = 0,\\
e_1 = 0, & e_2 = 0, & e_3 = 1, & e_4 = 0,\\
f_1 = 0, & f_2 = 0, & f_3 = 0, & f_4 = 1.
\end{array}$$

Then $\widetilde{N}_1(\xi)$, $\widetilde{N}_2(\xi)$, $\widetilde{N}_3(\xi)$, and $\widetilde{N}_4(\xi)$ become:

$$\widetilde{N}_1(\xi) = \begin{cases} 1+\xi^2(c_1+d_1(\xi-\alpha)) & \text{if } 0\le\xi\le\alpha,\\ (\xi-1)^2(g_1+h_1(\xi-\alpha)) & \text{if } \alpha\le\xi\le 1,\end{cases}$$

$$\widetilde{N}_2(\xi) = \begin{cases} \xi+\xi^2(c_2+d_2(\xi-\alpha)) & \text{if } 0\le\xi\le\alpha,\\ (\xi-1)^2(g_2+h_2(\xi-\alpha)) & \text{if } \alpha\le\xi\le 1,\end{cases}$$

$$\widetilde{N}_3(\xi) = \begin{cases} \xi^2(c_3+d_3(\xi-\alpha)) & \text{if } 0\le\xi\le\alpha,\\ 1+(\xi-1)^2(g_3+h_3(\xi-\alpha)) & \text{if } \alpha\le\xi\le 1,\end{cases}$$

$$\widetilde{N}_4(\xi) = \begin{cases} \xi^2(c_4+d_4(\xi-\alpha)) & \text{if } 0\le\xi\le\alpha,\\ (\xi-1)+(\xi-1)^2(g_4+h_4(\xi-\alpha)) & \text{if } \alpha\le\xi\le 1.\end{cases}$$

By using the rigid connection conditions, the coefficients c_i, d_i, g_i, and h_i, $i = 1, 2, 3, 4$, can be determined by solving the following systems of equations:

For $\widetilde{N}_1(\xi)$:

$$\begin{aligned}
1+c_1\alpha^2 &= g_1(\alpha-1)^2,\\
2c_1\alpha+d_1\alpha^2 &= 2g_1(\alpha-1)+h_1(\alpha-1)^2,\\
B^-(2c_1+4d_1\alpha) &= B^+(2g_2+4h_1(\alpha-1)),\\
B^-(6d_1) &= B^+(6h_1).
\end{aligned}$$

For $\widetilde{N}_2(\xi)$:

$$\begin{aligned}
\alpha+c_2\alpha^2 &= g_2(\alpha-1)^2,\\
1+2c_2\alpha+d_2\alpha^2 &= 2g_2(\alpha-1)+h_2(\alpha-1)^2,\\
B^-(2c_2+4d_2\alpha) &= B^+(2g_2\alpha+4h_2(\alpha-1)),\\
B^-(6d_2) &= B^+(6h_2).
\end{aligned}$$

For $\widetilde{N}_3(\xi)$:

$$\begin{aligned} c_3\alpha^2 &= 1 + g_2(\alpha-1)^2, \\ 2c_3\alpha + d_3\alpha^2 &= 2g_3(\alpha-1) + h_3(\alpha-1)^2, \\ B^-(2c_3 + 4d_3\alpha) &= B^+(2g_3 + 4h_3(\alpha-1)), \\ B^-(6d_3) &= B^+(6h_3). \end{aligned}$$

For $\widetilde{N}_4(\xi)$:

$$\begin{aligned} c_4\alpha^2 &= (\alpha-1) + g_4(\alpha-1)^2. \\ 2c_4\alpha + d_4\alpha^2 &= 1 + 2g_4(\alpha-1) + h_4(\alpha-1)^2. \\ B^-(2c_4 + 4d_4\alpha) &= B^+(2g_4 + 4h_4(\alpha-1)). \\ B^-(6d_4) &= B^+(6h_4). \end{aligned}$$

Hence, we can solve the following linear systems for c_i, d_i, g_i, and h_i:

$$\begin{pmatrix} \alpha^2 & 0 & -(\alpha-1)^2 & 0 \\ 2\alpha & \alpha^2 & -2(\alpha-1) & -(\alpha-1)^2 \\ 2B^- & 4\alpha B^- & -2B^+ & -4(\alpha-1)B^+ \\ 0 & 6B^- & 0 & -6B^+ \end{pmatrix} \begin{pmatrix} c_i \\ d_i \\ g_i \\ h_i \end{pmatrix} = \overrightarrow{q}_i \tag{3.6}$$

where

$$\overrightarrow{q}_1 = \begin{pmatrix} -1 \\ 0 \\ 0 \\ 0 \end{pmatrix}, \quad \overrightarrow{q}_2 = \begin{pmatrix} -\alpha \\ -1 \\ 0 \\ 0 \end{pmatrix}, \quad \overrightarrow{q}_3 = \begin{pmatrix} 1 \\ 0 \\ 0 \\ 0 \end{pmatrix}, \quad \overrightarrow{q}_4 = \begin{pmatrix} \alpha-1 \\ 1 \\ 0 \\ 0 \end{pmatrix}.$$

We first want to show that the determinant of the coefficients matrix in (3.6) is nonzero, which further implies the solution to (3.6) exists and is unique.

Lemma 3.1.1 *The determinant of the coefficient matrix*

$$A = \begin{pmatrix} \alpha^2 & 0 & -(\alpha-1)^2 & 0 \\ 2\alpha & \alpha^2 & -2(\alpha-1) & -(\alpha-1)^2 \\ 2B^- & 4\alpha B^- & -2B^+ & -4(\alpha-1)B^+ \\ 0 & 6B^- & 0 & -6B^+ \end{pmatrix} \tag{3.7}$$

is nonzero.

Proof: We first evaluate the determinant of A and get:

$$\det(A) = 12\left((B^-)^2(\alpha-1)^4 - 2B^-B^+\alpha(\alpha-1)(\alpha^2-\alpha+2) + (B^+)^2\alpha^4\right).$$

Now we have to show that $\det(A) \neq 0$. It is clear that $(\alpha-1)^4(B^-)^2 + \alpha^4(B^+)^2 > 0$, so if $-2B^-B^+\alpha(\alpha-1)(\alpha^2-\alpha+2) \geq 0$, we have $\det(A) > 0$. Since $\alpha \in (0,1)$, we have $(\alpha-1) < 0$ and it follows that $(-2B^-B^+\alpha(\alpha-1)) > 0$. Thus, if $(\alpha^2-\alpha+2) \geq 0$, we have $\det(A) > 0$. To prove that $(\alpha^2-\alpha+2) \geq 0$, let us consider a function $f : \Omega \to \mathbf{R}$ by

$$f(\alpha) = (\alpha^2 - \alpha + 2).$$

Then by taking derivative of f with respect to α, we have $f'(\alpha) = 2\alpha - 1$. So $f(\alpha)$ has an absolute minimum at $\alpha = \frac{1}{2}$. But $f(\frac{1}{2}) = \frac{1}{4} - \frac{1}{2} + 2 > 0$, and thus the term $(\alpha^2-\alpha+2) > 0$. Therefore, it is true that $\det(A) > 0$, so $\det(A) \neq 0$.

■

Since the determinant of A in (3.7) is nonzero, we know the linear systems in (3.6), have unique solutions. Then by solving the linear systems in (3.6), the coefficients c_i, d_i, g_i, and h_i can be found as follows:

$$\begin{aligned}
c_1 &= B^+(B^-(\alpha+3)(\alpha-1) - \alpha^2B^+)/D,\\
d_1 &= -2B^+(\alpha B^- - B^- - \alpha B^+)/D,\\
g_1 &= B^-(-2\alpha B^- + B^- - \alpha^2B^+ + B^-\alpha^2 + 4\alpha B^+)/D,\\
h_1 &= -2B^-((\alpha-1)B^- - \alpha B^+)/D,\\
\\
c_2 &= B^+(\alpha^3(-B^+ + B^-) + (\alpha-2)B^-)/D,\\
d_2 &= -B^+(B^-\alpha^2 - B^- - \alpha^2B^+)/D,\\
g_2 &= \alpha B^-(-\alpha B^+(-2+\alpha) + B^-(\alpha-1)^2)/D,\\
h_2 &= -B^-(B^-\alpha^2 - B^- - \alpha^2B^+)/D,\\
\\
c_3 &= -B^+((-B^+ + B^-)\alpha^2 + B^-(2\alpha-3))/D,\\
d_3 &= 2B^+(\alpha B^- - B^- - \alpha B^+)/D,\\
g_3 &= -B^-(-2\alpha B^- + B^- - \alpha^2B^+ + B^-\alpha^2 + 4\alpha B^+)/D,\\
h_3 &= 2B^-(\alpha B^- - B^- - \alpha B^+)/D,\\
\\
c_4 &= -B^+(\alpha-1)((-B^+ + B^-)\alpha^2 - B^-)/D,\\
d_4 &= B^+((-B^+ + B^-)\alpha^2 + (-2B^- + 2B^+)\alpha + B^-)/D,\\
g_4 &= -B^-(\alpha^3(-B^+ + B^-) + (3B^+ - 3B^-)\alpha^2 + (3B^- - 4B^+)\alpha - B^-)/D,\\
h_4 &= B^-((-B^+ + B^-)\alpha^2 + (-2B^- + 2B^+)\alpha + B^-)/D,
\end{aligned}$$

where

$$D = (B^-)^2(\alpha-1)^4 - 2B^-B^+\alpha(\alpha-1)(\alpha^2-\alpha+2) + (B^+)^2\alpha^4. \tag{3.8}$$

Notice that $D = (\det A)/12$ where A is the matrix defined in (3.7), and since $\det(A) \neq 0$, so we have $D \neq 0$. Therefore, we have obtained unique solutions for coefficients c_i, d_i, g_i, and h_i, for $i = 1, 2, 3, 4$. Thus, our immersed Hermite local nodal basis functions $\widetilde{N}_i(\xi)$, $i = 1, 2, 3, 4$, are uniquely defined.

Here, we examine $\widetilde{N}_i(\xi)$, $i = 1, 2, 3, 4$, with a fixed interface, α, at $\pi/6$ and the piecewise constant coefficient function $B(x)$ in the following cases:
Case 1:

$$B(x) = \begin{cases} 2 & \text{if } x < \alpha \\ 5 & \text{if } \alpha < x, \end{cases}$$

Case 2:

$$B(x) = \begin{cases} 2 & \text{if } x < \alpha \\ 500 & \text{if } \alpha < x, \end{cases}$$

Case 3:

$$B(x) = \begin{cases} 2 & \text{if } x < \alpha \\ 50000 & \text{if } \alpha < x. \end{cases}$$

Note that the three cases illustrate the ratio in discontinuity $B(x)$ as small, moderate, and large, respectively. The plot for each of the cases are shown in Figure 3.1, Figure 3.2, and Figure 3.3.

As with the standard Hermite cubic local nodal basis functions, we can define the functions $\widetilde{\psi}_i(x) : [x_l, x_r] \to \mathbf{R}$ as the immersed Hermite cubic local nodal basis functions on an arbitrary interval $[x_l, x_r]$ with an interface $\alpha \in (x_l, x_r)$ as follows:

$$\begin{array}{ll} \widetilde{\psi}_1(x) = \widetilde{N}_1(\zeta(x)), & \widetilde{\psi}_2(x) = (x_r - x_l)(\widetilde{N}_2(\zeta(x))), \\ \widetilde{\psi}_3(x) = \widetilde{N}_3(\zeta(x)), & \widetilde{\psi}_4(x) = (x_r - x_l)(\widetilde{N}_4(\zeta(x))), \end{array} \tag{3.9}$$

where $\zeta : [x_l, x_r] \to [0, 1]$ defined as

$$\zeta(x) = \frac{x - x_l}{x_r - x_l}.$$

Now we will construct the immersed Hermite cubic finite element space with the Hermite cubic local nodal basis functions $\psi_1(x)$, $\psi_2(x)$, $\psi_3(x)$, and $\psi_4(x)$ defined in (2.31), and also the immersed Hermite cubic local nodal basis functions $\widetilde{\psi}_1(x)$, $\widetilde{\psi}_2(x)$, $\widetilde{\psi}_3(x)$, and $\widetilde{\psi}_4(x)$ defined in (3.9).

First, let us introduce a partition of $\overline{\Omega} = [0, 1]$:

$$\widetilde{\mathcal{T}}_h = \bigcup_{k=1}^{n} e_k,$$

where

$$e_k = [x_k, x_{k+1}], \tag{3.10}$$

and $k = 1, 2, \ldots, n-1$, are intervals in Ω formed by node points

$$0 = x_1 < x_2 < \cdots < x_{n-1} < x_n = 1,$$

with n being the number of elements. In addition, let us suppose that an interface α is in Ω.

Before we define the global basis functions, let us classify the elements according the definitions as follows:

Definition 3.1.1 *An element e_k is said to be an **interface-element** if e_k contains only one interface α such that α is an interior point of e_k, i.e., $e_{k-1} < \alpha < e_k$. An element e_k is said to be a **non-interface-element** if e_k there is no interface α such that $e_{k-1} < \alpha < e_k$.*

And in addition, let us define a function $\eta_{k,i} : e_k \to \mathbf{R}$ for $i = 1, 2, 3, 4$ as follows:

$$\eta_{k,i}(x) = \begin{cases} \psi_{k,i}(x), & \text{if } e_k \text{ is an non-interface-element.} \\ \widetilde{\psi}_{k,i}(x), & \text{if } e_k \text{ is an interface-element.} \end{cases}$$

We now ready to define the global basis functions, $\widetilde{\phi}_i$, $i = 1, 2, \ldots, 2n-1, 2n$, over Ω as follows:

At x_1, we define

$$\widetilde{\phi}_1(x) = \begin{cases} 0, & \text{if } x \notin [x_1, x_2] \\ \eta_{1,1}(x) & \text{if } x \in [x_1, x_2], \end{cases}$$

and

$$\widetilde{\phi}_2(x) = \begin{cases} 0, & \text{if } x \notin [x_1, x_2] \\ \eta_{1,2}(x) & \text{if } x \in [x_1, x_2], \end{cases}$$

At $x_k, k = 2, 3, \cdots, n-1$, we define

$$\widetilde{\phi}_{2k-1}(x) = \begin{cases} 0, & \text{if } x \notin [x_{k-1}, x_{k+1}] \\ \eta_{k-1,3}(x) & \text{if } x \in [x_{k-1}, x_k] \\ \eta_{k,1}(x) & \text{if } x \in [x_k, x_{k+1}], \end{cases}$$

$$\widetilde{\phi}_{2k}(x) = \begin{cases} 0, & \text{if } x \notin [x_{k-1}, x_{k+1}] \\ \eta_{k-1,4}(x) & \text{if } x \in [x_{k-1}, x_k] \\ \eta_{k,2}(x) & \text{if } x \in [x_k, x_{k+1}], \end{cases}$$

and at x_n, we define

$$\phi_{2n-1}(x) = \begin{cases} 0, & \text{if } x \notin [x_{n-1}, x_n] \\ \eta_{n-1,3}(x) & \text{if } x \in [x_{n-1}, x_n], \end{cases}$$

and

$$\widetilde{\phi}_{2n}(x) = \begin{cases} 0, & \text{if } x \notin [x_{n-1}, x_n] \\ \eta_{n-1,4}(x) & \text{if } x \in [x_{n-1}, x_n]. \end{cases}$$

Thus, the nodal values $\widetilde{\phi}_k(x_j)$ for $k = 1, 2, \ldots, 2n$ and $j = 1, 2, \ldots, n$ are given as follows:

$$\widetilde{\phi}_{2i-1}(x_j) = \begin{cases} 0, & \text{if } x_j \neq x_i \\ 1. & \text{if } x_j = x_i, \end{cases}$$

for $i = 1, 2, \ldots, n$, and

$$\widetilde{\phi}_{2i}(x_j) = \begin{cases} 0, & \text{if } x_j \neq x_i \\ 1. & \text{if } x_j = x_i, \end{cases}$$

for $i = 1, 2, \ldots, n$.

Note that the nodal values for $\widetilde{\phi}_k$, $k = 1, 2, \ldots, 2n-1, 2n$, are carried from the properties of the immersed Hermite cubic local nodal basis functions $\eta_{k,i}(x)$, $i = 1, 2, 3, 4$.

Finally, our Hermite cubic immersed finite element space is defined as:

$$\widetilde{S}_h(\overline{\Omega}) = span\{\widetilde{\phi}_1, \widetilde{\phi}_2, \ldots, \widetilde{\phi}_{2n-1}, \widetilde{\phi}_{2n}\}.$$

When using the Hermite cubic finite element space S_h to do the interpolations, we can except the order of convergence as follows:

$$||u - I_h u||_0 + h||u - I_h u||_1 + h^2||u - I_h u||_2 + h^3||u - I_h u||_3 \leq C(|u|_4)h^4,$$

where u is a function in $H^4(\Omega)$ and $I_h u$ is its interpolation using the Hermite cubic finite element space. We would like to know whether the immersed Hermite cubic finite element space $\widetilde{S}_h$ also has the same order of convergence, i.e.,

$$||u - \widetilde{I_h u}||_0 + h||u - \widetilde{I_h u}||_1 + h^2||u - \widetilde{I_h u}||_2 + h^3||u - \widetilde{I_h u}||_3 \leq C(|u|_4)h^4,$$

where $\widetilde{I_h u}$ is the interpolation of u by the immersed Hermite cubic finite element space. We will numerically investigate our immersed Hermite finite element space to see its approximation capability later on in the chapter.

3.2 Some properties of the immersed Hermite cubic local nodal basis functions

Here, we will show that the immersed Hermite cubic local nodal basis functions introduced in the previous section have following properties:

(i) If $\alpha \to x_l$ or $\alpha \to x_r$, then $\widetilde{\psi}_i(x) = \psi_i(x)$ for $i = 1, 2, 3, 4$.

(ii) If the piecewise continuous coefficients across the interface are the same, then the immersed Hermite cubic nodal basis functions become the usual Hermite nodal basis functions. In other words, if $B^- = B^+$ then $\widetilde{\psi}_i(x) = \psi_i(x)$ for $i = 1, 2, 3, 4$.

However, since $\widetilde{\psi}_i(x)$ and $\psi_i(x)$ are the transformation of $\widetilde{N}_i(x)$ and $N_i(x)$ from the reference interval $[0, 1]$ to an arbitrary interval $[x_l, x_r]$, respectively, proof of the following will give the equivalent result as in (i) and (ii):

(I) If $\alpha \to 0$ or $\alpha \to 1$, then $\widetilde{N}_i(\xi) = N(\xi)$ for $i = 1, 2, 3, 4$.

(II) If $B^- = B^+$ then $\widetilde{N}_i(\xi) = N(\xi)$ for $i = 1, 2, 3, 4$.

Here, we will first prove that $\lim_{\alpha\to 0} D = (B^-)^2$ and $\lim_{\alpha\to 1} D = (B^+)^2$ for the convenience of proving (I).

Lemma 3.2.1 *For D defined in (3.8), we have $\lim_{\alpha\to 0} D = (B^-)^2$ and $\lim_{\alpha\to 0} D = (B^+)^2$.*

Proof:

$$\begin{aligned}\lim_{\alpha\to 0} D &= \lim_{\alpha\to 0}\left((B^-)^2(\alpha-1)^4 - 2B^-B^+\alpha(\alpha-1)(\alpha^2-\alpha+2) + (B^+)^2\alpha^4\right)\\ &= (B^-)^2 - 0 + 0\\ &= (B^-)^2.\end{aligned}$$

Also,

$$\begin{aligned}\lim_{\alpha\to 1} D &= \lim_{\alpha\to 0}\left((B^-)^2(\alpha-1)^4 - 2B^-B^+\alpha(\alpha-1)(\alpha^2-\alpha+2) + (B^+)^2\alpha^4\right)\\ &= 0 - 0 + (B^+)^2\\ &= (B^+)^2.\end{aligned}$$

■

For property (I), we have

Theorem 3.2.1 *If $\alpha \to 0$ or $\alpha \to 1$, then $\widetilde{N}_i(\xi) = N(\xi)$ for $i = 1, 2, 3, 4$.*

Proof: First let us define the notations $f|_0$ and $f|_1$ as

$$f|_0 = \lim_{\alpha \to 0} f,$$
$$f|_1 = \lim_{\alpha \to 1} f.$$

Then

$$\begin{aligned}
\lim_{\alpha\to 0} \widetilde{N}_1(\xi) &= \lim_{\alpha\to 0} \begin{cases} 1+\xi^2(c_1+d_1(\xi-\alpha)) & \text{if } 0 \le \xi \le \alpha, \\ (\xi-1)^2(g_1+h_1(\xi-\alpha)) & \text{if } \alpha \le \xi \le 1, \end{cases} \\
&= (\xi-1)^2(g_1|_0 + h_1|_0(\xi-0)) \quad 0 \le \xi \le 1, \\
&= (\xi-1)^2\left(\tfrac{B^-(B^-)}{(B^-)^2}\right) + (\xi-1)^2\left(\tfrac{-2B^-(-B^-)\xi}{(B^-)^2}\right) \quad \text{if } 0 \le \xi \le 1, \\
&= (\xi-1)^2\left(\tfrac{B^-(B^-)}{(B^-)^2} - \tfrac{2B^-(-B^-)(\xi)}{(B^-)^2}\right) \quad 0 \le \xi \le 1, \\
&= (\xi-1)^2(1+2\xi) \quad 0 \le \xi \le 1, \\
&= (\xi^2-2\xi+1)(1+2\xi) \quad 0 \le \xi \le 1, \\
&= 2\xi^3 - 3\xi^2 + 1 \quad 0 \le \xi \le 1, \\
&= N_1(\xi).
\end{aligned}$$

$$\begin{aligned}
\lim_{\alpha\to 1} \widetilde{N}_1(\xi) &= \lim_{\alpha\to 1} \begin{cases} 1+\xi^2(c_1+d_1(\xi-\alpha)) & \text{if } 0 \le \xi \le \alpha, \\ (\xi-1)^2(g_1+h_1(\xi-\alpha)) & \text{if } \alpha \le \xi \le 1, \end{cases} \\
&= 1+\xi^2(c_1|_1 + d_1|_1(\xi-\alpha)) \quad 0 \le \xi \le 1, \\
&= 1+\xi^2\left(\tfrac{B^+(-B^+)}{(B^+)^2}\right) + \xi^2\left(\tfrac{2B^+(-B^+)(\xi-1)}{(B^+)^2}\right) \quad 0 \le \xi \le 1, \\
&= 1+\xi^2\left(\tfrac{B^+(-B^+)}{(B^+)^2} + \tfrac{-2B^+(-B^+)(\xi-1)}{(B^+)^2}\right) \quad 0 \le \xi \le 1, \\
&= 1+\xi^2(-1+2(\xi-1)) \quad 0 \le \xi \le 1, \\
&= 1-\xi^2+2\xi^3-2\xi^2(\xi-1) \quad 0 \le \xi \le 1, \\
&= 2\xi^3 - 3\xi^2 + 1 \quad 0 \le \xi \le 1, \\
&= N_1(\xi).
\end{aligned}$$

$$\begin{aligned}
\lim_{\alpha\to 0} \widetilde{N}_2(\xi) &= \lim_{\alpha\to 0} \begin{cases} \xi+\xi^2(c_2+d_2(\xi-\alpha)) & \text{if } 0 \le \xi \le \alpha, \\ (\xi-1)^2(g_2+h_2(\xi-\alpha)) & \text{if } \alpha \le \xi \le 1, \end{cases} \\
&= (\xi-1)^2(g_2|_0 + h_2|_0(\xi)) \quad 0 \le \xi \le 1, \\
&= (\xi-1)^2\left(\tfrac{-B^-(-B^-)\xi}{(B^-)^2}\right) \quad 0 \le \xi \le 1, \\
&= (\xi-1)^2\xi \quad 0 \le \xi \le 1, \\
&= \xi^3 - 2\xi^2 + \xi \quad 0 \le \xi \le 1, \\
&= N_2(\xi).
\end{aligned}$$

$$\begin{aligned}
\lim_{\alpha\to 1}\widetilde{N}_2(\xi) &= \lim_{\alpha\to 1}\begin{cases} \xi+\xi^2(c_2+d_2(\xi-\alpha)) & \text{if } 0\le\xi\le\alpha,\\ (\xi-1)^2(g_2+h_2(\xi-\alpha)) & \text{if } \alpha\le\xi\le 1,\end{cases}\\
&= \xi+\xi^2(c_2|_1+d_2|_1(\xi-1)) \quad 0\le\xi\le 1,\\
&= \xi+\xi^2\left(\tfrac{B^+(-B^++B^-+(-1)B^-)}{(B^+)^2}\right)+\xi^2\left(\tfrac{-B^+(B^--B^--B^+)(\xi-1)}{(B^+)^2}\right) \quad 0\le\xi\le 1,\\
&= \xi+\xi^2(-1+1(\xi-1)) \quad \text{if } 0\le\xi\le\alpha,\\
&= \xi-\xi^2+\xi^3-\xi^2 \quad \text{if } 0\le\xi\le\alpha,\\
&= \xi^3-2\xi^2+\xi \quad \text{if } \alpha\le\xi\le 1,\\
&= N_2(\xi).
\end{aligned}$$

$$\begin{aligned}
\lim_{\alpha\to 0}\widetilde{N}_3(\xi) &= \lim_{\alpha\to 0}\begin{cases} \xi^2(c_3+d_3(\xi-\alpha)) & \text{if } 0\le\xi\le\alpha,\\ 1+(\xi-1)^2(g_3+h_3(\xi-\alpha)) & \text{if } \alpha\le\xi\le 1,\end{cases}\\
&= 1+(\xi-1)^2(g_3|_0+h_3|_0\xi) \quad 0\le\xi\le 1,\\
&= 1+(\xi-1)^2\left(\tfrac{-B^-(B^-)}{(B^-)^2}\right)+(\xi-1)^2\left(\tfrac{2B^-(-B^-)\xi}{(B^-)^2}\right) \quad 0\le\xi\le 1,\\
&= 1+(\xi-1)^2\left(\tfrac{-B^-(B^-)}{(B^-)^2}+\tfrac{2B^-(-B^-)(\xi)}{(B^-)^2}\right) \quad \alpha\le\xi\le 1,\\
&= 1+(\xi-1)^2(-1-2(\xi)) \quad 0\le\xi\le 1,\\
&= 1-(\xi^2-2\xi+1)-2\xi^3+4\xi^2-2\xi \quad 0\le\xi\le 1,\\
&= -2\xi^3+3\xi^2 \quad 0\le\xi\le 1,\\
&= N_3(\xi).
\end{aligned}$$

$$\begin{aligned}
\lim_{\alpha\to 1}\widetilde{N}_3(\xi) &= \lim_{\alpha\to 1}\begin{cases} \xi^2(c_3+d_3(\xi-\alpha)) & \text{if } 0\le\xi\le\alpha,\\ 1+(\xi-1)^2(g_3+h_3(\xi-\alpha)) & \text{if } \alpha\le\xi\le 1,\end{cases}\\
&= \xi^2(c_3|_1+d_3|_1(\xi-1)) \quad 0\le\xi\le 1,\\
&= \xi^2\left(\tfrac{-B^+((-B^++B^-)+B^-(2-3))}{(B^+)^2}\right)+\xi^2\left(\tfrac{2B^+(B^--B^--B^+)(\xi-1)}{(B^+)^2}\right) \quad \text{if } 0\le\xi\le 1,\\
&= \xi^2\left(\tfrac{-B^+(-B^+)}{(B^+)^2}+\tfrac{2B^+(-B^+)(\xi-1)}{(B^+)^2}\right) \quad \text{if } 0\le\xi\le 1,\\
&= \xi^2(1-2(\xi-1)) \quad 0\le\xi\le 1,\\
&= \xi^2-2\xi^3+2\xi^2)) \quad 0\le\xi\le 1,\\
&= -2\xi^3+3\xi^2 \quad \text{if } 0\le\xi\le 1,\\
&= N_3(\xi).
\end{aligned}$$

$$\begin{aligned}
\lim_{\alpha\to 0}\widetilde{N}_4(\xi) &= \lim_{\alpha\to 0}\begin{cases} \xi^2(c_4+d_4(\xi-\alpha)) & \text{if } 0\le\xi\le 1,\\ (\xi-1)+(\xi-1)^2(g_4+h_4(\xi-\alpha)) & \text{if } 0\le\xi\le 1,\end{cases}\\
&= (\xi-1)+(\xi-1)^2(g_4|_0+h_4|_0(\xi-\alpha)) \quad 0\le\xi\le 1,\\
&= (\xi-1)+(\xi-1)^2\left(\tfrac{-B^-(-B^-)}{(B^-)^2}+\tfrac{B^-(B^-)(\xi)}{(B^-)^2}\right) \quad 0\le\xi\le 1,
\end{aligned}$$

$$
\begin{aligned}
&= (\xi-1)+(\xi-1)^2(1+\xi) \quad 0\le\xi\le 1,\\
&= (\xi-1)(1+\xi^2-1) \quad 0\le\xi\le 1,\\
&= \xi^3-\xi^2 \quad 0\le\xi\le 1,\\
&= N_4(\xi).
\end{aligned}
$$

$$
\begin{aligned}
\lim_{\alpha\to 1}\widetilde{N}_4(\xi) &= \lim_{\alpha\to 1}\begin{cases} \xi^2(c_4+d_4(\xi-\alpha)) & \text{if } 0\le\xi\le\alpha,\\ (\xi-1)+(\xi-1)^2(g_4+h_4(\xi-\alpha)) & \text{if } \alpha\le\xi\le 1,\end{cases}\\
&= \xi^2(c_4|_1+d_4|_1(\xi-1)) \quad \text{if } 0\le\xi\le 1,\\
&= \xi^2\left(\tfrac{B^+((-B^++B^-)+(-2B^-+2B^+)+B^-)(\xi-1)}{(B^+)^2}\right) \quad 0\le\xi\le 1,\\
&= \xi^2\left(\tfrac{B^+(B^+)(\xi-1)}{(B^+)^2}\right) \quad 0\le\xi\le 1,\\
&= \xi^2(\xi-1) \quad 0\le\xi\le 1,\\
&= \xi^3-\xi^2 \quad 0\le\xi\le 1,\\
&= N_4(\xi).
\end{aligned}
$$

Thus (I) is proved.

■

Again, before proving (II), we will first show that if $B^- = b = B^+$ then $D = b^2$, for the convenience of proving (II).

Lemma 3.2.2 *If $B^- = b = B^+$ then D defined in (3.8) becomes b^2.*

Proof: Suppose $B^- = b = B^+$, then

$$
\begin{aligned}
D &= (\alpha-1)^4(B^-)^2 - 2B^-B^+\alpha(\alpha-1)(\alpha^2-\alpha+2)+\alpha^4(B^+)^2\\
&= (\alpha-1)^4b^2 - 2b^2\alpha(\alpha-1)(\alpha^2-\alpha+2)+\alpha^4b^2\\
&= b^2((\alpha-1)^4 - 2\alpha(\alpha-1)(\alpha^2-\alpha+2)+\alpha^4))\\
&= b^2(\alpha^4-4\alpha^3+6\alpha^2-4\alpha+1-2\alpha^4+4\alpha^3-6\alpha^2+4\alpha+\alpha^4)\\
&= b^2.
\end{aligned}
$$

■

Now we are ready to prove (II).

Theorem 3.2.2 *If the coefficients B^- and B^+ across the interface are the same, then the immersed Hermite cubic nodal basis functions become the usual Hermite nodal basis functions.*

Proof: Suppose $B^- = B^+ = b$, then

$$\begin{aligned}
\widetilde{N}_1(\xi) &= \begin{cases} 1+\xi^2(c_1+d_1(\xi-\alpha)) & \text{if } 0\le\xi\le\alpha, \\ (\xi-1)^2(g_1+h_1(\xi-\alpha)) & \text{if } \alpha\le\xi\le 1, \end{cases} \\
&= \begin{cases} 1+\xi^2\left(\frac{b(b(\alpha+3)(\alpha-1)-\alpha^2 b)}{D}-\frac{2b(\alpha b-b-\alpha b)(\xi-\alpha)}{D}\right) & \text{if } 0\le\xi\le\alpha, \\ (\xi-1)^2\left(\frac{b(-2\alpha b+b-\alpha^2 b+b\alpha^2+4\alpha b)}{D}-\frac{2b((\alpha-1)b-\alpha b)(\xi-\alpha)}{D}\right) & \text{if } \alpha\le\xi\le 1, \end{cases} \\
&= \begin{cases} 1+\xi^2\left(\frac{b(b(\alpha+3)(\alpha-1)-\alpha^2 b)}{b^2}-\frac{2b(\alpha b-b-\alpha b)(\xi-\alpha)}{b^2}\right) & \text{if } 0\le\xi\le\alpha, \\ (\xi-1)^2\left(\frac{b(-2\alpha b+b-\alpha^2 b+b\alpha^2+4\alpha b)}{b^2}-\frac{2b((\alpha-1)b-\alpha b)(\xi-\alpha)}{b^2}\right) & \text{if } \alpha\le\xi\le 1, \end{cases} \\
&= \begin{cases} 1+\xi^2(((\alpha+3)(\alpha-1)-\alpha^2)+2(\xi-\alpha)) & \text{if } 0\le\xi\le\alpha, \\ (\xi-1)^2(1+2\alpha+2(\xi-\alpha)) & \text{if } \alpha\le\xi\le 1, \end{cases} \\
&= \begin{cases} 1+\xi^2(-3+2\xi) & \text{if } 0\le\xi\le\alpha, \\ (\xi-1)^2(1+2\xi) & \text{if } \alpha\le\xi\le 1, \end{cases} \\
&= \begin{cases} 2\xi^3-3\xi^2+1 & \text{if } 0\le\xi\le\alpha, \\ 2\xi^3-3\xi^2+1 & \text{if } \alpha\le\xi\le 1, \end{cases} \\
&= N_1(\xi).
\end{aligned}$$

$$\begin{aligned}
\widetilde{N}_2(\xi) &= \begin{cases} \xi+\xi^2(c_2+d_2(\xi-\alpha)) & \text{if } 0\le\xi\le\alpha, \\ (\xi-1)^2(g_2+h_2(\xi-\alpha)) & \text{if } \alpha\le\xi\le 1, \end{cases} \\
&= \begin{cases} \xi+\xi^2\left(\frac{B^+(\alpha^3(-B^++B^-)+(\alpha-2)B^-)}{D}-\frac{B^+(B^-\alpha^2-B^--\alpha^2B^+)(\xi-\alpha)}{D}\right) & \text{if } 0\le\xi\le\alpha, \\ (\xi-1)^2\left(\frac{\alpha B^-(-\alpha B^+(-2+\alpha)+B^-(\alpha-1)^2)}{D}-\frac{B^-(B^-\alpha^2-B^--\alpha^2B^+)(\xi-\alpha)}{D}\right) & \text{if } \alpha\le\xi\le 1, \end{cases} \\
&= \begin{cases} \xi+\xi^2(-2+\xi) & \text{if } 0\le\xi\le\alpha, \\ (\xi-1)^2(\alpha(-\alpha(-2+\alpha)+(\alpha-1)^2)+(\xi-\alpha)) & \text{if } \alpha\le\xi\le 1, \end{cases} \\
&= \begin{cases} \xi^3-2\xi^2+\xi & \text{if } 0\le\xi\le\alpha, \\ \xi^3-2\xi^2+\xi & \text{if } \alpha\le\xi\le 1, \end{cases} \\
&= N_2(\xi).
\end{aligned}$$

$$\begin{aligned}
\widetilde{N}_3(\xi) &= \begin{cases} \xi^2(c_3+d_3(\xi-\alpha)) & \text{if } 0\le\xi\le\alpha, \\ 1+(\xi-1)^2(g_3+h_3(\xi-\alpha)) & \text{if } \alpha\le\xi\le 1, \end{cases} \\
&= \begin{cases} \xi^2\left(\frac{-b((-b+b)\alpha^2+B^-(2\alpha-3))}{D}+\frac{2b(\alpha b-b-\alpha b)(\xi-\alpha)}{D}\right) & \text{if } 0\le\xi\le\alpha, \\ 1+(\xi-1)^2\left(\frac{-b(-2\alpha b+b-\alpha^2 b+b\alpha^2+4\alpha b)}{D}+\frac{2B^-(\alpha b-b-\alpha b)(\xi-\alpha)}{D}\right) & \text{if } \alpha\le\xi\le 1, \end{cases} \\
&= \begin{cases} \xi^2(-(2\alpha-3)-2(\xi-\alpha)) & \text{if } 0\le\xi\le\alpha, \\ 1+(\xi-1)^2(-1-2\xi) & \text{if } \alpha\le\xi\le 1, \end{cases} \\
&= \begin{cases} \xi^2(3-2\xi)) & \text{if } 0\le\xi\le\alpha, \\ 1+(\xi^2-2\xi+1)(-1-2\xi) & \text{if } \alpha\le\xi\le 1, \end{cases} \\
&= \begin{cases} -2\xi^3+3\xi^2 & \text{if } 0\le\xi\le\alpha, \\ -2\xi^3+3\xi^2 & \text{if } \alpha\le\xi\le 1, \end{cases}
\end{aligned}$$

$$= \quad N_3(\xi).$$

$$\begin{aligned}
\widetilde{N}_4(\xi) &= \begin{cases} \xi^2(c_4 + d_4(\xi-\alpha)) & \text{if } 0 \le \xi \le \alpha, \\ (\xi-1) + (\xi-1)^2(g_4 + h_4(\xi-\alpha)) & \text{if } \alpha \le \xi \le 1. \end{cases} \\
&= \begin{cases} \xi^2\left(\frac{-b(\alpha-1)(-b)}{D} + \frac{b(b)(\xi-\alpha)}{D}\right) & \text{if } 0 \le \xi \le \alpha, \\ (\xi-1) + (\xi-1)^2\left(\frac{-b((3b-4b)\alpha-b)}{D} + \frac{b(b)(\xi-\alpha)}{D}\right) & \text{if } \alpha \le \xi \le 1. \end{cases} \\
&= \begin{cases} \xi^2((\alpha-1) + (\xi-\alpha)) & \text{if } 0 \le \xi \le \alpha, \\ (\xi-1) + (\xi-1)^2(1+\xi) & \text{if } \alpha \le \xi \le 1. \end{cases} \\
&= \begin{cases} \xi^2(-1+\xi) & \text{if } 0 \le \xi \le \alpha, \\ \xi - 1 + (\xi^2 - 2\xi + 1)(1+\xi) & \text{if } \alpha \le \xi \le 1. \end{cases} \\
&= \begin{cases} \xi^3 - \xi^2 & \text{if } 0 \le \xi \le \alpha, \\ \xi^3 - \xi^2 & \text{if } \alpha \le \xi \le 1. \end{cases} \\
&= N_4(\xi).
\end{aligned}$$

Thus (II) is proved.

■

Therefore, by the properties of transformation on $N_i(\xi) \to \psi_i(x)$ and $\widetilde{N}_i(\xi) \to \widetilde{\psi}_i(x)$, it follows that $\widetilde{\psi}_i(x)$ reduces to $\psi_i(x)$ when the interface α is such that $\alpha \to x_l$ or $\alpha \to x_r$, and when the piecewise constant coefficients are equal over the interface α, for α in the interval $[x_l, x_r]$.

3.3 The immersed Hermite finite element solution

In this section, we will discuss the immerse Hermite finite element solution to our BVP (1.2) and (1.4). Recall that the weak form for this boundary value problem is listed in (2.12) as:

Find $w \in S = \{w | w \in H^2, w(0) = b_1, w'(0) = b_2, w(1) = b_3, w'(1) = b_4\}$ such that
$\int_0^1 v''(x)B(x)w''(x)dx = \int_0^1 v(x)f(x)dx,$
for any $v \in T = \{w | w \in H^2, w(0) = w(1) = w'(0) = w'(1) = 0\}$,

Since the immersed Hermite cubic finite element space defined in Section 3.1 is a subspace of H^2, we can use its basis functions to form the immersed Hermite cubic finite element spaces for both of our test function space and trial function set. Specifically, we let

$$\begin{aligned}
S_h(\overline{\Omega}) &= span\{\widetilde{\phi}_1, \widetilde{\phi}_2, \cdots, \widetilde{\phi}_{2n-1}, \widetilde{\phi}_{2n}\} \cap S, \\
T_h(\overline{\Omega}) &= span\{\widetilde{\phi}_3, \widetilde{\phi}_4, \cdots, \widetilde{\phi}_{2n-3}, \widetilde{\phi}_{2n-2}\} \subset T.
\end{aligned}$$

Using this weak form of the BVP and following the same framework in Section 2.3.2, we can obtain the IFE equation for our BVP in vector form as follows:

$$K\vec{u} = \vec{f} + \vec{B}_e, \tag{3.11}$$

where

$$\begin{aligned}
\vec{u} &= (u_i)_{i=3}^{2n-2}, \widetilde{u}_h(x) = \sum_{j=1}^{2n} u_j \widetilde{\phi}_j(x) \\
K &= (K_{i,j})_{i=3,j=3}^{2n-2}, K_{i,j} = \int_0^1 \widetilde{\phi}_i''(x) B(x) \widetilde{\phi}_j''(x) dx \\
\vec{f} &= \left(\int_0^1 \widetilde{\phi}_i(x) f(x) dx \right)_{i=3}^{2n-2}, \\
\vec{B}_e &= (B_{e,i})_{i=3}^{2n-2}, \text{ where } B_{e,i} = -b_1 K_{i,1} - b_2 K_{i,2} - b_3 K_{i,2n-1} - b_4 K_{i,2n}.
\end{aligned}$$

We should note that when h is small, K is a banded matrix, and most of the entries of B_e are zero. In addition, the matrix K can also assembled by the local matrix K_{e_k} with the standard procedure, where

$$\begin{aligned}
K_{e_k} &= (K_{e_k,i,j})_{i,j=1}^{4}, \\
K_{e_k,i,j} &= \int_{e_k} \widetilde{\phi}_{k,i}''(x) B(x) \widetilde{\phi}_{k,j}''(x) dx, i, j = 1, 2, 3, 4.
\end{aligned}$$

Over most of the elements, $K_{e_k,i,j}$ can be computed in the same way as for the standard Hermite local basis functions. However, if $e_k = [x_k, x_{k+1}]$ is an interface-element, we calculate the entries of K_{e_k} as follows:

$$K_{e_k,i,j} = \int_{x_k}^{\alpha} \widetilde{\phi}_{k,i}''(x) B(x) \widetilde{\phi}_{k,j}''(x) dx + \int_{\alpha}^{x_{k+1}} \widetilde{\phi}_{k,i}''(x) B(x) \widetilde{\phi}_{k,j}''(x) dx,$$

for $i = 1, 2, 3, 4$ and $j = 1, 2, 3, 4$. A similar piecewise integration procedure applies to the components of $\vec{f}$.

By solving the linear system in (3.11), we will obtain the vector $\vec{u}$ which can then be used to form the immersed finite element solution:

$$\widetilde{u}_h(x) = u_1 \widetilde{\phi}_1(x) + u_2 \widetilde{\phi}_2(x) + \ldots + u_{2n-1} \widetilde{\phi}_{2n-1}(x) + u_{2n} \widetilde{\phi}_{2n}(x).$$

Since $\widetilde{u}_h$ is an approximation of w, we would like to know the accuracy of $\widetilde{u}_h$. Since the Hermite finite element space has an accuracy of $||w - u_h||_0 \leq Ch^4$ and $|w - u_h|_2 \leq Ch^2$, we would like to know if our immersed Hermite finite element solution also has this accuracy, i,e., $||w - \widetilde{u}_h||_0 \leq Ch^4$ and $|w - \widetilde{u}_h|_2 \leq Ch^2$. We will investigate this numerically in the next two sections.

3.4 Approximation capability of the Hermite cubic IFE space

In this subsection, we numerically investigate the approximation orders of the interpolation in the IFE space. Our main goal is to identify the order of accuracy of the immersed Hermite cubic finite element space with rigid interface connection condition from the point of view of interpolation.

To investigate the order of accuracy of IFE methods developed here, we first create a function $u(x)$ that satisfies the rigid interface condition. Specifically, we let

$$u(x) = \begin{cases} a\cos(x) + b\sin(x) & \text{if } 0 \le x < \alpha, \\ ce^x + dx^3 + 5 & \text{if } \alpha \le x \le 1 \end{cases} \tag{3.12}$$

and

$$B(x) = \begin{cases} B^-, & 0 \le x < \alpha, \\ B^+, & \alpha < x \le 1. \end{cases} \tag{3.13}$$

We determine the constants a, b, c, and d such that $u(x)$ satisfies the rigid connection condition:

$$\begin{aligned} u(\alpha-) &= u(\alpha+), \\ u'(\alpha-) &= u'(\alpha+), \\ B(\alpha-)u''(\alpha-) &= B(\alpha+)u''(\alpha+), \\ (B(\alpha-)u''(\alpha-))' &= (B(\alpha+)u''(\alpha+))'. \end{aligned}$$

These equations lead to

$$\begin{aligned} a\cos(\alpha) + b\sin(\alpha) &= ce^\alpha + d\alpha^3 + 5, \\ -a\sin(\alpha) + b\cos(\alpha) &= ce^\alpha + 3d\alpha^2, \\ B^-(-a\cos(\alpha) - b\sin(\alpha)) &= B^+(ce^\alpha + 6d\alpha), \\ B^-(a\sin(\alpha) - b\cos(\alpha)) &= B^+(ce^\alpha + 6d). \end{aligned}$$

By putting the above equations into the matrix form, it becomes:

$$\begin{pmatrix} \cos(\alpha) & \sin(\alpha) & -e^\alpha & -\alpha^3 \\ -\sin(\alpha) & \cos(\alpha) & -e^\alpha & -3\alpha^2 \\ -B^-\cos(\alpha) & -B^-\sin(\alpha) & -B^+(e^\alpha) & -6B^+\alpha \\ B^-\sin(\alpha) & -B^-\cos(\alpha) & -B^+(e^\alpha) & -6B^+ \end{pmatrix} \begin{pmatrix} a \\ b \\ c \\ d \end{pmatrix} = \begin{pmatrix} 5 \\ 0 \\ 0 \\ 0 \end{pmatrix}. \tag{3.14}$$

Generally, the determinant of the matrix above does not equal zero for arbitrary α, B^- and B^+ chosen.

Here, we will conduct several experiments with a fixed interface at $\alpha = \pi/6$ and choose

$$\begin{aligned}&\text{Case 1: } B^- = 2, B^+ = 5,\\ &\text{Case 2: } B^- = 2, B^+ = 500,\\ &\text{Case 3: } B^- = 2, B^+ = 50000.\end{aligned}$$

These configurations are chosen to represent small, moderate, and large discontinuities of the coefficient.

In each of these cases, we let $h = \frac{1}{10 \cdot 2^{i-1}}$, $i = 1, 2, \ldots, 8$ to generate $\widetilde{I_h u}(x) \in \widetilde{S}_h(\overline{\Omega})$. We then compute the actual errors in various commonly used norms or semi-norms. Let error in the interpolation by using the IFE space be $\widetilde{E}_h$, then we expect $\widetilde{E}_h \approx Ch^r$, where r is the order of accuracy. By taking the natural log of both sides of the expression $\widetilde{E}_h \approx Ch^r$, we get $\ln(\widetilde{E}_h) \approx \ln|C| + r\ln(h)$. Then the values C and r can be determined by applying the linear regression on a set of values of $\ln(\widetilde{E}_h)$ and $\ln(h)$ generated by the numerical experiments.

The related data for each of the cases are listed in Tables 7.1, 7.2, and 7.3; the constant C and the order of accuracy r for each norm and semi-norms taken on $\widetilde{E} = |u(x) - \widetilde{I_h u}(x)|$ are found as follows:

For Case 1:

$$\begin{aligned}||\widetilde{E}||_0 &\approx 5.3522 \times 10^{-003} h^{3.9983},\\ |\widetilde{E}|_1 &\approx 1.8675 \times 10^{-002} h^{3.0003},\\ |\widetilde{E}|_2 &\approx 1.2123 \times 10^{-001} h^{2.0006}.\end{aligned}$$

For Case 2:

$$\begin{aligned}||\widetilde{E}||_0 &\approx 5.3945 \times 10^{-003} h^{3.9888},\\ |\widetilde{E}|_1 &\approx 1.9077 \times 10^{-002} h^{2.9943},\\ |\widetilde{E}|_2 &\approx 1.2415 \times 10^{-001} h^{1.9950}.\end{aligned}$$

For Case 3:

$$\begin{aligned}||\widetilde{E}||_0 &\approx 5.4416 \times 10^{-003} h^{3.9896},\\ |\widetilde{E}|_1 &\approx 1.9166 \times 10^{-002} h^{2.9939},\\ |\widetilde{E}|_2 &\approx 1.2470 \times 10^{-001} h^{1.9947}.\end{aligned}$$

It is important to note that in all of these experiments, the orders of accuracy of the Hermite cubic immersed finite element space in $H^s(0,1), s = 0, 1, 2$ norms match that of the standard Hermite cubic finite element space. This strongly suggests that our IFE space have an approximation capability similar to the standard Hermite cubic finite element space.

The data $\left|\left|u(x) - \widetilde{I_h u}(x)\right|\right|$, $\left|\left|u'(x) - \widetilde{I_h u}'(x)\right|\right|$, and $\left|\left|u''(x) - \widetilde{I_h u}''(x)\right|\right|$ for each case and for each h are shown in the appendix.

3.5 Accuracy of the IFE solution of the interface beam problem

In this section, we numerically investigate the order of accuracy of the Hermite cubic IFE solution to the interface beam problem. First, we set up an interface beam problem to which we know the exact solution. Here, we will choose a function $w(x)$ and then find $f(x)$ such that $(B(x)w''(x))'' = f(x)$ with $B(x)$ as piecewise continuous constants. For simplicity, we choose $x \in \Omega = [0, 1]$ and the interface, α, in (0, 1). Let

$$w(x) = \begin{cases} a\cos(x) + b\sin(x) & \text{if } 0 \le x < \alpha, \\ ce^x + dx^3 + 5 & \text{if } \alpha \le x \le 1 \end{cases} \tag{3.15}$$

and

$$B(x) = \begin{cases} B^-, & 0 \le x < \alpha, \\ B^+, & \alpha \le x \le 1, \end{cases} \tag{3.16}$$

Then

$$(B(x)w(x)'')'' = f(x) = \begin{cases} B^-(a\cos(x) + b\sin(x)) & \text{if } 0 \le x < \alpha, \\ B^+(ce^x) & \text{if } \alpha \le x \le 1 \end{cases} \tag{3.17}$$

Then, we determine the constants a, b, c, and d such that $w(x)$ satisfies the rigid connection condition:

$$\begin{aligned} w(\alpha-) &= w(\alpha+), \\ w'(\alpha-) &= w'(\alpha+), \\ B(\alpha-)w''(\alpha-) &= B(\alpha+)w''(\alpha+), \\ (B(\alpha-)w''(\alpha-)' &= (B(\alpha+)w''(\alpha+)', \end{aligned}$$

or

$$\begin{aligned} a\cos(\alpha) + b\sin(\alpha) &= ce^\alpha + d\alpha^3 + 5, \\ -a\sin(\alpha) + b\cos(\alpha) &= ce^\alpha + 3d\alpha^2, \\ B^-(-a\cos(\alpha) - b\sin(\alpha)) &= B^+(ce^\alpha + 6d\alpha), \\ B^-(a\sin(\alpha) - b\cos(\alpha)) &= B^+(ce^\alpha + 6d). \end{aligned}$$

Putting the equations above into matrix form, it becomes:

$$\begin{pmatrix} \cos(\alpha) & \sin(\alpha) & -e^\alpha & -\alpha^3 \\ -\sin(\alpha) & \cos(\alpha) & -e^\alpha & -3\alpha^2 \\ -B^-\cos(\alpha) & -B^-\sin(\alpha) & -B^+(e^\alpha) & -6B^+\alpha \\ B^-\sin(\alpha) & -B^-\cos(\alpha) & -B^+(e^\alpha) & -6B^+ \end{pmatrix} \begin{pmatrix} a \\ b \\ c \\ d \end{pmatrix} = \begin{pmatrix} 5 \\ 0 \\ 0 \\ 0 \end{pmatrix}. \tag{3.18}$$

Generally, the determinant of the matrix above does not equal zero for arbitrary α, B^- and B^+ chosen.

So the boundary value problem for our numerical experiments becomes:

Find $w(x)$ such that

$$\begin{array}{ll} (B^- w''(x))'' = B^-(a\cos(x) + b\sin(x)), & 0 \le x < \pi/6 \\ (B^+ w''(x))'' = B^+(6ce^x), & \pi/6 \le x \le 1 \end{array} \tag{3.19}$$

and

$$w(0) = a, \quad w'(0) = b, \quad w(1) = ce + d + 5, \quad w'(1) = ce + 3d, \tag{3.20}$$

where the constants, a, b, c, and d comprise the solution of the matrix equation in (3.18).

In the following numerical experiments, we let $\alpha = \pi/6$ and choose

$$\begin{aligned} &\text{Case 1: } B^- = 2, B^+ = 5, \\ &\text{Case 2: } B^- = 2, B^+ = 500, \\ &\text{Case 3: } B^- = 2, B^+ = 50000. \end{aligned}$$

And in each of the cases, we let $h = \frac{1}{5i}$, $i = 1, 2, \ldots, 10$. As before, we let the error in the IFE solution be E_h, then we expect $E_h \approx Ch^r$, where r is the order of convergence. Since $E_h \approx Ch^r$, by taking the natural log of both sides of $E_h \approx Ch^r$, we get $\ln(E_h) \approx \ln|C| + r\ln(h)$. Then the values C and r can be determined by using a least squares linear regression on a set of values of $\ln(E_h)$, and $\ln(h)$ generated for each of h. The error for $||w(x) - \widetilde{w}_h(x)||$, $||w'(x) - \widetilde{w}'_h(x)||$, and $||w'(x) - \widetilde{w}'_h(x)||$ for each h are shown in Table 7.4, 7.5, and 7.6 in the Appendix chapter. The order of convergence, r, and C for each of the cases are as follows:

For Case 1:

$$\begin{aligned} ||\widetilde{E}||_0 &\approx 5.0140 \times 10^{-003} h^{3.9797}, \\ |\widetilde{E}|_1 &\approx 1.7440 \times 10^{-002} h^{2.9809}, \\ |\widetilde{E}|_2 &\approx 1.1370 \times 10^{-001} h^{1.9825}. \end{aligned}$$

For Case 2:

$$\begin{aligned} ||\widetilde{E}||_0 &\approx 4.5946 \times 10^{-003} h^{3.9373}, \\ |\widetilde{E}|_1 &\approx 1.6671 \times 10^{-002} h^{2.9546}, \\ |\widetilde{E}|_2 &\approx 1.1014 \times 10^{-001} h^{1.9596}. \end{aligned}$$

For Case 3:

$$\begin{aligned} ||\widetilde{E}||_0 &\approx 4.8851e-003 h^{3.9314}, \\ |\widetilde{E}|_1 &\approx 1.6759e-002 h^{2.9541}, \\ |\widetilde{E}|_2 &\approx 1.1061e-001 h^{1.9592}. \end{aligned}$$

It is important to note that in all of these experiments, the orders of accuracy of the Hermite cubic IFE solution in $H^s(0,1), s = 0, 1, 2$ norms match that of the standard Hermite cubic finite element solution. This strongly suggests that our IFE space has an approximation capability similar to the standard Hermite cubic finite element space.

3.6 Accuracy of the Hermite cubic IFE Space with multiple interfaces

In this subsection, we discuss the accuracy of the Hermite cubic IFE space for the interface beam problem that contains multiple interfaces. To investigate the order of accuracy, we first set up an interface beam problem to which we know the exact solution. We will choose a function $w(x)$, and find $f(x)$ such that $(B(x)w''(x))'' = f(x)$ with $B(x)$ as piecewise continuous constants. For simplicity, we choose $\Omega = (0,1)$ and the interfaces, α, β, in (0, 1) such that $\alpha < \beta$ and no element e_k contains both α and β. We let

$$w(x) = \begin{cases} a\cos(x) + b\sin(x) & \text{if } 0 \le x < \alpha, \\ ce^x + dx^3 + 5 & \text{if } \alpha \le x < \beta, \\ sx^{-1} + tx^2 + ux + v & \text{if } \beta \le x \le 1 \end{cases} \tag{3.21}$$

$$B(x) = \begin{cases} B_1, & 0 \le x < \alpha, \\ B_2, & \alpha \le x < \beta, \\ B_3, & \beta \le x \le 1. \end{cases} \tag{3.22}$$

Then

$$(B(x)w(x)'')'' = f(x) = \begin{cases} B_1(a\cos(x) + b\sin(x)) & \text{if } 0 \le x < \alpha, \\ B_2(ce^x) & \text{if } \alpha \le x < \beta, \\ B_3(24sx^{-5}) & \text{if } \beta \le x \le 1. \end{cases} \tag{3.23}$$

Now, we find the constants a, b, c, d, s, t, u and v such that $w(x)$ satisfies the rigid connection condition:

$$\begin{aligned} w(\alpha-) &= w(\alpha+), \\ w'(\alpha-) &= w'(\alpha+), \\ B(\alpha-)w''(\alpha-) &= B(\alpha+)w''(\alpha+), \\ (B(\alpha-)w''(\alpha-))' &= (B(\alpha+)w''(\alpha+))'. \end{aligned}$$

and

$$\begin{aligned} w(\beta-) &= w(\beta+), \\ w'(\beta-) &= w'(\beta+), \\ B(\beta-)w''(\alpha-) &= B(\beta+)w''(\beta+), \\ (B(\beta-)w''(\beta-))' &= (B(\beta+)w''(\beta+))', \end{aligned}$$

or

$$\begin{aligned} a\cos(\alpha) + b\sin(\alpha) &= ce^{\alpha} + d\alpha^3 + 5, \\ -a\sin(\alpha) + b\cos(\alpha) &= ce^{\alpha} + 3d\alpha^2, \\ B_1(-a\cos(\alpha) - b\sin(\alpha)) &= B_2(ce^{\alpha} + 6d\alpha), \\ B_1(a\sin(\alpha) - b\cos(\alpha)) &= B_2(ce^{\alpha} + 6d). \end{aligned}$$

and

$$\begin{aligned} ce^{\beta} + d\beta^3 + 5 &= s\beta^{-1} + t\beta^2 + u\beta + v, \\ ce^{\beta} + d(3\beta^2) &= -s\beta^{-2} + 2t\beta + u, \\ B_2(ce^{\beta} + d(6\beta)) &= B_3(2s\beta^{-3} + 2t), \\ B_2(ce^{\beta} + 6d) &= B_3(-6s\beta^{-4}). \end{aligned}$$

By putting the above equations into the form of a linear system, we get:

$$\begin{pmatrix} \cos(\alpha) & \sin(\alpha) & -e^{\alpha} & -\alpha^3 \\ -\sin(\alpha) & \cos(\alpha) & -e^{\alpha} & -3\alpha^2 \\ -B^{-}\cos(\alpha) & -B^{-}\sin(\alpha) & -B^{+}(e^{\alpha}) & -6B^{+}\alpha \\ B^{-}\sin(\alpha) & -B^{-}\cos(\alpha) & -B^{+}(e^{\alpha}) & -6B^{+} \end{pmatrix} \begin{pmatrix} a \\ b \\ c \\ d \end{pmatrix} = \begin{pmatrix} 5 \\ 0 \\ 0 \\ 0 \end{pmatrix}.$$

and

$$\begin{pmatrix} \beta^{-1} & \beta^2 & \beta & 1 \\ -\beta^{-2} & 2\beta & 1 & 0 \\ 2B_3\beta^{-3} & 2B_3 & 0 & 0 \\ -6B_3\beta^{-4} & 0 & 0 & 0 \end{pmatrix} \begin{pmatrix} s \\ t \\ u \\ v \end{pmatrix} = \begin{pmatrix} ce^{\beta} + d\beta^3 + 5 \\ ce^{\beta} + 3d\beta^2 \\ B_2ce^{\beta} + 6B_2d\beta \\ B_2ce^{\beta} + 6B_2d \end{pmatrix}.$$

Generally, the determinant of the matrices above does not equal zero for arbitrary α, β, B_1, B_2, and B_3 chosen. Notice that a, b, c, d, s, t, u, and v can be found by solving the first system of equations and then solving the second system of equations.

So the boundary value problem becomes:

Find $w(x)$ such that

$$\begin{aligned} &(B_1w''(x))'' = B_1(a\cos(x) + b\sin(x)), && 0 \le x < \pi/12 \\ &(B_2w''(x))'' = B_2(ce^{x}), && \pi/12 \le x < \pi/6 \\ &(B_3w''(x))'' = B_3(24sx^{-5}), && \pi/6 \le x \le 1 \end{aligned}$$

and

$$w(0) = a, \quad w'(0) = b, \quad w(1) = s + t + u + v, \quad w'(1) = -s + 2t + u.$$

In the following numerical experiment, we choose $\alpha = \pi/12$, $\beta = \pi/6$ and

$$\begin{aligned}&\text{Case 1: } B_1 = 2, B_2 = 5, B_3 = 2.\\ &\text{Case 2: } B_1 = 2, B_2 = 5, B_3 = 200.\\ &\text{Case 3: } B_1 = 2, B_2 = 5, B_3 = 20000.\end{aligned}$$

In each of the cases, we let $h = \frac{1}{5i}$, $i = 1, 2, \ldots, 12$. Let error in the IFE solution be E_h, then $E_h \approx Ch^r$, where r is the order of convergence which can be determined by numerical data as before. The data for $||w(x) - \widetilde{w}_h(x)||$, $||w'(x) - \widetilde{w}'_h(x)||$, and $||w''(x) - \widetilde{w}''_h(x)||$ for each of the cases are shown in Tables 7.7, 7, and 7.9 of the Appendix section.

According to these data, the order of convergence, r, and C for each case are as follows:

For Case 1:

$$\begin{aligned}||\widetilde{E}||_0 &\approx 3.3334 \times 10^{-003} h^{3.9834},\\ |\widetilde{E}|_1 &\approx 1.1622 \times 10^{-002} h^{2.9850},\\ |\widetilde{E}|_2 &\approx 7.6690 \times 10^{-002} h^{1.9895}.\end{aligned}$$

For Case 2:

$$\begin{aligned}||\widetilde{E}||_0 &\approx 2.5621 \times 10^{-003} h^{3.9271},\\ |\widetilde{E}|_1 &\approx 9.0631 \times 10^{-003} h^{2.9339},\\ |\widetilde{E}|_2 &\approx 5.9600 \times 10^{-002} h^{1.9375}.\end{aligned}$$

For Case 3:

$$\begin{aligned}||\widetilde{E}||_0 &\approx 2.7994 \times 10^{-003} h^{3.9649},\\ |\widetilde{E}|_1 &\approx 9.0196 \times 10^{-003} h^{2.9326},\\ |\widetilde{E}|_2 &\approx 5.9407 \times 10^{-002} h^{1.9367}.\end{aligned}$$

Thus, our numerical data suggest that for multiple interfaces, the order of accuracy for each of the norms and the semi-norms remains the same, as in the case of only one interface involved.

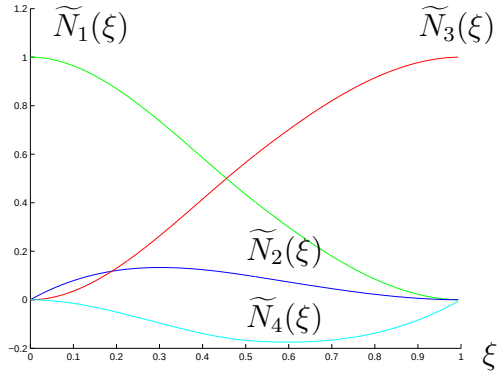

Figure 3.1: The immersed Hermite cubic local nodal basis functions $\widetilde{N}_i(\xi)$, $i = 1, 2, 3, 4$ with $B^- = 2$, $B^+ = 5$ and $\alpha = \pi/6$.

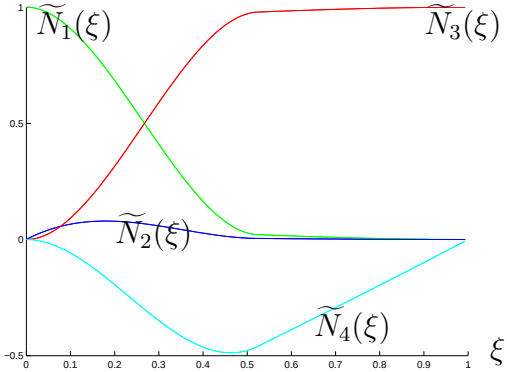

Figure 3.2: The immersed Hermite cubic local nodal basis functions $\widetilde{N}_i(\xi)$, $i = 1, 2, 3, 4$ with $B^- = 2$, $B^+ = 500$ and $\alpha = \pi/6$.

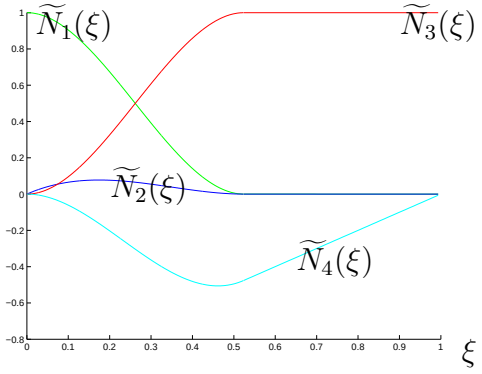

Figure 3.3: The immersed Hermite cubic local nodal basis functions $\widetilde{N}_i(\xi)$, $i = 1, 2, 3, 4$ with $B^- = 2$, $B^+ = 50000$ and $\alpha = \pi/6$.

Chapter 4

Solving the Inverse Problem by the Immersed Finite Element Space

In this chapter we will apply the immersed Hermite cubic IFE space to solve an interface inverse problem of the beam equation numerically. The uses of one uniform mesh in the iteration procedure for the solution of interface problems with the interface parameter (i.e., the position of α) being adjusted makes the use of the immersed Hermite cubic IFE space desirable.

4.1 A procedure for solving the inverse problem

In this section, we will develop a sequence of procedures that will generate the solution to our inverse problem. First, let us recall our model beam interface problem: find w such that

$$\begin{array}{c}(B(x)w''(x))'' = f(x), x \in \Omega = (0,1), \\ w(0) = b_1, w'(0) = b_2, w(1) = b_3, w'(1) = b_4,\end{array} \tag{4.1}$$

where

$$B(x) = \begin{cases} B^-, & 0 \le x < \alpha, \\ B^+, & \alpha < x \le 1. \end{cases}$$

Now, let us consider an inverse beam interface problem as follows:

Given b_1, b_2, b_3, b_4, B^-, B^+, f, and partial information about w: $B(1)w''(1) \approx \gamma$ (i.e., the bending moment at the right end of the beam is γ), our inverse problem is to find all $\alpha^* \in \Omega$ such that

$$g(\alpha^*) \equiv B(1)w''(1, \alpha^*) = \gamma \tag{4.2}$$

if possible; otherwise, find $\alpha^* \in \Omega$ for which

$$|g(\alpha^*) - \gamma| < |g(\alpha) - \gamma|, \qquad \forall \alpha \in \Omega. \tag{4.3}$$

However, instead of solving $g(\alpha)$ directly and finding the solution to the inverse problem, we will solve it numerically with

$$g_h(\alpha_h) \equiv B(1)\widetilde{w}_h''(1, \alpha_h) \approx g(\alpha) = B(1)w''(1, \alpha),$$

and find the solution to our inverse problem as:

Find all $\alpha_h^* \in \Omega$ such that

$$g_h(\alpha_h^*) = \gamma \tag{4.4}$$

if possible; otherwise, find $\alpha_h^* \in \Omega$ for which

$$|g_h(\alpha_h^*) - \gamma| < |g_h(\alpha) - \gamma|, \qquad \forall \alpha \in \Omega. \tag{4.5}$$

Thus, there are two cases involved in solving our inverse problem. In the first case, we try to find all the α^* that satisfies (4.4). In the second case, we assume that there are no α^* satisfying (4.4), then we try to find α_h^* that satisfies (4.5).

In the first case, the solution α_h^* exists if

$$\gamma \in [\min_{\alpha \in \Omega} g_h(\alpha), \max_{\alpha \in \Omega} g_h(\alpha)].$$

Therefore, if we can determine the absolute maximum of g_h and the absolute minimum of g_h, we can then determine whether the solution of the condition in (4.4) can be found. Moreover, we then will know whether to solve for α^* in (4.4) or solve for α^* in (4.5) in the process of finding the solution to our inverse problem. Hence, let us first develop a procedure to find the absolute maximum and absolute minimum of g_h.

Recall that we already have discussed how to obtain the solution $\widetilde{w}_h(x, \alpha)$ in the forward problem with Hermite cubic immersed finite element space, thus we can determine function $g_h(\alpha) \equiv B(1)\widetilde{w}_h''(1, \alpha)$ from solving the forward problem (4.1). To determine the absolute maximum of g_h and the absolute minimum of g_h, we assume that g_h has finitely many local extremes. Then let us consider a partition p of $\overline{\Omega}$ be such that

$$p = \{0 = p_0, p_1, p_2, \ldots, p_n = 1\}$$

for which no more than one α in the interval $[p_l, p_{l+2}]$, $l = 0, 1, \ldots, n-2$ gives a local extreme of g_h; i.e., no two consecutive intervals formed by p exit such that both contain an α that gives a local extreme of g_h. Notice that such partition p is possible because we assume that g_h contains finitely many local extremes. Now we will approximate the position of α's such

that local extreme of g_h occurs at these α's. From calculus, we know that the local extreme of g_h occurs when the slope of the function g_h changes either from positive to negative or from negative to positive. So we will use our nodes in the partition p to determine the intervals $E_j = [a_j, b_j]$, $j = 1, 2, \ldots, m$ such that each of E_j contains an α such that α gives a local extreme of g_h, where m is the number of local extremes of g_h in Ω. To do this, let us define a function s such that

$$s(i) = g_h(x_i) - g_h(x_{i-1}), \qquad i = 1, 2, \ldots, n-1.$$

Then if

$$s(i) \cdot s(i+1) < 0$$

for some i, we know that the slope of the function g has a sign change over the interval $[x_{i-1}, x_{i+1}]$. Thus, by this method, we can find the intervals $E_j = [a_j, b_j]$, $j = 1, 2, \ldots, m$ such that each of E_j contains α_j that gives a local extreme of g_h. Here, we use the Algorithm 4.1.1 to assemble this interval E_j, $j = 1, 2, \ldots, m$.

After we have obtained E_j, $j = 1, 2, \ldots, m$, we now want to determine each of the position $\alpha_j \in E_j$. The golden section (golden ratio) search [3, 15, 19] is one of the methods that can be use to determine the position of α_j given the interval E_j for each α_j. The golden section search algorithm is designed to search for absolute minimum (maximum) of a *unimodal* function in a given interval.

Definition 4.1.1 *The function $f(x)$ is unimodal on $[a, b]$ if there exists a unique number p in $[a, b]$ such that $f(x)$ is decreasing (increasing) on $[a, p]$ and $f(x)$ is increasing (decreasing) on $[p, b]$.*

For convenience, we will modify the golden section search for minimum and the golden section search for maximum into one single algorithm that searches for the absolute maximum or the absolute minimum of the function f in a given interval according to user input. One problem that arises is that we do not know each of the α_j in E_j that gives local maximum or local minimum of g_h. However, due to the property of the partition p, we know that each of the intervals $[p_l, p_{l+2}]$, $l = 0, 1, \ldots, n-2$ contains no more than one α that gives an extreme of g_h. Thus, to determine whether α_j contained in E_j is a local maximum or local minimum, we can seek the intervals formed by the nodes of p prior to E_j or seek the interval formed by the nodes of p after E_j. If the function g_h in the interval prior to E_j is increasing or the function g_h in the interval right after E_j is decreasing, then we know that α_j is a local maximum in E_j; otherwise, we know that α_j is a local minimum in E_j. Note here we know g_h is either non-increasing or non-decreasing over the intervals that is prior to E_j and right after E_j because the intervals right before and right after E_j contains no local extremes of g_h. Therefore, we can easily check to see if α_j in E_j is a local maximum or a local minimum of g_h; or in other words, we can now obtain $\alpha_j, j = 1, 2, \ldots, m$, by applying the golden section search algorithm. Here, the golden section search algorithm is shown in Algorithm 4.1.3.

After we have obtained a list of α_j's such that $\alpha_1 < \alpha_2 < \cdots < \alpha_m$ yield the local extremes of g_h, we simply add the boundary points of Ω, namely 0 and 1 to obtained an array $E = \{0, \alpha_1, \alpha_2, \ldots, \alpha_m, 1\}$ for which each element in E yields local extremes of g_h. Note here the array E can be obtained by applying the Algorithms 4.1.1, 4.1.2, and 4.1.3.

Finally, we can obtain the absolute maximum and the absolute minimum of g_h by evaluating g_h at each of the points in E and by computing their values. Therefore, we can now determine whether α^* exists for the condition in (4.4), or equivalently, we can determine whether

$$\gamma \in [\min_{\alpha\in\Omega} g_h(\alpha), \max_{\alpha\in\Omega} g_h(\alpha)].$$

Thus, we know whether to seek for α_h^* in equation (4.4) or to seek for α_h^* in the condition (4.5).

First, let us consider the case that α_h^* exists in (4.4). Then we want to obtain the values of α_h^*, i.e., find all the α_h^*s such that

$$g_h(\alpha_h^*) = \gamma. \tag{4.6}$$

Since

$$\gamma \in [\min_{\alpha\in\Omega} g_h(\alpha), \max_{\alpha\in\Omega} g_h(\alpha)], \tag{4.7}$$

we can define a continuous function $J_h : \overline{\Omega} \to \mathbf{R}$ as

$$J_h(x) = g_h(x) - \gamma,$$

and then obtain an α^* by using iterative algorithms for solving a root in J_h such as bisection algorithm. When ξ is a root of J_h, we have $\alpha^* = \xi$ is a solution to our inverse problem.

However, if we wish to obtain all the α^*s, we have to use another procedure. Since we have already obtained the set E, we can then find all the extremes of g_h. So if γ falls within two consecutive local extremes of g_h, i.e., $g_h(E(i)) < \gamma < g_h(E(i+1))$ for some $i \in \{1, 2, \ldots, m+1\}$, then we know there exists an $\alpha^* \in [E(i), E(i+1)]$ that is a solution to our inverse problem. Now suppose the interval $[E(i), E(i+1)]$ contains α^*, then we can find α^* by seeking a root of J_h in the interval $[E(i), E(i+1)]$. If ξ is the root of J_h in this interval, then we have $\alpha^* = \xi$ is a solution to our inverse problem. Again, this α^* can be found by using iterative algorithms such as the bisection method with initial interval $[E(i), E(i+1)]$. However, we will use both the bisection method and the secant method (Algorithms 4.1.5 and 4.1.6) to obtain the root of j and compare the difference between these two methods. Therefore, all the α_h^*s can be obtained.

Now we consider the case in which no α_h^* satisfies (4.4). Thus, we need to find α_h^* for which $\alpha_h^* \in \Omega$ satisfies (4.5). Since we have already determined the array E that yields all the extremes of g_h, we can then search for ξ_1 and ξ_2 such that $g_h(\xi_1)$ gives the absolute maximum of g_h and $g_h(\xi_2)$ gives the absolute minimum of g. Now if $\gamma > g_h(\xi_1)$, we will have $\alpha_h^* = \xi_1$ satisfies the condition in (4.5); otherwise we have $\alpha_h^* = \xi_2$ satisfies the condition in (4.5). Thus, we have obtained the α_h^* as the solution to our inverse problem.

Algorithm 4.1.1 *To approximate the positions such that local extremes of* $g_h(\alpha) = B(1)\widetilde{w}_h''(1,\alpha)$ *occur.*
Given: m

Step 1: Set $j = 1$
Step 2:
    for $i = 1 : m-1$
        p = *1/m*i*
        if $s(i) * s(i+1) < 0$
            $a(j) = 1/m * (i-1)$, $b(j) = 1/m * (i+1)$
            $j = j + 1$
        end if
    end for
Step 3: evaluate g(0) and g(1)
Step 4: Return a, b, $g(0)$, *and* $g(1)$.

Here m is the number of partitions in $\Omega = (0,1)$ such that $1/h = m$, and we now have $p = \{0, h, 2h, \ldots, mh = 1\}$ that gives the partition of $\overline{\Omega}$. Moreover, we assume that m is chosen such that the intervals $[p_l, p_{l+2}]$, $l = 0, 1, m-2$, contain at most one local extreme of g. Also, s is defined as

$$s(i) = g(1/m * i) - g(1/m * (i-1)).$$

We output the arrays of a and b such that the interval $[a(j), b(j)]$ contains the local extremes of g. Notice that $g(0)$ and $g(1)$ are the values at the boundary of $\overline{\Omega}$ so $g(0)$ and $g(1)$ are two of the local extremes of g.

Algorithm 4.1.2 *Refinement for local extremes.*
Given: a, b, tol.
Step 1:
    for $i = 1 : size(a)$
        Run The Golden Section Search Algorithm.
Step 2: Return the local extremes.
END

Here a and b are vectors obtained from Algorithm 1, and the tolerance is given by $(b-a) \leq tol$.

Algorithm 4.1.3 *The Golden section search algorithm.*
Given: a, b, N, maxORmin

Step 1:
Set $n = 1$, $\varsigma = (\sqrt{5} - 1)/2$
Step 2:
for $i = 1 : N$
Set $m_1 = b - \varsigma(b - a)$, $m_2 = b + \varsigma(b - a)$.
if $maxORmin = -1$
if $g(m_1) \leq g(m_2)$
Set $b = m_2$
else Set $a = m_1$
end if
elseif $maxORmin = 1$
if $g(m_1) \geq g(m_2)$
Set $b = m_2$
else Set $a = m_1$
end if
end if
if $|a - b| < tol$
Set $\iota = (m1 + m2)/2$
Return ι
elseif $n = N$
Return error message: Exceeded the max number of iterations.
end if
Set $n = n + 1$.
end for.
End

Input: a and b such that the interval $[a, b]$ contains the local extremes of g. $maxORmin = -1$ indicates the search of the absolute minimum in $[a, b]$, and $maxORmin = 1$ indicate the search of absolute maximum in $[a, b]$. N is the maximum number of iterations allowed in the algorithm.

Output: ι is the position in $[a, b]$ such that $g(\iota)$ gives a local extreme of g.

Algorithm 4.1.4 *Search for locations of* α^*.
Given: E, tol, N, γ.

Step 1:
for $i = 1 : size(E) - 1$
if $g(E(i)) \leq \gamma \leq g(E(i + 1))$

OPTION I: Run Bisection Method Algorithm.
OPTION II: Run Secant Method Algorithm.
OPTION III: Run Semi-Secant Method Algorithm.
OPTION IV: Run Method of False Position Algorithm.
end if
end for
Return α^*.
Step 2:
Set $Min = E(1)$, $Max = E(1)$
for $i = 2 : size(E)$
if $E(i) > Max$
Set $Max = E(i)$
else if $E(i) < Min$
Set $Min = E(i)$
end if
end for
Step 3:
if $\gamma > Max$,
set $\alpha^* = Max$,
else
set $\alpha^* = Min$.
end if
Step 4: Return α^*.

Here, E is an array that contains positions giving the local extremes of g in an ascending order, i.e., $E = [g(0), e_1, e_2, \ldots, e_n, g(1)]$. *tol* is defined as $(b - a) < tol$, where $[a, b]$ forms the interval that contains α^* and γ is the given bending moment of the beam at the right end. N is the same as defined in Algorithm 3.

Algorithm 4.1.5 *Bisection Method Algorithm.*
Given: a, b, γ, N, *tol*.

Step 1:
Set $c = (a + b)/2$, $n = 1$.
if $g(a) - \gamma = 0$, *Set* $\alpha^* = a$, *return* α^*,
if $g(b) - \gamma = 0$, *Set* $\alpha^* = b$, *return* α^*.
Step 2:
while $(b - a) > tol$
Set $c = (a + b)/2$
if $|g(c) - \gamma| = 0$
Set $\alpha^* = c$
Return α^*

elseif $(g(a)-\gamma)(g(c)-\gamma)<0$
Set $b=c$
else
Set $a=c$
end if
Set $n=n+1$
if $n=N$
Return error message: 'maximum number of iteration exceeded'.
end if
end while.
Step 3:
Return α^*.

Input: a and b forms the interval $[a,b]$ such that $\alpha^* \in [a,b]$. N, tol, and γ are the same as defined Algorithm 4.1.4.
Output: α^*, where α^* satisfy the condition in (4.5) is the solution to our inverse problem.

Algorithm 4.1.6 *Secant Method Algorithm [5].*
Given: a, b, γ*, N, tol*

Step 1:
Set $p0=a$, $p1=b$, $q0=g(a)-\gamma$, $q1=g(b)-\gamma$, $i=2$.
Step 2:
while $(i<N)$
Set $p=p1-q1*(p1-p0)/(q1-q0)$
$if(p<0)|(p>1)$
Return error message: 'Secant method fall out of the interval $[a,b]$*'.*
STOP.
elseif $|p-p1|<tol$
Set: $\alpha^*=p$, *return* α^*.
else
Set: $i=i+1, p0=p1, q0=q1, p1=p, q1=g(p)-\gamma$.
end if
end while
disp('maximum number of iteration exceeded').
END

Input / Output : Same as in the Bisection Algorithm.

Now we are ready to examine the accuracy of the solution to the inverse problem with the immersed Hermite cubic finite element space.

4.2 IFE solution to an example inverse interface problem

In this subsection we will solve an example inverse interface problem by the IFE method and discuss its accuracy. Since we have already created an interface boundary value problem in Section 3.5, we can set up our inverse problem as follows:

Consider the boundary value problem given in (3.19), (3.20), with $B^- = 2$ and $B^+ = 5$. Find α^* such that

$$|B(1)w''(1,\alpha^*) - \gamma|^2 \leq |B(1)w''(1,\alpha) - \gamma|^2$$

for all $\alpha \in \Omega$, where $\gamma = -4.088054047173819$. Note here the value of γ is derived from $B(1)w''(1,\pi/6)$. We will examine the accuracy of the inverse problem by using $h = 1/10, 1/20, \ldots 1/200$ when solving the forward problem $\widetilde{w}_h(x,\alpha_h)$ to obtain

$$g(\alpha_h) \equiv B(1)\widetilde{w}_h''(1,\alpha_h).$$

To solve the inverse problem for each h, we will use the algorithms described in the previous section with the following specified input values:

For Algorithm 4.1.1, we choose the number of sampling partition $m = 20$.

For Algorithm 4.1.2, 4.1.3, 4.1.4, and 4.1.5, we choose our $tol = 10^{-12}$ and $N = 200$.

Notice that we only use the bisection method to obtain the α_h^* that satisfy the following:

$$B(1)\widetilde{w}_h''(1,\alpha_h^*) = \gamma.$$

After executing these Algorithms, the approximations of α_h^* with corresponding partition parameter h can be found and are listed in Table 4.1.

We note that our algorithms generate two distinct approximated solutions $\alpha_{h,1}^*$ and $\alpha_{h,2}^*$ to the inverse problem. The plot of $g(\alpha)$ shown in Figure 4.1 verifies that there are in fact two solutions to our inverse problem. Thus, additional information is needed to determine which of the $\alpha_{h,i}^*, i = 1,2$ should be chosen. Here we present two possible extra conditions. First, we can enforce the additional restriction on choosing $\alpha_{h,i}^*$ such that the corresponding bending moment at the left end of the beam is close to a given value λ. This means that we can choose the numerical approximation $\alpha_{h,i}^*$ such that

$$|B(0)\widetilde{w}''(0,\alpha_{h,i}^*) - \lambda|^2 = \min_{j=1,2} |B(0)\widetilde{w}''(0,\alpha_{h,j}^*) - \lambda|^2.$$

For our specific example, we note that

$$\lambda = -6.178942957146504,$$

and

$$|B(0)\widetilde{w}''(0,\alpha^*_{h,1}) - \lambda| = 1.377483321984840e - 005,$$
$$|B(0)\widetilde{w}''(0,\alpha^*_{h,2}) - \lambda| = 6.083541362525849e + 000.$$

These results clearly indicate that we should choose $\alpha^*_{h,2}$ as the solution to the inverse problem.

Secondly, our choice of solution can be based on the desired design. For example, we can demand that the interface of the two materials be close to the right end of the beam instead of the left. For our example, this means we should choose $\alpha^*_{h,2}$ instead of $\alpha^*_{h,1}$.

Then with the choice of $\alpha^*_{h,2}$ as the inverse problem solution, we would like to know the order of accuracy in our inverse problem. By a procedure similar to that used to investigate the order of accuracy in forward problems, we can find that the data in Table 4.2 obey

$$\left|\frac{\pi}{6} - \alpha^*_{h,2}\right| \approx 16.2551h^{2.7475}.$$

The error $\left|\frac{\pi}{6} - \alpha^*_{h,2}\right|$ for each h are shown in Table 4.2.

To see how reliable our solution procedure is, we consider a perturbation on our γ by δ_k where $\delta_k = \delta * k$ for which δ is a random number in the interval $[-1, 1]$ and $k = 1/10, 1/20, 1/30, \ldots, 1/200$. So let us pick a uniform partition of $h = 1/200$ for solving the forward problems. Also, for Algorithm 1, we choose the number of sampling partition as $m = 20$. For Algorithm 2, 3, 4, and 5, we choose our $tol = 10^{-12}$ and $N = 200$. Here, the solutions to our inverse problem obtained for each value of k are shown in Table 4.3. And from this table, we can see that the procedures used to obtain the solutions of the inverse problem is stable because, when the magnitude of the perturbation decreases, our numerical solution converges to the numerical solution for the pure data.

Finally, we will use the secant method in the process of finding $\alpha^*_{h,1}$ and $\alpha^*_{h,2}$ with the same tolerance (tol), maximum number of iterations (N), and sampling partition (m) used previously, and compare the result with the $\alpha^*_{h,1}$ and $\alpha^*_{h,2}$ obtained from the bisection method. First let us note that, according to the authors of [5], for a continuous function f and $f(a)f(b) < 0$, the bisection method generates a sequence $\{p_n\}_{n=1}^{\infty}$ approximating a zero p of f with

$$|p_n - p| \leq \frac{b-a}{2^n}, \qquad \text{when } n \geq 1.$$

Then the number of iterations required for the bisection method to reach a given tolerance can be determined by solving the following inequality for n:

$$\frac{b-a}{2^n} \leq tol.$$

Thus, with a given initial interval [0, 1] and tolerance 10^{-12}, we can find the number of iterations n that are guaranteed to satisfy a given tolerance as follows:

$$\frac{1}{2^n} \leq 10^{-12} \text{ or } n \geq 40.$$

Now, after we proceed to obtain $\alpha^*_{h,1}$ and $\alpha^*_{h,2}$ with the secant method, we have the results listed in the Table 4.4. From the table, we see that in many cases the secant method tends to fall out of the interval $[0, 1]$ (indicated as $STOP$ in the table) and the number of iterations n used in order to obtain $\alpha^*_{h,1}$ or $\alpha^*_{h,2}$ are not necessarily better than the bisection method.

This difficulty can be alleviated by replacing first four iterations of the secant method with the bisection method in solving of $\alpha^*_{h,1}$ and $\alpha^*_{h,2}$. In this way, we will have a faster convergence in general, and all $\alpha^*_{h,1}$ and $\alpha^*_{h,2}$ can be obtained. We call this method the semi-secant method and the results generated by this method are listed in Table 4.5.

However, we still see that in some cases, with the uses of the semi-secant method, the number of iterations required to reach the tolerance still exceeds the number of iterations required to reach the tolerance with the bisection method. Since we already know that we can obtain an interval $[a, b]$ such that $(g_h(a) - \gamma)(g_h(b) - \gamma) < 0$, we will propose to use the method of false position to find $\alpha^*_{h,1}$ and $\alpha^*_{h,2}$ because these values a and b satisfy the initial input requirements of this method [5]. The algorithm of the method of false position is as follows:

Algorithm 4.2.1 *Method of False Position [5].*
Given: a, b, γ, N, tol

Step 1:
    Set $p0 = a$, $p1 = b$, $q0 = g(a) - \gamma$, $q1 = g(b) - \gamma$, $i = 2$.
Step 2:
    while $(i < N)$
        Set $p = p1 - q1(p1 - p0)/(q1 - q0)$
            if $|p - p1| < tol$
                Set: $\alpha^* = p$, *return* α^*.
            else
                Set: $i = i + 1, q = g(p) - \gamma$.
            end if
            Set $p1 = p$, $q1 = q$.
    end while
Step 3 disp('maximum number of iteration exceeded').
END

Input / Output: Same as in the Bisection Algorithm.

The result of $\alpha^*_{h,1}$, $\alpha^*_{h,2}$ and the number of iterations used with method of false position are given in Table 4.6. We see that the method of false position requires a much lower number of iterations to solve for $\alpha^*_{h,1}$ and $\alpha^*_{h,2}$ than bisection. Also, the number of iterations required is much more consistent in the method of false position as compared to the secant method or semi-secant method. Moreover, similar to the bisection method, the method of false position is guaranteed to converge and the method of false position has the same order of accuracy as secant method. Thus, we conclude that the method of false position is a highly suitable method for solving our inverse problem.

Table 4.1: The $\alpha^*_{h,1}$ and $\alpha^*_{h,2}$ generated from the inverse problem with $B_1 = 2$, $B_2 = 5$ and $\gamma \approx -4.088054047173819e + 000$ using the bisection method.

h	$\alpha^*_{h,1}$	$\alpha^*_{h,2}$
1/20	6.849315544419826e-002	5.229870843318960e-001
1/40	6.568983766019579e-002	5.304483971089439e-001
1/60	6.821690088654403e-002	5.235299181321175e-001
1/80	6.689797399086715e-002	5.266277437958722e-001
1/100	6.819324350517173e-002	5.235739212480468e-001
1/120	6.731677024883333e-002	5.235815191776956e-001
1/140	6.818659279727379e-002	5.235860823069134e-001
1/160	6.752925522920029e-002	5.235890592898989e-001
1/180	6.818382594836434e-002	5.235910596727813e-001
1/200	6.765774908330761e-002	5.235926335162007e-001

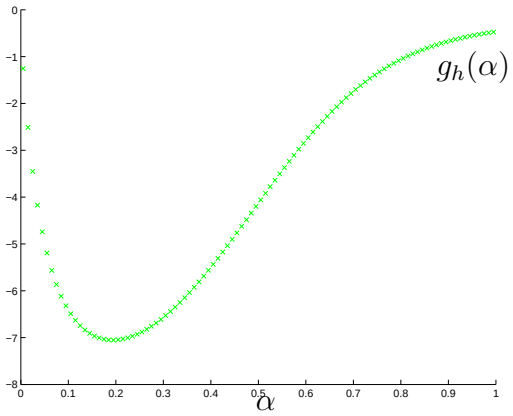

Figure 4.1: Plot of $g_h(\alpha) \equiv B(1)\widetilde{w}''_h(1,\alpha)$ with $h = 200$.

Table 4.2: Errors generated from the inverse problem with $B_1 = 2$, $B_2 = 5$ and $\gamma \approx -4.088054047173819e + 000$.

h	$\lvert\pi/6 - \alpha^*_{h,2}\rvert$
1/20	6.116912664028140e-004
1/40	6.849621510645054e-003
1/60	6.885746618134903e-005
1/80	3.028968197573367e-003
1/100	2.485435025201266e-005
1/120	1.725642060323995e-005
1/140	1.269329138542386e-005
1/160	9.716308399965179e-006
1/180	7.715925517515210e-006
1/200	6.142082098148372e-006

Table 4.3: Errors generated from the inverse problem with perturbation with $B_1 = 2$, $B_2 = 5$ and $\gamma \approx -4.088054047173819e + 000$.

k	$(\alpha^*_1)_k$	$(\alpha^*_2)_k$	$\left\lvert\alpha^*_{200,1} - (\alpha^*_1)_k\right\rvert$	$\left\lvert\alpha^*_{200,2} - (\alpha^*_2)_k\right\rvert$
1/20	6.95608866e-002	5.19211608e-001	1.90313750e-003	4.38102546e-003
1/40	6.82286018e-002	5.23483678e-001	5.70852703e-004	1.08955275e-004
1/60	6.77537961e-002	5.24698201e-001	9.60470177e-005	1.10556717e-003
1/80	6.88026880e-002	5.22022927e-001	1.14493889e-003	1.56970662e-003
1/100	6.82490442e-002	5.23431520e-001	5.91295080e-004	1.61113321e-004
1/120	6.79482077e-002	5.24200204e-001	2.90458588e-004	6.07570163e-004
1/140	6.80217894e-002	5.24011977e-001	3.64040280e-004	4.19343170e-004
1/160	6.82527148e-002	5.23422153e-001	5.94965770e-004	1.70480333e-004
1/180	6.79599417e-002	5.24170179e-001	3.02192575e-004	5.77545042e-004
1/200	6.79949413e-002	5.24080642e-001	3.37192179e-004	4.88008195e-004

Table 4.4: The $\alpha^*_{h,1}$ and $\alpha^*_{h,2}$ generated from the inverse problem with $B_1 = 2$, $B_2 = 5$ and $\gamma \approx -4.088054047173819e + 000$ using the secant method, along with the number of iterations required and comparison of the results to the bisection method.

h	$\alpha^*_{h,1}$	n	$\alpha^*_{h,2}$	$\left\|(\alpha^*_{200,1})_{bisect} - \alpha^*_{h,1}\right\|$	n	$\left\|(\alpha^*_{200,2})_{bisect} - \alpha^*_{h,2}\right\|$
$\frac{1}{20}$	6.84931554e-002	11	5.22987084e-001	8.354063605-004	21	4.38102546e-003
$\frac{1}{40}$	STOP	3	5.30448397e-001	N/A	45	1.08955275e-004
$\frac{1}{60}$	STOP	3	5.23529919e-001	N/A	14	1.10556717e-003
$\frac{1}{80}$	STOP	3	5.26627744e-001	N/A	15	1.56970662e-003
$\frac{1}{100}$	STOP	3	5.23573922e-001	N/A	61	1.61113321e-004
$\frac{1}{120}$	STOP	3	5.23581512e-001	N/A	46	6.07570163e-004
$\frac{1}{140}$	STOP	3	5.23586076e-001	N/A	28	4.19343170e-004
$\frac{1}{160}$	STOP	3	5.23589053e-001	N/A	58	1.70480333e-004
$\frac{1}{180}$	STOP	3	STOP	N/A	32	N/A
$\frac{1}{200}$	STOP	3	5.23592641e-001	N/A	18	4.88008195e-004

Table 4.5: The $\alpha^*_{h,1}$ and $\alpha^*_{h,2}$ generated from inverse problem with $B_1 = 2$, $B_2 = 5$ and $\gamma \approx -4.088054047173819e + 000$ using the semi-secant method, along with the number of iterations required and comparison of the results to the bisection method.

h	$\alpha^*_{h,1}$	n	$\alpha^*_{h,2}$	$\left\|(\alpha^*_{200,1})_{bisect} - \alpha^*_{h,1}\right\|$	n	$\left\|(\alpha^*_{200,2})_{bisect} - \alpha^*_{h,2}\right\|$
$\frac{1}{20}$	6.84931554e-002	10	5.22987084e-001	8.35406361e-004	10	6.05549182e-004
$\frac{1}{40}$	6.56898377e-002	12	5.30448397e-001	1.96791143e-003	9	6.85576374e-003
$\frac{1}{60}$	6.82169009e-002	13	5.23529918e-001	5.59151834e-004	15	6.27155349e-005
$\frac{1}{80}$	6.68979740e-002	15	5.26627742e-001	7.59775099e-004	17	3.03510882e-003
$\frac{1}{100}$	6.81932438e-002	19	5.23573922e-001	5.35494748e-004	41	1.87118259e-005
$\frac{1}{120}$	6.73167742e-002	26	5.25332099e-001	3.40974925e-004	28	1.73946556e-003
$\frac{1}{140}$	6.81865937e-002	53	5.23586084e-001	5.28844662e-004	19	6.54988333e-006
$\frac{1}{160}$	6.75292562e-002	63	5.23589059e-001	1.28492862e-004	20	3.57472634e-006
$\frac{1}{180}$	6.81838251e-002	28	5.23591068e-001	5.26076024e-004	145	1.56521158e-006
$\frac{1}{200}$	6.76577507e-002	42	5.23592638e-001	1.62350854e-009	23	4.56903648e-009

Table 4.6: The $\alpha^*_{h,1}$ and $\alpha^*_{h,2}$ generated from the inverse problem with $B_1 = 2$, $B_2 = 5$ and $\gamma \approx -4.088054047173819e + 000$ using the false position method, along with the number of iterations required and error of $|\pi/6 - \alpha^*_{h,2}|$.

h	$\alpha^*_{h,1}$	n	$\alpha^*_{h,2}$	n	$\left\|\pi/6 - \alpha^*_{h,2}\right\|$
$\frac{1}{20}$	6.849315544371809e-002	17	5.229870843222750e-001	11	6.116912760237847e-004
$\frac{1}{40}$	6.568983767056019e-002	21	5.304483971901582e-001	13	6.849621591859423e-003
$\frac{1}{60}$	6.821690069354543e-002	25	5.235299183392002e-001	21	6.885725909866469e-005
$\frac{1}{80}$	6.689797411625058e-002	26	5.266277437616306e-001	18	3.028968163331758e-003
$\frac{1}{100}$	6.819324379912631e-002	28	5.235739224290671e-001	18	2.485316923173109e-005
$\frac{1}{120}$	6.731677293115547e-002	23	5.235815115316871e-001	13	1.726406661173296e-005
$\frac{1}{140}$	6.818659940296604e-002	23	5.235860826966857e-001	18	1.269290161309833e-005
$\frac{1}{160}$	6.752925794552628e-002	30	5.235890524487018e-001	14	9.723149597018477e-006
$\frac{1}{180}$	6.818382553810209e-002	34	5.235910740329959e-001	23	7.701565302942193e-006
$\frac{1}{200}$	6.765775009628390e-002	34	5.235926311657972e-001	20	6.144432501575814e-006

Chapter 5

Immersed Finite Element Methods for Time-Dependent Beam Problems

In this chapter, we will consider how to use the IFE space to solve the time-dependent beam interface problem. First, let us recall the weak form for the Euler-Bernoulli beam equation:

Find $w \in S$ such that

$$\int_0^1 v(x)\rho(x)w_{tt}(x,t)dx + \int_0^1 v''(x)B(x)w_{xx}(x,t)dx = \int_0^1 v(x)f(x,t)dx, \forall v \in T,$$

where

$$S = \{w \in C^2((0,T_{end}), L^2(0,1)) \cap C((0,T_{end}), H^2(0,1)| \\ w(0,t) = b_1(t), w'(0,t) = b_2(t), w(1,t) = b_3(t), w'(1,t) = b_4(t)\}$$
$$T = \{v \in H^2(0,1) | v(0) = v'(0) = v(1) = v'(1) = 0\}.$$

Note that S is the solution set for the weak form and T is the test function space.

Now, in order to solve this problem, we will first discretize our weak form solution. We propose two discretization methods: a semi-discretized method and a fully-discretized method. However we will only use the fully-discretized method to solve our initial boundary value and examine the order of accuracy of the IFE solution at time level T_{end}.

The contents of this chapter are as follows. In Section 5.1, we introduce a semi-discrete IFE method for solving the forward time-dependent beam problem. In Section 5.2, we introduce a fully-discrete IFE method for solving our forward time-dependent beam problem. In Section 5.3, we have created an example of an initial boundary value problem and solved it with the fully-discretized method created in Section 5.2. Further, the order of accuracy at time level T_{end} are investigated. Finally, in Section 5.4, we propose a further investigation of our IFE space for solving the time-dependent beam problem when the involved interface varies with time.

5.1 A semi-discrete IFE method

In this section, we will discuss a semi-discrete IFE method. The idea of a semi-discrete scheme is to reduce the initial-boundary value problem of a PDE to an ODE system and then obtain an approximate solution to this initial-boundary value problem with an ODE solver [13].

Recall our weak form for time-dependent initial-boundary value problem: Find $w \in S$ such that

$$\int_0^1 v(x)\rho(x)w_{tt}(x,t)dx + \int_0^1 v''(x)B(x)w_{xx}(x,t)dx = \int_0^1 v(x)f(x,t)dx, \forall v \in T,$$

where

$$S = \{w \in C^2((0,T_{end}), L^2(0,1)) \cap C((0,T_{end}), H^2(0,1))| \\ w(0,t) = b_1(t), w'(0,t) = b_2(t), w(1,t) = b_3(t), w'(1,t) = b_4(t)\}$$

for any

$$v \in T = H_0^2(\Omega).$$

Now the semi-discrete method is to find

$$w_h(x,t) = \sum_{j=1}^{2n} w_j(t)\widetilde{\phi}_j(x)$$

such that

$$\int_0^1 \widetilde{\phi_i}(x)\rho(x)(w_h)_{tt}(x,t)dx + \int_0^1 \widetilde{\phi}_i''(x)B(x)(w_h)_{xx}(x,t)dx = \int_0^1 \widetilde{\phi}_i(x)f(x,t)dx,$$

for $i = 1, 2, \ldots, 2n$. In matrix form, we have

$$Mw''(t) + Kw(t) = \overrightarrow{f}(t) + \overrightarrow{B}_{eM}(t) + \overrightarrow{B}_{eK}(t),$$

where

$$\begin{aligned} M &= \left(\int_0^1 \rho(x)\widetilde{\phi}_i(x)\widetilde{\phi}_j(x)dx\right)_{i,j=3}^{2n-2}, \\ K &= \left(\int_0^1 B(x)\widetilde{\phi}_i''(x)\widetilde{\phi}_j''(x)dx\right)_{i,j=3}^{2n-2}, \\ \overrightarrow{B}_{eM} &= -\left(b_1''(t)\int_0^1 \rho(x)\widetilde{\phi}_i(x)\widetilde{\phi}_1(x)dx + b_2''(t)\int_0^1 \rho(x)\widetilde{\phi}_i(x)\widetilde{\phi}_2(x)dx\right)_{i=3}^{2n-2}, \\ &- \left(b_3''(t)\int_0^1 \rho(x)\widetilde{\phi}_i(x)\widetilde{\phi}_{2n-1}(x)dx + b_4''(t)\int_0^1 \rho(x)\widetilde{\phi}_i(x)\widetilde{\phi}_{2n}(x)dx\right)_{i=3}^{2n-2}, \end{aligned}$$

$$\begin{aligned}
\overrightarrow{B}_{eK} &= -\left(b_1(t)\int_0^1 B(x)\widetilde{\phi}_i''(x)\phi_1''(x) + b_2(t)\int_0^1 B(x)\widetilde{\phi}_i''(x)\widetilde{\phi}_2''(x)\right)_{i=3}^{2n-2}, \\
&- \left(b_3(t)\int_0^1 B(x)\widetilde{\phi}_i''(x)\widetilde{\phi}_{2n-1}''(x) + b_4(t)\int_0^1 B(x)\widetilde{\phi}_i''(x)\widetilde{\phi}_{2n}''(x)\right)_{i=3}^{2n-2}, \\
f(t) &= \left(\int_0^1 \widetilde{\phi}_i(x)f(x,t)dx\right)_{i=3}^{2n-2}.
\end{aligned}$$

After solving this ODE system numerically, we can obtain a sequence of vectors

$$\overrightarrow{w^k} \approx \overrightarrow{t^k}, \qquad t^k \in [0, T_{end}), \qquad k = 0, 1, 2, \cdots,$$

where

$$\overrightarrow{w^k} = \left(w_i(t^k)\right)_{i=3}^{2n-2},$$

which can be used to form a FE solution:

$$w_h^k(x) = \sum_{j=1}^{2n} w_j(t^k)\widetilde{\phi_j}(x) \approx w(x, t^k).$$

Note here that we are expecting fourth order accuracy in space, i.e.,

$$||w(x, T_{end}) - w_h^K(x)|| \approx Ch^4,$$

where $w_h^K(x) \approx w(x, T_{end})$. Thus we should choose the appropriate ODE solver that has enough accuracy in time.

5.2 A fully discrete IFE method

In this section, we give a derivation of a fully discretized method for solving our time-dependent beam with Hermite cubic IFE space. Recall our initial boundary value problem:

$$\begin{aligned}
&\rho(x)w_{tt}(x,t) + (B(x)w_{xx}(x,t))_{xx} = f(x,t), \qquad x \in (0,1), t \in (0,T), \\
&w(0,t) = b_1(t), w_x(0,t) = b_2(t), w(1,t) = b_3(t), w_x(1,t) = b_4(t). \\
&B(x)w(x,0) = g_1(x), B(x)w_t(x,0) = g_2(x),
\end{aligned}$$

and our weak form for this initial boundary value problem:

Find $w \in S$ such that

$$\int_0^1 v(x)\rho(x)w_{tt}(x,t)dx + \int_0^1 v''(x)B(x)w_{xx}(x,t)dx = \int_0^1 v(x)f(x,t)dx, \forall v \in T,$$

where

$$S = \{w \in C^2((0,T_{end}), L^2(0,1)) \cap C((0,T_{end}), H^2(0,1))| \\ w(0,t) = b_1(t), w'(0,t) = b_2(t), w(1,t) = b_3(t), w'(1,t) = b_4(t)\}$$

for any

$$v \in T = H_0^2(\Omega).$$

First, let us introduce a partition in the time variable as follows:

$$\begin{aligned} &0 = t^0 < t^1 < t^2 < \cdots < t^N = T_{end}, \\ &t^{k+1} = t^k + \tau, k = 0, 1, \cdots, N-1. \end{aligned} \tag{5.1}$$

Now we consider the approximation $w^k(x) \approx w(x, t^k)$ at time level t^k. Let

$$\begin{aligned} w^{k,1/4} &:= \frac{w^{k+1} + 2w^k + w^{k-1}}{4}, \\ w_t^k &:= \frac{w^{k+1} - w^{k-1}}{2\tau}, \\ w_{tt}^k &:= \frac{w^{k+1} - 2w^k + w^{k-1}}{\tau^2}, \end{aligned} \tag{5.2}$$

where τ is the step size in time level [14]. Note here, since $w(x,0) = g_1(x)$ and $w'(x,0) = g_2(x)$ are given, we can obtain $w^0(x)$ from $g_1(x)$ and $g_1'(x)$, also, $w^1(x)$ can be approximated by $g_1(x) + g_2(x)\tau$ and $g_1'(x) + g_2'(x)\tau$.

Now, let $w^k(x)$ be:

$$w^k(x) = \sum_{j=1}^{2n} w_j^k \widetilde{\phi}_j(x) \approx w(x, t^k). \tag{5.3}$$

Then we want

$$\begin{aligned} &\int_0^1 \widetilde{\phi}_i(x)\rho(x) \left(\frac{w^{k+1}(x) - 2w^k(x) + w^{k-1}(x)}{\tau^2} \right) dx \\ &\quad + \int_0^1 \widetilde{\phi}_i''(x) B(x) \left(\frac{w^{k+1}(x) + 2w^k(x) + w^{k-1}(x)}{4} \right)'' dx \\ &\quad = \int_0^1 \widetilde{\phi}_i(x) f(x,t) dx, \end{aligned}$$

or

$$\begin{aligned} &\int_0^1 \frac{\widetilde{\phi}_i(x)\rho(x)w^{k+1}(x)}{\tau^2} dx - \int_0^1 \frac{\widetilde{\phi}_i(x)\rho(x)2w^k(x)}{\tau^2} dx + \int_0^1 \frac{\widetilde{\phi}_i(x)\rho(x)w^{k-1}(x)}{\tau^2} dx \\ + &\int_0^1 \frac{\widetilde{\phi}_i''(x)B(x)(w^{k+1}(x))''}{4} dx + \int_0^1 \frac{\widetilde{\phi}_i''(x)B(x)(w^k(x))''}{2} dx + \int_0^1 \frac{\widetilde{\phi}_i''(x)B(x)(w^{k-1}(x))''}{4} dx \\ = &\int_0^1 \widetilde{\phi}_i(x) f(x,t) dx, \end{aligned}$$

where $i = 2, 3, \ldots, 2n-2$. By rearrange terms, we get

$$\begin{aligned}
&\int_0^1 \frac{\widetilde{\phi}_i(x)\rho(x)w^{k+1}(x)}{\tau^2}dx + \int_0^1 \frac{\widetilde{\phi}_i''(x)B(x)(w^{k+1}(x))''}{4}dx \\
&\quad = \int_0^1 \frac{\widetilde{\phi}_i(x)\rho(x)(2w^k(x))}{\tau^2}dx - \int_0^1 \frac{\widetilde{\phi}_i''(x)B(x)(w^k(x))''}{2}dx \\
&\qquad - \int_0^1 \frac{\widetilde{\phi}_i(x)\rho(x)w^{k-1}(x)}{\tau^2}dx - \int_0^1 \frac{\widetilde{\phi}_i''(x)B(x)(w^{k-1}(x))''}{4}dx \\
&\qquad + \int_0^1 \widetilde{\phi}_i(x)f(x,t)dx.
\end{aligned}$$

Now, by multiplying $4\tau^2$ on both side of the equation, we get

$$\begin{aligned}
&\int_0^1 4\widetilde{\phi}_i(x)\rho(x)w^{k+1}(x)dx + \int_0^1 \tau^2\widetilde{\phi}_i''(x)B(x)(w^{k+1}(x))''dx \\
&\quad = \int_0^1 8\widetilde{\phi}_i(x)\rho(x)w^k(x)dx - \int_0^1 2\tau^2\widetilde{\phi}_i''(x)B(x)(w^k(x))''dx \\
&\qquad - \int_0^1 4\widetilde{\phi}_i(x)\rho(x)w^{k-1}(x)dx - \int_0^1 \tau^2\widetilde{\phi}_i''(x)B(x)(w^{k-1}(x))''dx \\
&\qquad + \int_0^1 4\tau^2\widetilde{\phi}_i(x)f(x,t)dx.
\end{aligned}$$

Using the equation (5.3), we obtain the matrix form for the fully-discrete finite element solution as follows:

$$\begin{aligned}
(4M+\tau^2K)\overrightarrow{w}^{k+1} &= (8M-2\tau^2K)\overrightarrow{w}^k - (4M+\tau^2K)\overrightarrow{w}^{k-1} + 4\tau^2\overrightarrow{f}(t^{k+1}) \\
&- 4\overrightarrow{B}_{eM}(t^{k+1}) - \tau^2\overrightarrow{B}_{eK}(t^{k+1}) \\
&+ 8\overrightarrow{B}_{eM}(t^k) - 2\tau^2\overrightarrow{B}_{eK}(t^k) \\
&- 4\overrightarrow{B}_{eM}(t^{k-1}) - \tau^2\overrightarrow{B}_{eK}(t^{k-1}),
\end{aligned}$$

where

$$\overrightarrow{w}^k = \left(w_i^k\right)_{i=3}^{2n-2},$$

and

$$\begin{aligned}
M &= \left(\int_0^1 \rho(x)\widetilde{\phi}_i(x)\widetilde{\phi}_j(x)dx\right)_{i,j=3}^{2n-2}, \\
K &= \left(\int_0^1 B(x)\widetilde{\phi}_i''(x)\widetilde{\phi}_j''(x)dx\right)_{i,j=3}^{2n-2}, \\
\overrightarrow{B}_{eM}(t) &= \left(b_1(t)\int_0^1 \rho(x)\widetilde{\phi}_i(x)\widetilde{\phi}_1(x)dx + b_2(t)\int_0^1 \rho(x)\widetilde{\phi}_i(x)\widetilde{\phi}_2(x)dx\right)_{i=3}^{2n-2}, \\
&+ \left(b_3(t)\int_0^1 \rho(x)\widetilde{\phi}_i(x)\widetilde{\phi}_{2n-1}(x)dx + b_4(t)\int_0^1 \rho(x)\widetilde{\phi}_i(x)\widetilde{\phi}_{2n}(x)dx\right)_{i=3}^{2n-2},
\end{aligned}$$

$$\begin{aligned}
\overrightarrow{B}_{eK}(t) &= \left(b_1(t)\int_0^1 B(x)\widetilde{\phi}_i''(x)\widetilde{\phi}_1''(x)dx + b_2(t)\int_0^1 B(x)\widetilde{\phi}_i''(x)\widetilde{\phi_2}''(x)dx\right)_{i=3}^{2n-2}, \\
&+ \left(b_3(t)\int_0^1 B(x)\widetilde{\phi}_i''(x)\widetilde{\phi}_{2n-1}''(x)dx + b_4(t)\int_0^1 B(x)\widetilde{\phi}_i''(x)\widetilde{\phi}_{2n}''(x)dx\right)_{i=3}^{2n-2}, \\
\overrightarrow{f}(t) &= \left(\int_0^1 \widetilde{\phi}_i(x)f(x,t)dx\right)_{i=3}^{2n-2}.
\end{aligned}$$

Note that the matrices M, K, and the vector f can be assembled in the same way as before.

5.3 Accuracy of the IFE solution of the time dependent interface beam problem

In this subsection, we will numerically examine the order of accuracy of the Hermite cubic IFE solution for the time dependent interface beam problem.

To investigate the order of accuracy of the IFE method developed here, we first set up an interface beam problem to which we know the exact solution. First we choose $w(x,t)$, and find $f(x,t)$ such that $\rho(x)w_{tt}(x,t) + (B(x)w_{xx}(x))_{xx} = f(x,t)$ with $\rho(x)$ (the mass of the material at cross-section x) and $B(x)$ ($B(x) = EI(x)$ where E is the Young's modulus of the material and $I(x)$ is the moment of inertia at the cross-section x) being piecewise continuous constants

For simplicity, we let our domain be $\overline{\Omega} = [0,1]$ and let our interface $\alpha \in \Omega = (0,1)$. Here, let

$$w(x,t) = \begin{cases} a(t)\cos(x) + b(t)\sin(x) + e^{-t/10} + xe^{-t/20} & \text{if } 0 \le x \le \alpha,\ t \ge 0, \\ c(t)e^x + d(t)x^3 + 5 + x\cos t + x^2\sin t & \text{if } \alpha \le x \le 1,\ t \ge 0 \end{cases} \tag{5.4}$$

with

$$B(x) = \begin{cases} B_1, & 0 \le x < \alpha, t \ge 0, \\ B_2, & \alpha < x \le 1, t \ge 0, \end{cases} \tag{5.5}$$

and

$$\rho(x) = \begin{cases} \rho_1, & 0 \le x < \alpha, \quad t \ge 0, \\ \rho_2, & \alpha < x \le 1, \quad t \ge 0. \end{cases} \tag{5.6}$$

Now, find $a(t)$, $b(t)$, $c(t)$, and $d(t)$ such that $w(x,t)$ satisfies the rigid connection condition:

$$\begin{aligned}
w(\alpha-,t) &= w(\alpha+,t), \\
w'(\alpha-,t) &= w'(\alpha+,t), \\
B(\alpha-)w_{xx}(\alpha-,t) &= B(\alpha+)w_{xx}(\alpha+,t), \\
(B(\alpha-)w_{xx}(\alpha-,t))_x &= (B(\alpha+)w_{xx}(\alpha+,t))_x,
\end{aligned}$$

or

$$\begin{aligned}
a(t)\cos(\alpha) + b(t)\sin(\alpha) + e^{-t/10} + \alpha e^{-t/20} &= c(t)e^{\alpha} + d(t)\alpha^3 + 5 + \alpha\cos t + 2\alpha\sin t,\\
-a(t)\sin(\alpha) + b(t)\cos(\alpha) + e^{-t/20} &= c(t)e^{\alpha} + 3d(t)\alpha^2 + \cos t + 2\alpha\sin t,\\
B_1(-a(t)\cos(\alpha) - b(t)\sin(\alpha)) &= B_2(c(t)e^{\alpha} + 6d(t)\alpha + 2\sin t),\\
B_1(a(t)\sin(\alpha) - b(t)\cos(\alpha)) &= B_2(c(t)e^{\alpha} + 6d(t)).
\end{aligned}$$

And by putting the above equations into the form of linear systems, we get:

$$\begin{pmatrix}
\cos(\alpha) & \sin(\alpha) & -e^{\alpha} & -\alpha^3\\
-\sin(\alpha) & \cos(\alpha) & -e^{\alpha} & -3\alpha^2\\
-B_1\cos(\alpha) & -B_1\sin(\alpha) & -B_2(e^{\alpha}) & -6B_2\alpha\\
B_1\sin(\alpha) & -B_1\cos(\alpha) & -B_2(e^{\alpha}) & -6B_2
\end{pmatrix}
\begin{pmatrix} a(t)\\ b(t)\\ c(t)\\ d(t)\end{pmatrix} = RHS,$$

where

$$RHS = \begin{pmatrix} 5 + \alpha\cos t + \alpha^2\sin t - e^{-t/10} - \alpha e^{-t/20}\\ \cos t + 2\alpha\sin t - e^{-t/20}\\ B_2 2\sin t\\ 0\end{pmatrix}.$$

After solving the linear system above, $a(t)$, $b(t)$, $c(t)$, and $d(t)$ can be found as follows:

$$\begin{aligned}
a(t) &= \frac{(A_a - \sin(t)B_a + 2\cos(t)C_a - 2e^{-t/20}D_a - 3e^{-t/10}E_a)B_2}{R},\\
b(t) &= \frac{-(A_b + \sin(t)B_b + 2\cos(t)C_b - 2e^{-t/20}D_b - 3e^{-t/10}E_b)B_2}{R},\\
c(t) &= \frac{(A_c + \sin(t)B_c + 2\cos(t)C_c - 2e^{-t/20}D_c - 3e^{-t/10}E_c)}{Re^{\alpha}},\\
d(t) &= \frac{-(A_d + \sin(t)B_d + \cos(t)C_d - e^{-t/20}D_d - e^{-t/10}E_d)}{\alpha^2 B_1(\alpha - 3) + 6B_2(\alpha - 1)},
\end{aligned}$$

where

$$\begin{aligned}
A_a &= 15(\sin(\alpha) - \cos(\alpha))B_1\alpha^2 + 30\cos(\alpha)\mathcal{B}\alpha - 30\sin(\alpha)B_1 - 30\cos(\alpha)B_2\\
B_a &= -(\sin(\alpha) - \cos(\alpha))B_1\alpha^4 - 4\cos(\alpha)\mathcal{B}\alpha^3 + 6\mathcal{B}(\sin(\alpha) + \cos(\alpha))\alpha^2 - 12\sin(\alpha)\mathcal{B}\alpha\\
&+ 12B_2(\sin(\alpha) - \cos(\alpha))\\
C_a &= (\sin(\alpha) - \cos(\alpha))B_1\alpha^3 + 3\cos(\alpha)\mathcal{B}\alpha^2 - 3\mathcal{B}(\sin(\alpha) + \cos(\alpha))\alpha + 3\sin(\alpha)\mathcal{B}\\
D_a &= (\sin(\alpha) - \cos(\alpha))B_1\alpha^3 + 3\cos(\alpha)\mathcal{B}\alpha^2 - 3\mathcal{B}(\sin(\alpha) + \cos(\alpha))\alpha + 3\sin(\alpha)\mathcal{B}\\
E_a &= (\sin(\alpha) - \cos(\alpha))B_1\alpha^2 + 2\cos(\alpha)\mathcal{B}\alpha - 2\sin(\alpha)B_1 - 2\cos(\alpha)B_2
\end{aligned}$$

$$A_b = 15B_1(\cos(\alpha) + \sin(\alpha))\alpha^2 - 30\sin(\alpha)\mathcal{B}\alpha - 30B_1\cos(\alpha) + 30\sin(\alpha)B_2$$

$$
\begin{aligned}
B_b &= B_1(\cos(\alpha)+\sin(\alpha))\alpha^4 - 4\sin(\alpha)\mathcal{B}\alpha^3 + 6\mathcal{B}(-\cos(\alpha)+\sin(\alpha))\alpha^2 + 12\cos(\alpha)\mathcal{B}\alpha \\
&- 12B_2(\cos(\alpha)+\sin(\alpha)) \\
C_b &= B_1(\sin(\alpha)+\cos(\alpha))\alpha^3 - 3\sin(\alpha)\mathcal{B}\alpha^2 + 3(\sin(\alpha)-\cos(a))\mathcal{B}\alpha + 3\cos(\alpha)\mathcal{B} \\
D_b &= B_1(\sin(\alpha)+\cos(\alpha))\alpha^3 - 3\sin(\alpha)\mathcal{B}\alpha^2 + 3(\sin(\alpha)-\cos(a))\mathcal{B}\alpha + 3\cos(\alpha)\mathcal{B} \\
E_b &= B_1(\sin(\alpha)+\cos(\alpha))\alpha^2 - 2\sin(\alpha)\mathcal{B}\alpha - 2B_1\cos(\alpha) + 2\sin(\alpha)B_2
\end{aligned}
$$

$$
\begin{aligned}
A_c &= 15B_1(2B_2+\alpha^2 B_1) \\
B_c &= (12B_2^2+\alpha^4 B_1^2) \\
C_c &= \alpha^3 B_1^2 \\
D_c &= \alpha^3 B_1^2 \\
E_c &= B_1(\alpha^2 B_1 + 2B_2)
\end{aligned}
$$

$$
\begin{aligned}
A_d &= 5B_1 \\
B_d &= 2B_2 - 2\alpha B_1 + \alpha^2 B_1 \\
C_d &= B_1(\alpha-1) \\
D_d &= B_1(\alpha-1) \\
E_d &= B_1
\end{aligned}
$$

$$
R = \mathcal{B}(\alpha^2 B_1(\alpha-3) + 6B_2(\alpha-1))
$$

where

$$
\mathcal{B} = B_1 + B_2.
$$

After we have obtained $a(t)$, $b(t)$, $c(t)$, and $d(t)$, we can determine the force function, $f(x,t)$, and create a time dependent beam problem. From the partial differential equation of the time dependent beam problem:

$$
\rho(x)u_{tt}(x,t) + (B(x)u_{xx})_{xx} = f(x,t), \tag{5.7}
$$

we can derive the force function $f(x,t)$ as follows:

$$
f(x,t) = \begin{cases} \rho_1(t)\left(a''(t)\cos(x) + b''(t)\sin(x) + \frac{e^{-t/10}}{100} + \frac{xe^{-t/20}}{400}\right) + B_1(a\cos(x)+b\sin(x)), \\ \qquad\qquad \text{if } 0 \le x < \alpha,\ t \ge 0, \\ \rho_2(t)\left(c''(t)e^x + d''(t)x^3 - x\cos t - x^2\sin t\right) + B_2(ce^x), \\ \qquad\qquad \text{if } \alpha < x \le 1,\ t \ge 0, \end{cases}
$$

where

$$
a''(t) = \frac{\left(\sin(t)B_a - 2\cos(t)C_a - 2e^{-t/20}D_a/400 - 3e^{-t/10}E_a/100\right)B_2}{R},
$$

$$
\begin{aligned}
b''(t) &= \frac{\left(\sin(t)B_b + 2\cos(t)C_b + 2e^{-t/20}D_b/400 + 3e^{-t/10}E_b/100\right)B_2}{R},\\
c''(t) &= \frac{-\left(\sin(t)B_c + 2\cos(t)C_c + 2e^{-t/20}D_c/400 + 3e^{-t/10}E_c/100\right)}{Re^{\alpha}},\\
d''(t) &= \frac{\left(\sin(t)B_d + \cos(t)C_d + e^{-t/20}D_d/400 + e^{-t/10}E_d/100\right)}{\alpha^2 B_1(\alpha-3) + 6B_2(\alpha-1)}.
\end{aligned}
$$

And finally, we have boundary conditions:

$$
\begin{aligned}
u(0,t) &= a(t) + e^{-t/10}, && (5.8)\\
u_x(0,t) &= b(t) + e^{-t/20} && (5.9)\\
u(1,t) &= c(t)e + d(t) + 5 + \cos(t) + \sin(t), && (5.10)\\
u_x(1,t) &= c(t)e + 3d(t) + \cos(t) + 2\sin(t), && (5.11)
\end{aligned}
$$

for $t \geq 0$, and initial conditions:

$$
u(x,0) = \begin{cases} a(0)\cos(x) + b(0)\sin(x) + 1 + x & \text{if } 0 \leq x < \alpha, \\ c(0)e^x + d(0)x^3 + 5 + x & \text{if } \alpha \leq x \leq 1, \end{cases} \quad (5.12)
$$

$$
u_t(x,0) = \begin{cases} a'(0)\cos(x) + b'(0)\sin(x) - 1/10 - x/20 & \text{if } 0 \leq x \leq \alpha, \\ c'(0)e^x + d'(0)x^3 + x^2 & \text{if } \alpha \leq x \leq 1, \end{cases} \quad (5.13)
$$

where

$$
\begin{aligned}
a'(t) &= \frac{(-\cos(t)B_a - 2\sin(t)C_a + 2e^{-t/20}D_a/20 + 3e^{-t/10}E_a/10)B_2}{R}\\
b'(t) &= \frac{-(\cos(t)B_b - 2\sin(t)C_b + 2e^{-t/20}D_b/20 + 3e^{-t/10}E_b/10)B_2}{R}\\
c'(t) &= \frac{(\cos(t)B_c - 2\sin(t)C_c + 2e^{-t/20}D_c/20 + 3e^{-t/10}E_c/10)}{Re^{\alpha}}\\
d'(t) &= \frac{-(\cos(t)B_d - \sin(t)C_d + e^{-t/20}D_d/20 + e^{-t/10}E_d/10)}{\alpha^2 B_1(\alpha-3) + 6B_2(\alpha-1)}
\end{aligned}
$$

Now, we are ready to test the accuracy of the immersed Hermite cubic IFE space on the time dependent interface beam problem by the differential equation (5.4), boundary conditions (5.8) – (5.11) and initial conditions (5.12) – (5.13). We will use the fully discrete IFE method discussed in the previous section in this experiment. Note here $\overrightarrow{w}^0$ can be generated from initial conditions, and $\overrightarrow{w}^1$ can be generated by various approximation methods; however, we will use the exact solution to obtain $\overrightarrow{w}^1(x)$ and then conduct our experiments.

As in the static beam problems, we will use the following configurations of the discontinuity of the piecewise continuous coefficient $B(x)$ at the interface α:

$$\begin{array}{l}\text{Case 1: } B_1 = 2, B_2 = 5,\\ \text{Case 2: } B_1 = 2, B_2 = 500,\\ \text{Case 3: } B_1 = 2, B_2 = 50000.\end{array}$$

We will fix the interface at $\pi/6$ and use $\tau = 1/2500$ as the time step in the discretization with $t \in [0, T_{end}]$. Moreover, for simplicity, we choose $\rho_1(x) = \rho_2(x) = 1$.

To investigate the order of accuracy numerically, we use

$$h = \frac{1}{5 \times i}, \qquad i = 1, 2, \ldots, 10,$$

to generate $\widetilde{w}_h(x,t) \in \widetilde{S}_h(\overline{\Omega})$, and let the error $\widetilde{E}_h$ in our initial-boundary value be such that

$$\widetilde{E}_h = |w(x, T_{end}) - w_h^N(x)|.$$

The related data for each of the cases are listed in Tables 7.10, 7.11, and 7.12, of the Appendix section.

We expect $||\widetilde{E}_h|| \approx Ch^r$, where r is the order of accuracy and C is a constant independent of h. As before, we can estimate the values of C and r numerically applying regression to the data in Tables 7.10, 7.11, and 7.12.

For Case 1:

$$\begin{aligned} ||\widetilde{E}||_0 &\approx 7.1606 \times 10^{-003} h^{4.0120},\\ |\widetilde{E}|_1 &\approx 2.3868 \times 10^{-002} h^{2.9956},\\ |\widetilde{E}|_2 &\approx 1.5516 \times 10^{-001} h^{1.9963}. \end{aligned}$$

For Case 2:

$$\begin{aligned} ||\widetilde{E}||_0 &\approx 9.5144 \times 10^{-003} h^{4.0991},\\ |\widetilde{E}|_1 &\approx 3.6535 \times 10^{-002} h^{3.1071},\\ |\widetilde{E}|_2 &\approx 2.6338 \times 10^{-001} h^{2.0435}. \end{aligned}$$

For Case 3:

$$\begin{aligned} ||\widetilde{E}||_0 &\approx 9.9145 \times 10^{-003} h^{4.0195},\\ |\widetilde{E}|_1 &\approx 3.7577 \times 10^{-002} h^{2.9945},\\ |\widetilde{E}|_2 &\approx 2.6454 \times 10^{-001} h^{1.8951}. \end{aligned}$$

In all of these experiments, the orders of accuracy of the Hermite cubic immersed finite element in $H^s(0,1)$, $s = 0, 1, 2$ norms seem to match the orders of accuracy in the standard Hermite cubic finite element space. These results strongly suggest that our IFE space has the same orders of accuracy as the standard Hermite cubic finite element space.

5.4 A proposed IFE method for the beam problem with a time-dependent interface

In this section, we will propose a method for further investigation of our IFE method created in this thesis for solving the time dependent beam problem where the interface changes with time. Thus, we now have $\rho(x,t)$ and $B(x,t)$ is depends on both space and time. The initial-boundary value problem (IBVP) is then as follows:

$$\begin{aligned}
&\rho(x,t)w_{tt}(x,t) + (B(x,t)w_{xx}(x,t))_{xx} = f(x,t), \qquad x \in (0,1), t \in (0,T),\\
&w(0,t) = b_1(t), w_x(0,t) = b_2(t), w(1,t) = b_3(t), w_x(1,t) = b_4(t).\\
&B(x,t)w(x,0) = g_1(x), B(x,t)w_t(x,0) = g_2(x),
\end{aligned}$$

The weak for this IBVP is: Find $w \in S$ such that

$$\int_0^1 v(x)\rho(x,t)w_{tt}(x,t)dx + \int_0^1 v''(x)B(x,t)w_{xx}(x,t)dx = \int_0^1 v(x)f(x,t)dx, \forall v \in T,$$

where

$$\begin{aligned}
S = \{w \in C^2((0,T_{end}), L^2(0,1)) \cap C((0,T_{end}), H^2(0,1))| \\
w(0,t) = b_1(t), w'(0,t) = b_2(t), w(1,t) = b_3(t), w'(1,t) = b_4(t)\}
\end{aligned}$$

for any $v \in T = H_0^2(\Omega)$.

We will use the partition in the time variable as defined in equation (5.1) and finite difference schemes defined in equations (5.2). Because the interface α is a function of time, at each time level, the position of α, i.e., the point of discontinuity, can be different. Therefore, we define our IFE solution at time level t^k as

$$w^k(x) \;=\; \sum_{j=1}^{2n} w_j^k \widetilde{\phi}_j^k(x) \approx w(x,t^k) \tag{5.14}$$

and let

$$\rho^k(x) = \rho(x,t^k),\ B^k(x) = B(x,t^k).$$

Further, we propose to use the test function defined at the time level t^{k+1}. Then we want

$$\int_0^1 \widetilde{\phi}_i^{k+1}(x)\rho^k(x)\left(\frac{w^{k+1}(x) - 2w^k(x) + w^{k-1}(x)}{\tau^2}\right)dx$$

$$+\int_0^1 (\widetilde{\phi}_i^{k+1}(x))'' B^k(x) \left(\frac{w^{k+1}(x)+2w^k(x)+w^{k-1}(x)}{4}\right)'' dx$$
$$= \int_0^1 \widetilde{\phi}_i^{k+1}(x) f(x,t) dx,$$

where $i = 3, 4, \ldots, 2n-3, 2n-2$.

By expanding terms and simplifying the equation above as in the procedures used in Section 5.2, we get the matrix form for this fully-discrete finite element solution when the interface α changes through time as follows:

$$\int_0^1 4\widetilde{\phi}_i^{k+1}(x)\rho^k(x)w^{k+1}(x)dx + \int_0^1 \tau^2(\widetilde{\phi}_i^{k+1}(x))''B^k(x)(w^{k+1}(x))''dx$$
$$= \int_0^1 8\widetilde{\phi}_i(x)\rho^k(x)w^k(x)dx - \int_0^1 2\tau^2(\widetilde{\phi}_i^{k+1}(x))''B^k(x)(w^k(x))''dx$$
$$- \int_0^1 4\widetilde{\phi}_i^{k+1}(x)\rho^k(x)w^{k-1}(x)dx - \int_0^1 \tau^2(\widetilde{\phi}_i^{k+1}(x))''B^k(x)(w^{k-1}(x))''dx$$
$$+ \int_0^1 4\tau^2\widetilde{\phi}_i^{k+1}(x)f(x,t)dx.$$

Now, by applying equation (5.14) on the equation above, we get:

$$\int_0^1 4\widetilde{\phi}_i^{k+1}(x)\rho^k(x)\sum_{j=1}^{2n} w_j^{k+1}\widetilde{\phi}_j^{k+1}(x)dx + \int_0^1 \tau^2(\widetilde{\phi}_i^{k+1}(x))''B^k(x)\left(\sum_{j=1}^{2n} w_j^{k+1}\widetilde{\phi}_j^{k+1}(x)\right)''dx$$
$$= \int_0^1 8\widetilde{\phi}_i^{k+1}(x)\rho^k(x)\sum_{j=1}^{2n} w_j^{k}\widetilde{\phi}_j^{k}(x)dx - \int_0^1 2\tau^2(\widetilde{\phi}_i^{k+1}(x))''B^k(x)\left(\sum_{j=1}^{2n} w_j^{k}\widetilde{\phi}_j^{k}(x)\right)''dx$$
$$- \int_0^1 4\widetilde{\phi}_i^{k+1}(x)\rho^k(x)\sum_{j=1}^{2n} w_j^{k-1}\widetilde{\phi}_j^{k-1}(x)dx - \int_0^1 \tau^2(\widetilde{\phi}_i^{k+1}(x))''B(x)\left(\sum_{j=1}^{2n} w_j^{k-1}\widetilde{\phi}_j^{k-1}(x)\right)''dx$$
$$+ \int_0^1 4\tau^2\widetilde{\phi}_i^{k+1}(x)f(x,t)dx.$$

So the matrix form for the fully-discrete finite element solution is:

$$\begin{aligned}
(4M^{k+1,k+1} + \tau^2 K^{k+1,k+1})\overrightarrow{w}^{k+1} &= (8M^{k+1,k} - 2\tau^2 K^{k+1,k})\overrightarrow{w}^{k} \\
&- (4M^{k+1,k-1} + \tau^2 K^{k+1,k-1})\overrightarrow{w}^{k-1} \\
&+ 4\tau^2\overrightarrow{f}(t^{k+1}) \\
&- 4\overrightarrow{B}_{eM}^{k+1,k+1}(t^{k+1}) - \tau^2\overrightarrow{B}_{eK}^{k+1,k+1}(t^{k+1}) \\
&+ 8\overrightarrow{B}_{eM}^{k+1,k}(t^{k}) - 2\tau^2\overrightarrow{B}_{eK}^{k+1,k}(t^{k}) \\
&- 4\overrightarrow{B}_{eM}^{k+1,k-1}(t^{k-1}) - \tau^2\overrightarrow{B}_{eK}^{k+1,k-1}(t^{k-1}),
\end{aligned}$$

where

$$\overrightarrow{w}^k = \left(w_i^k\right)_{i=3}^{2n-2},$$

and for $r = k+1, s = k+1, k, k-1$, we have

$$
\begin{aligned}
M^{r,s} &= \left(\int_0^1 \rho^k(x) \widetilde{\phi}_i^r(x) \widetilde{\phi}_j^s(x) dx \right)_{i,j=3}^{2n-2}, \\
K^{r,s} &= \left(\int_0^1 B^k(x) \left(\widetilde{\phi}_i^r(x) \right)'' \left(\widetilde{\phi}_j^s(x) \right)'' dx \right)_{i,j=3}^{2n-2}, \\
\overrightarrow{B}_{eM}^{r,s}(t) &= \left(b_1(t) \int_0^1 \rho^k(x) \widetilde{\phi}_i^s(x) \widetilde{\phi}_1^r(x) dx + b_2(t) \int_0^1 \rho^k(x) \widetilde{\phi}_i^s(x) \widetilde{\phi}_2^r(x) dx \right)_{i=3}^{2n-2}, \\
&+ \left(b_3(t) \int_0^1 \rho^k(x) \widetilde{\phi}_i^s(x) \widetilde{\phi}_{2n-1}^r(x) dx + b_4(t) \int_0^1 \rho^k(x) \widetilde{\phi}_i^s(x) \widetilde{\phi}_{2n}^r(x) dx \right)_{i=3}^{2n-2}, \\
\overrightarrow{B}_{eK}^{r,s}(t) &= \left(b_1(t) \int_0^1 B^k(x) \left(\widetilde{\phi}_i^s(x) \right)'' \left(\widetilde{\phi}_1^r(x) \right)'' dx + b_2(t) \int_0^1 B^k(x) \left(\widetilde{\phi}_i^s(x) \right) \left(\widetilde{\phi_2^r}(x) \right)'' dx \right)_{i=3}^{2n-2}, \\
&+ \left(b_3(t) \int_0^1 B^k(x) \left(\widetilde{\phi}_i^s(x) \right)'' \left(\widetilde{\phi}_{2n-1}^r(x) \right)'' dx + b_4(t) \int_0^1 B^k(x) \left(\widetilde{\phi}_i^s(x) \right)'' \left(\widetilde{\phi}_{2n}^r(x) \right)'' dx \right)_{i=3}^{2n-2}, \\
\overrightarrow{f}^r(t) &= \left(\int_0^1 \widetilde{\phi}_i^r(x) f(x,t) dx \right)_{i=3}^{2n-2}.
\end{aligned}
$$

Note that the matrices M and K, and the vector f are to be assembled the same way as that for the static state beam problem.

Chapter 6

Conclusion

The focus of this thesis is to develop an immersed finite element space that is suitable for solving beam design problems in $\Omega \in \mathbf{R}$ that have piecewise constant coefficients. The solution of interface beam problems are required to satisfy the interface requirements: namely that the deflection, bending angle, bending moment, and shear of the beam be continuous on the domain Ω. Immersed finite element spaces are finite element spaces which are constructed so that the basis functions can satisfy these interface conditions. Thus, defining the finite element basis functions in this way allows the partition upon which the immersed finite element space is constructed to be independent of the interface, thereby immersing it in the partition of the domain.

The Hermite cubic immersed IFE space developed in this thesis is uniquely determined by the interface conditions and the usual nodal value specifications of the basis functions.

The approximation capability of the Hermite cubic IFE space is numerically tested by the interpolation of a set of appropriate testing functions. These numerical results strongly suggest that the order of accuracies of this IFE space is the same as that of the standard Hermite cubic FE space, which performs optimally in interpolating functions that have differentiable bending moment and continuous shear.

Also, when this IFE space is used to solve the forward beam problems, **Problem**($\mathbf{F}$), described in Chapter 1, the numerical results again strongly suggest that the order of accuracies for this IFE space is the same as that for the standard Hermite cubic FE space, which performs optimally in solving the forward beam problems that have piecewise continuous coefficients.

When this IFE space is used to solve the inverse problem described in Chapter 1, we see that the order of accuracy is higher than what we expected. Note that in the forward problem, the order of accuracy for approximating the bending moment is 2; however, the order of

accuracy for our inverse problem, **Problem**(**I**), is about 2.75.

The method of false position is the best method for searching for α^* because it takes the advantages of both the bisection method, which guarantees convergence, and the secant method, which preserves the order of convergence of the secant method.

Finally, when this IFE space is used to solve the forward time-dependent interface beam problems, our numerical examples indicate that its order of accuracies is the same as the order of accuracies in static state beam problems, which is as expected.

IFE spaces can be applied efficiently to moving interface problems such as the inverse problem, **Problem**(**I**), presented in Chapter 4.

There are questions to be answered in future research. For example, we do not know whether the order of accuracy is preserved for the beam problem if the interface α is a time-dependent. Section 5.4 proposed an idea that may be used in the future investigation for answering this question. Also, it is very interesting to see how we can extend this Hermite cubic IFE space to a two dimensional problem, e.g., solving the differential equation of plates. If we can, does it preserve the order of accuracy as in one dimensional problems?

Chapter 7

Appendix

This section gives all the table mentioned in the previous Chapters.

Table 7.1: Errors generated from the interpolation problem with $\alpha = \pi/6$, $B^- = 2$, $B^+ = 5$.

h	$\|\|u(x) - \widetilde{I_h u}(x)\|\|$	$\|\|u'(x) - \widetilde{I_h u}'(x)\|\|$	$\|\|u''(x) - \widetilde{I_h u}''(x)\|\|$
1/10	5.450781630798945e-007	1.887448982629727e-005	1.224861539885773e-003
1/20	3.330035788546192e-008	2.308308437125189e-006	2.992977246640569e-004
1/40	2.099907274228335e-009	2.910381704953534e-007	7.544628263873330e-005
1/80	1.312779942741883e-010	3.638571207246578e-008	1.886484434151407e-005
1/160	8.206347625846279e-012	4.548760379561024e-009	4.716912485421274e-006
1/320	5.130741270957564e-013	5.687946326771858e-010	1.179639386737241e-006
1/640	3.211087892877039e-014	7.117833080648714e-011	2.952640915699698e-007
1/1280	2.042082781944379e-015	8.911694543159438e-012	7.382785223567168e-008

Table 7.2: Errors generated from the interpolation problem with $\alpha = \pi/6$, $B^- = 2$, $B^+ = 500$.

h	$\|\|u(x) - \widetilde{I_h u}(x)\|\|$	$\|\|u'(x) - \widetilde{I_h u}'(x)\|\|$	$\|\|u''(x) - \widetilde{I_h u}''(x)\|\|$
1/10	5.565712476440778e-007	1.928554187601933e-005	1.252440031020260e-003
1/20	3.477072388543133e-008	2.409552254058297e-006	3.126264520529968e-004
1/40	2.208196697148401e-009	3.065632507247138e-007	7.963873165026163e-005
1/80	1.382891684470896e-010	3.837002695980558e-008	1.992334419342868e-005
1/160	8.666612304220051e-012	4.805613858608100e-009	4.986622325247083e-006
1/320	5.430905916813267e-013	6.020262279793338e-010	1.248648966177118e-006
1/640	3.402348376228674e-014	7.537240444309487e-011	3.126477341891240e-007
1/1280	2.225727442374852e-015	9.451881431759503e-012	7.820819809194944e-008

Table 7.3: Errors generated from the interpolation problem with $\alpha = \pi/6$, $B^- = 2$, $B^+ = 50000$.

h	$\|\|u(x) - \widetilde{I_h u}(x)\|\|$	$\|\|u'(x) - \widetilde{I_h u}'(x)\|\|$	$\|\|u''(x) - \widetilde{I_h u}''(x)\|\|$
1/10	5.597798140383150e-007	1.939158982217396e-005	1.256802521924881e-003
1/20	3.498315751039832e-008	2.424249703296664e-006	3.145319594616157e-004
1/40	2.221692143017617e-009	3.084423709669514e-007	8.013022997207119e-005
1/80	1.391365784057778e-010	3.860567823577036e-008	2.004634871933782e-005
1/160	8.719934967553024e-012	4.835227325552972e-009	5.017429026452119e-006
1/320	5.464138661688798e-013	6.057503966733879e-010	1.256375063786582e-006
1/640	3.423436844468838e-014	7.583284597121441e-011	3.145677475544004e-007
1/1280	2.224935676982436e-015	9.531175969391846e-012	7.866238929501791e-008

Table 7.4: Errors generated from the boundary value problem with $\alpha = \pi/6$, $B^- = 2$, $B^+ = 5$.

h	$\|\|w(x) - \widetilde{w}_h(x)\|\|$	$\|\|w'(x) - \widetilde{w}'_h(x)\|\|$	$\|\|w''(x) - \widetilde{w}''_h(x)\|\|$
1/5	8.033612932480310e-006	1.396249110972903e-004	4.546488622723493e-003
1/10	5.450781568289168e-007	1.887448982369008e-005	1.224861539919153e-003
1/15	1.053274772607739e-007	5.477217189065275e-006	5.325550804525035e-004
1/20	3.330038211071103e-008	2.308308462417520e-006	2.992977246706625e-004
1/25	1.391346425969246e-008	1.204183208861189e-006	1.956434181792296e-004
1/30	6.591260626467974e-009	6.852932856825524e-007	1.333001383125106e-004
1/35	3.589065530895787e-009	4.350889506309022e-007	9.870403029911372e-005
1/40	2.100230432971302e-009	2.910384598901390e-007	7.544628292224312e-005
1/45	1.304508048906979e-009	2.034669423775661e-007	5.936029402216212e-005
1/50	8.657124266167434e-010	1.497698031282741e-007	4.855291348178408e-005

Table 7.5: Errors generated from the boundary value problem with $\alpha = \pi/6$, $B^- = 2$, $B^+ = 500$.

h	$\|\|w(x) - \widetilde{w}_h(x)\|\|$	$\|\|w'(x) - \widetilde{w}'_h(x)\|\|$	$\|\|w''(x) - \widetilde{w}''_h(x)\|\|$
1/5	7.907845860343327e-006	1.377744431411709e-004	4.530854982540894e-003
1/10	5.565712197048426e-007	1.928554187098851e-005	1.252440031048368e-003
1/15	1.078248616009723e-007	5.640432789883273e-006	5.532394512471659e-004
1/20	3.477086825444591e-008	2.409552275556433e-006	3.126264519463314e-004
1/25	1.457507692297920e-008	1.260084876095401e-006	2.042846046628071e-004
1/30	6.875412493331874e-009	7.160788999001547e-007	1.396609370164878e-004
1/35	3.733349249257488e-009	4.564623127254135e-007	1.035589547277694e-004
1/40	2.168521011945155e-009	3.065605733792501e-007	7.963873132906642e-005
1/45	1.448412327638124e-009	2.141230167773431e-007	6.250046739538347e-005
1/50	9.694815930646745e-010	1.575207602366631e-007	5.107323944186823e-005

Table 7.6: Errors generated from the boundary value problem with $\alpha = \pi/6$, $B^- = 2$, $B^+ = 50000$.

h	$\|\|w(x) - \widetilde{w}_h(x)\|\|$	$\|\|w'(x) - \widetilde{w}'_h(x)\|\|$	$\|\|w''(x) - \widetilde{w}''_h(x)\|\|$
1/5	7.951116898431485e-006	1.385335950244084e-004	4.556948973841448e-003
1/10	5.597798241774828e-007	1.939158982908795e-005	1.256802521977542e-003
1/15	1.084510265125043e-007	5.673653018745095e-006	5.566068202655337e-004
1/20	3.498253483437706e-008	2.424249654554797e-006	3.145319594477523e-004
1/25	3.238969730250826e-008	1.276511265258283e-006	2.054278131828696e-004
1/30	6.918035362269439e-009	7.204114225539409e-007	1.405154063995368e-004
1/35	3.803039003547921e-009	4.592453197825760e-007	1.041788199460846e-004
1/40	2.217705467183558e-009	3.084420944619696e-007	8.013022946967847e-005
1/45	1.442135575023129e-009	2.154359927317846e-007	6.288455848459465e-005
1/50	9.053384861447290e-010	1.584735772890988e-007	5.135169267112095e-005

Table 7.7: Errors generated from the boundary value problem with $\alpha = \pi/6$, $B_1 = 2$, $B_2 = 5$, $B_3 = 2$.

h	$\|\|w(x) - \widetilde{w}_h(x)\|\|$	$\|\|w'(x) - \widetilde{w}'_h(x)\|\|$	$\|\|w''(x) - \widetilde{w}''_h(x)\|\|$
1/5	5.650445455609324e-006	9.806437667292311e-005	3.223299238197469e-003
1/10	3.229783286995079e-007	1.125206148413369e-005	7.331082152120475e-004
1/15	7.075673709614115e-008	3.682716613866055e-006	3.599519325980711e-004
1/20	2.235184461666597e-008	1.550534671084527e-006	2.011884347151966e-004
1/25	8.783703529699052e-009	7.627449439697021e-007	1.238207086811235e-004
1/30	4.383675210483903e-009	4.559361017332668e-007	8.895317506848140e-005
1/35	2.373623430786107e-009	2.882342390032495e-007	6.540645818037033e-005
1/40	1.388227630116316e-009	1.914895566101761e-007	4.987903105443399e-005
1/45	8.661621659674413e-010	1.350189730634128e-007	3.944984138516576e-005
1/50	5.684645563379808e-010	9.872659480459300e-008	3.203400874852876e-005

Table 7.8: Errors generated from the boundary value problem with $\alpha = \pi/6$, $B_1 = 2$, $B_2 = 5$, $B_3 = 200$.

h	$\|\|w(x) - \widetilde{w}_h(x)\|\|$	$\|\|w'(x) - \widetilde{w}'_h(x)\|\|$	$\|\|w''(x) - \widetilde{w}''_h(x)\|\|$
1/5	4.522032088691862e-006	7.877466233659703e-005	2.574034053010097e-003
1/10	3.011674325898141e-007	1.049319715538321e-005	6.857777382801694e-004
1/15	6.315341737566420e-008	3.308255327635678e-006	3.234621564471598e-004
1/20	2.054175814563237e-008	1.423622481786424e-006	1.847231466320649e-004
1/25	8.292822257048479e-009	7.195301854345285e-007	1.168562719826064e-004
1/30	4.052967839733834e-009	4.193212448968838e-007	8.170545703192923e-005
1/35	2.232293396405442e-009	2.704288940876806e-007	6.141778964367835e-005
1/40	1.283676703496137e-009	1.778045455605023e-007	4.619976336087248e-005
1/45	8.112533711179220e-010	1.252985579025156e-007	3.657597163572107e-005
1/50	5.440897571692117e-010	9.326457896141421e-008	3.027217330486957e-005

Table 7.9: Errors generated from the boundary value problem with $\alpha = \pi/6$, $B_1 = 2$, $B_2 = 5$, $B_3 = 20000$.

h	$\|\|w(x) - \widetilde{w}_h(x)\|\|$	$\|\|w'(x) - \widetilde{w}'_h(x)\|\|$	$\|\|w''(x) - \widetilde{w}''_h(x)\|\|$
1/5	4.502430478529783e-006	7.847489492285749e-005	2.568893363324766e-003
1/10	3.010776174539863e-007	1.048813111370550e-005	6.844688123517986e-004
1/15	6.303734938738698e-008	3.305466998357899e-006	3.234419645217433e-004
1/20	2.052606594196815e-008	1.422331007245879e-006	1.845238339671191e-004
1/25	8.753755300592911e-009	7.198130579560463e-007	1.168505875380573e-004
1/30	4.022449010961474e-009	4.190991959617839e-007	8.169428168601149e-005
1/35	2.229282302303115e-009	2.703319916549174e-007	6.136716961769257e-005
1/40	9.466680887698802e-010	1.779612879925245e-007	4.620191445458718e-005
1/45	8.031478140374838e-010	1.252478363677807e-007	3.656551371542485e-005
1/50	5.353637697405486e-010	9.325742815266898e-008	3.026642409557121e-005

Table 7.10: Errors generated from the initial-boundary value problem with $\alpha = \pi/6$, $B_1 = 2$, $B_2 = 5$, $\tau = 1/2500$, $T_{end} = 1$

h	$\left\|\left\|w\left(x, T_{end}\right) - w_h^N(x)\right\|\right\|$	$\left\|\left\|w'\left(x, T_{end}\right) - \left(w_h^N(x)\right)'\right\|\right\|$	$\left\|\left\|w''\left(x, T_{end}\right) - \left(w_h^N(x)\right)''\right\|\right\|$
1/5	1.086065064385945e-005	1.883324728734923e-004	6.109206697649410e-003
1/10	7.201021026506174e-007	2.491585495740149e-005	1.621260807418160e-003
1/15	1.366722002704458e-007	7.104137821175691e-006	6.906394165919926e-004
1/20	4.364506247707457e-008	3.028956625611993e-006	3.927105710535730e-004
1/25	1.805628999618895e-008	1.567345385332355e-006	2.550618132094556e-004
1/30	8.501455991771155e-009	8.895903747952418e-007	1.729860436258231e-004
1/35	4.613197779024254e-009	5.667534556386855e-007	1.286787758022503e-004
1/40	2.665327601498983e-009	3.766678264416339e-007	9.764291917760779e-005
1/45	1.644973760436220e-009	2.646154965212138e-007	7.717250103543801e-005
1/50	1.068070372048264e-009	1.944891073240859e-007	6.308145485896282e-005

Table 7.11: Errors generated from the initial-boundary value problem with $\alpha = \pi/6$, $B_1 = 2$, $B_2 = 500$, $\tau = 1/2500$, $T_{end} = 1$

h	$\left\|\left\|w(x,T_{end}) - w_h^N(x)\right\|\right\|$	$\left\|\left\|w'(x,T_{end}) - \left(w_h^N(x)\right)'\right\|\right\|$	$\left\|\left\|w''(x,T_{end}) - \left(w_h^N(x)\right)''\right\|\right\|$
1/5	9.531368902678647e-006	1.676971552813939e-004	5.494260394738412e-003
1/10	1.607284982777645e-006	7.372443517049330e-005	9.788962500086098e-003
1/15	1.076624438384095e-007	5.601254144502309e-006	5.447438867441547e-004
1/20	4.367620124143166e-008	3.181601702100117e-006	4.464373612927664e-004
1/25	1.608477694482543e-008	1.518539256488534e-006	7.004255620079135e-004
1/30	6.684504207675700e-009	7.032750361646511e-007	1.368288512470282e-004
1/35	5.795379561708469e-009	8.260025176604919e-007	2.687068971024875e-004
1/40	2.152442132347095e-009	2.971528863661436e-007	7.702856971949780e-005
1/45	1.412638290322878e-009	2.171887795191454e-007	6.369056212618448e-005
1/50	1.283410979717634e-009	2.687504255331464e-007	1.992995006147033e-004

Table 7.12: Errors generated from the initial-boundary value problem with $\alpha = \pi/6$, $B_1 = 2$, $B_2 = 50000$, $\tau = 1/2500$, $T_{end} = 1$

h	$\left\|\left\|w(x,T_{end}) - w_h^N(x)\right\|\right\|$	$\left\|\left\|w'(x,T_{end}) - \left(w_h^N(x)\right)'\right\|\right\|$	$\left\|\left\|w''(x,T_{end}) - \left(w_h^N(x)\right)''\right\|\right\|$
1/5	9.545262641331915e-006	1.680608229528997e-004	5.509592565850187e-003
1/10	2.666419629350337e-006	1.289240263685724e-004	1.771583294922764e-002
1/15	1.072667045237088e-007	5.580902680867959e-006	5.427759553241485e-004
1/20	4.460838514135333e-008	3.265900220812373e-006	4.614476997454541e-004
1/25	6.993801161352304e-008	1.275447425192097e-005	1.124596251507745e-002
1/30	6.628707876421416e-009	7.008245906221602e-007	1.363521856630357e-004
1/35	6.664250038092902e-009	9.817781590088675e-007	3.325769109725078e-004
1/40	2.120500317618399e-009	2.964623891372976e-007	7.680730626088641e-005
1/45	1.616456770337265e-009	2.197655908507971e-007	6.339983072550670e-005
1/50	2.455010063989352e-009	6.621523553273841e-007	5.808482415533415e-004

Bibliography

[1] Hyochoong Bang and Young W, Kwon, *The Finite Element Method Using Matlab*. CRC Press, New York, 1997.

[2] Haym Benaroya, *Mechanical Vibration. Analysis, Uncertainties, and Control.*. Prentice-Hall, New Jersey, 1998.

[3] Brian D. Camp, A Class of Immersed Finite Element Spaces and Their Application to Forward and Inverse Interface Problems, Ph.D Thesis, Virginia Tech, 2003. 2003.

[4] B. Camp, T. Lin, Y. Lin, and W.W.Sun, Quadratic immersed finite element spaces and their approximation capabilities. *Advances in Computational Mathematics*, 2003. (to appear).

[5] Richard L. Burden and J. Douglas Faires, *Numerical Analysis*. Library of Congress Cataloging in Publishcation Data, United States, 2001.

[6] Michael A. Celia and William G. Gray, *Numerical Methods for Differential Equations*. Prentice-Hall, New Jersey, 1992.

[7] Lloyd Hamilton Donnell, *Beams, Plates, and Shells*. McGraw-Hill, New York, 1976.

[8] John O. Dow, *A Unified Approach to the Finite Element Method and Error Analysis Procedures*. Academic Press, New York, 1999.

[9] R.E. Ewing, Z. Li, T. Lin and Y. Lin, The immersed finite volume element methods for the elliptic interface problems, *Mathematics and Computers in Simulations*, Vol. 30 (1999) 63-76.

[10] A. Ford, R. Freedman, T. Sandin, and H. Young, *University Physics with Modern Physics*. Addison-Wesley, New York, 2000.

[11] M. Hetényi, *Beams on Elastic Foundation, Theory with Applications in the Fields of Civil and Mechanical Engineering*. Waverly Press, Baltimore, 1946.

[12] Thomas J.R. Hughes, *The Finite Element Method. Linear Static and Dynamic Finite Element Analysis*. Dover Publications, Inc, New York, 1987.

[13] T. Lin, Finite Element Methods, letcutre notes, Virginia Tech, 2004.

[14] Tao Lin and D.L. Russell, A Superconvergent Method for Approximating the Bending Moment of Elastic Beam with Hysteresis Damping. *Applied Numerical Mathematics*, 38(2001), pp 145-165.

[15] John H. Mathews, *Numerical Methods for Computer Science, Engineering, and Mathematics*. Prentice-Hall, New Jersey, 1987.

[16] James Michalos and Edward N. Wilson, *Structural Mechanics and Analysis*. Macmillan Publishing Co., Inc., New York, 1965.

[17] G. Prathap, *The Finite Element Methods in Structural Mechanics*. Kluwer Academic Publishers, Boston, 1993

[18] Frank L. Stasa, *Applied Finite Element Analysis For Engineers*. CBS Publishing, New York, 1985.

[19] G. Zoutendijk, *Mathematical Programming Methods*. North-Holland Publishing Company, New York, 1992.

Vita

Tzin Wang was born in Taiwan 1979 and immigrated into the United States in 1995. Tzin has lived in Virginia since he moved to the U.S. and went to Grafton High School where he met an inspiring mathematics teacher, Linda Osborne. During his senior year of high school, he attended New Horizons Governor School and received college level education from many of the teachers that dedicated their lives to teaching. In August 2001, Tzin transferred from Old Dominion University to Virginia Polytechnic Institute and State University to pursue his mathematics education, and he received his bachelor degree in Mathematics in December 2003. Upon receiving the B.S. degree, Tzin saw many aspects of mathematics and decided to continue his education in mathematics. In January 2004, Tzin entered the Virginia Polytechnic Institute and State University's Graduate School to further study mathematics under the guidance of Dr. Tao Lin, whom Tzin met during his undergraduate years and was inspired by his teaching and research. Under the guidance of Dr. Lin, Tzin learned the finite element method and the immersed finite element method in depth, and in May 2005, Tzin received the degree of master of sciences in mathematics.